For Reference

NOT TO BE TAKEN FROM THIS ROOM

Ex libris
universitatis
albertaensis


Digitized by the Internet Archive
in 2024 with funding from
University of Alberta Library

https://archive.org/details/Kushigbor1984

THE UNIVERSITY OF ALBERTA

**RELEASE FORM**

NAME OF AUTHOR CORNELIUS A KUSHIGBOR

TITLE OF THESIS DETAILED HEAT FLOW STUDIES IN THE WEST CENTRAL ALBERTA SEDIMENTARY BASIN FROM BOTTOM-HOLE TEMPERATURE VALUES

DEGREE FOR WHICH THESIS WAS PRESENTED MASTER OF SCIENCE

YEAR THIS DEGREE GRANTED SPRING 1984

Permission is hereby granted to THE UNIVERSITY OF ALBERTA LIBRARY to reproduce single copies of this thesis and to lend or sell such copies for private, scholarly or scientific research purposes only.

The author reserves other publication rights, and neither the thesis nor extensive extracts from it may be printed or otherwise reproduced without the author's written permission.

THE UNIVERSITY OF ALBERTA

# DETAILED HEAT FLOW STUDIES IN THE WEST CENTRAL ALBERTA SEDIMENTARY BASIN FROM BOTTOM-HOLE TEMPERATURE VALUES

by

CORNELIUS A KUSHIGBOR

A THESIS

SUBMITTED TO THE FACULTY OF GRADUATE STUDIES AND RESEARCH

IN PARTIAL FULFILMENT OF THE REQUIREMENTS FOR THE DEGREE

OF MASTER OF SCIENCE

IN

GEOPHYSICS

DEPARTMENT OF PHYSICS

EDMONTON, ALBERTA

SPRING 1984

81-60

THE UNIVERSITY OF ALBERTA

FACULTY OF GRADUATE STUDIES AND RESEARCH

The undersigned certify that they have read, and recommend to the Faculty of Graduate Studies and Research, for acceptance, a thesis entitled DETAILED HEAT FLOW STUDIES IN THE WEST CENTRAL ALBERTA SEDIMENTARY BASIN FROM BOTTOM-HOLE TEMPERATURE VALUES submitted by CORNELIUS A KUSHIGBOR in partial fulfilment of the requirements for the degree of MASTER OF SCIENCE in GEOPHYSICS.

## ABSTRACT

Detailed heat flow studies were carried out with bottom-hole temperature data, geological formation data and measured thermal conductivity values obtained from core samples taken from wells in west central Alberta.

The results indicate that high vertical geothermal gradients are observed bordering the eastern limit of the disturbed belt. Also, detailed subsurface temperature analysis indicates that lateral temperature gradients exist. These gradients originate along the disturbed belt and strike northward and northeastward. They are probably associated with fluid motion within the permeable Cretaceous, Mississippian and upper Devonian formations.

Calculated conductive heat flow was found to increase with depth. Heat flow across the Mesozoic formations was found to be 69.19mWm$^{-2}$, while 95.03mWm$^{-2}$ was obtained within the Paleozoic sediments. The difference in heat flow values above and below the Paleozoic erosional surface is attributed to fluid motion. A hydrodynamic model can explain the thermal regime. The model suggests that gravity induced water flow in the Rocky Mountains and the foothills region and along permeable Cretaceous, Mississippian and Devonian strata is a major influence on the thermal regime.

Finally, the evidence suggests that steady-state "background" heat flow can only be determined from careful measurements below the sedimentary strata in the deeply buried Precambrian basement formations which may be less

influenced by the water flow system.

## ACKNOWLEDGEMENTS

I am greatly indebted to Professor F. W. Jones, my supervisor, for the many valuable suggestions he made and the careful guidance he gave to me throughout the various stages in the preparation of this thesis.

I also wish to thank Dr. J. A. Majorowicz for his assistance and discussions during the course of this work, and for his careful reading of the thesis and subsequent suggestions.

I am also indebted to Drs. H. Lam and M. Rahman for their help in digital computer plotting programming and also for allowing me to reproduce some of their figures.

I am particularly grateful to Professor J. A. Kernahan, the Associate Chairman of the Physics Department of The University of Alberta, for his kindness and encouragement throughout my period of study. I also thank Dr. E. Nyland for his kindness.

Finally, but not the least, I wish to express my sincere gratitude to the Physics Department of The University of Alberta for granting me financial support in the form of a Graduate Teaching Assistantship during the period of my study.

C. A. Kushigbor

November, 1983.

## Table of Contents

## List of Figures

LIST OF TABLES

# 1. INTRODUCTION

## 1.1 GENERAL

Heat flow from the deep interior of the Earth toward its surface provides the energy to drive tectonic processes and to cause metamorphic and igneous activity. A study of such heat flow and related thermal processes is therefore important to better understand the nature of the Earth.

For a long time it has been known that temperature increases with depth into the Earth, and this temperature gradient produces an outward heat flow. The main source of the heat which flows outward from the interior of the Earth is believed to be from radioactive decay of long-lived isotopes (Birch et al, 1968; Roy et al, 1968) supplemented by slow cooling of the Earth as a whole (Bott, 1982).

Although a small fraction of the heat flowing outward is transmitted to the Earth's surface and lost to the surroundings, the majority is converted to other forms of energy to drive tectonic processes and to cause igneous and metamorphic activity. The near-surface heat flow ranges from 0-200 $mWm^{-2}$ over 99 percent of the Earth's surface (Elder, 1981), and a recent compilation by Sclater et al, (1980) indicates an average worldwide value of $82mWm^{-2}$. In addition, there are localized thermal areas where the heat flux is up to 100 times the normal value, and these areas are characterized by hot springs and steaming ground.

Heat may be transmitted to the Earth's surface by conduction through the solid crystalline rocks, by water motion, and by upward flowing volcanic material. Heat conduction occurs throughout the whole Earth, while volcanic action occurs in limited areas and may provide information from depths as great as 100 km (Elder, 1981). Hydrothermal systems are much more widespread, but can provide information only to depths of about 10 km.

Thermally conducted heat flow per unit area is equal to the temperature gradient ($\nabla T$) multiplied by the thermal conductivity K: $Q=\nabla T \times K$. Applying this to the Earth, the heat which escapes by conduction from the interior at a location on the surface can be determined by measuring

(i) the temperature gradient just below the Earth's surface, and

(ii) the thermal conductivity of the rocks.

The redistribution of heat by active groundwater flow has been the subject of heat flow studies for as long as measurements have been made (Van Ostrand, 1934; Bullard, 1939). It is clear that convecting systems play an important role in heat transport in thermal areas (Lachenbruch and Sass, 1977; Bodvarson, 1969). Also there is evidence that heat transport by both local and large scale water motion strongly affects the thermal regimes of wider areas such as sedimentary basins (Majorowicz and Jessop, 1981a,b; Smith and Chapman, 1982). As a consequence, study of the temperature regime and related heat flow in a basin can

provide important information about the nature of fluid motion and thermal interactions there.

Understandinig the temperature regime and heat flow in basins is important for evaluating the geothermal energy potential (Rybach and Muffer, 1981; Jessop, 1976; BRGM report, 1976). Also, although temperature information has not been used directly in hydrocarbon exploration, it is speculated that oil and gas deposits may be associated with temperature anomalies (Roberts, 1979). Water movement transports hydrocarbons and also influences the thermal regime, so some relationship between hydrocarbon reservoirs and temperature distribution can be expected.

### 1.1.1 Review of Basin Heat Flow Studies from Bottom-Hole Temperature Values

Sedimentary basin heat flow studies can assist in locating potential regions for low-grade geothermal energy recovery as well as provide information related to the generation and migration of hydrocarbons within the basin. Also, temperature surveying is becoming important for locating groundwater (O' Brien, 1970).

The temperature distribution within the sediments and their thermal conductivities need to be known to describe the thermal regime of the basin. Also, the porosities and permeabilities of the sediments are important parameters in assessing the presence of fluid and the nature of its motion.

Unfortunately, accurate temperature observations are seldom available, except perhaps at widely separated isolated locations. However, in most basins, petroleum exploration has taken place, and some temperature measurements have been associated with these efforts.

When service company logging is carried out in an exploration or development well, bottom-hole temperatures are usually taken during each logging run by a maximum reading thermometer as a matter of course. These temperature measurements abound with both human and mechanical errors, and conclusions from them must be considered with these errors in mind. Also, well temperatures are normally disturbed by circulation fluid during the drilling process,

and it may take a long time for temperature equilibrium to return to the well and its surroundings. This effect must also be taken into account when such measurements are used for subsurface temperature estimates.

Although many difficulties and uncertainties occur when bottom-hole temperature (BHT) values are used, it must be recognized that these measurements are the only data that exist in many areas. If many BHT values are used, and interpretation based on them made with care, useful information should be gained.

Bottom-hole temperature values from well logs have been used previously for basin studies in Europe, North America and elsewhere. Harper (1971) and Evans and Coleman (1979) were the first to use BHT data in estimating heat flow for the North Sea sedimentary basin. Recently Oxburgh and Andrews-Speed (1981) used BHT together with estimated rock thermal conductivities from measurements on 230 samples to evaluate heat flow in the south western North Sea. They found average heat flow values of 70-75mWm$^{-2}$ which were generally higher than the average value of 60mWm$^{-2}$ found on the mainland United Kingdom. Also, the heat flow distribution pattern exhibited a correlation with the main geological features.

Balling et al, (1980) used BHT to investigate the geothermal energy potential of the Danish sub-basin which is part of the west European sedimentary basin, and Gable (1979) used BHT data to estimate heat flow in the Paris

basin in France.

Reiter et al, (1982) have also used BHT to study the Northern Chihuahua geothermal field in Mexico. They used many uncorrected BHT values and have been able to delineate areas with heat flows ranging from 60mWm$^{-2}$ to approximately 90mWm$^{-2}$ in the region.

Reiter and Jessop (1983) have used BHT to identify heat flow regimes in the offshore eastern Canadian basin, and Anglin and Beck (1965) and Majorowicz and Jessop (1981a) have made regional heat flow estimates from BHT and temperatures from shut-in wells in the central Canadian plains region. In both the eastern Canadian offshore work of Reiter and Jessop (1983) and the plains work of Majorowicz and Jessop (1981a), it was suggested that fluid migration along permeable strata or along faults and fractures strongly affects the heat flow regime. Recently, Yorath and Hyndman (1983) estimated heat flow for the Queen Charlotte Basin in Canada using BHT data and effective thermal conductivity estimates based on the relationship between sonic velocity and thermal conductivity of rocks. Carvalho et al, (1980) estimated heat flow using BHT from Sumatra basin wells.

A variety of factors cause variable heat flow patterns in sedimentary basins. The basin age, distribution of radioactive heat sources, heat conductivity variations, magmatic heat sources and thermal effects of groundwater flows are among the most important factors influencing the

geothermal state of the basins.

### 1.1.2 Previous Heat Flow Studies in West Central Alberta

The first heat flow study in the western Canadian sedimentary basin in Alberta was undertaken by Garland and Lennox (1962). They measured equilibrium temperatures in two wells in Redwater and Leduc and used heat conductivity values from samples from nearby wells to determine heat flow values of $61 mWm^{-2}$ and $67 mWm^{-2}$ which are rather higher than the average value for sedimentary basins with Precambrian basements.

Anglin and Beck (1965) were the first to use temperature data collected from oil companies. From geothermal gradient estimates for 18 sites and assuming that the conductivity is reasonably constant for the basin, they found a northerly trending increase in heat flow values which they suggested may be due to crustal thickening. Also, they suggested a correlation of enhanced temperature with granitic basement intrusions and, furthermore, their results showed temperature gradient values that increased eastward in the direction of decreasing sediment thickness.

As mentioned in the previous section, Majorowicz and Jessop (1981a) made estimates of regional geothermal gradients and heat flow from available temperature data (AAPG, 1976) for the interior plains. They found that the heat flow values are generally higher than those found in other Precambrian platform areas. They found that radioactive heat generation estimated on the basis of uranium, thorium, and potassium studies by Burwash and

Cumming (1976) and Burwash (1979) could not explain the heat flow pattern and suggested that fluid motion is a major contributing factor to the regional heat flow pattern in the region.

Lam et al, (1982) used BHT values from west central Alberta and found a high geothermal gradient anomaly in the Hinton/Edson area. They suggested that this anomaly may be the result of hot water motion northeastward and upward toward the surface from the disturbed region to the west along southwestward dipping faults in the Devonian and Cambrian sediments.

A closely spaced magnetic variometer array study conducted by Ingham et al, (1983) has indicated a deep electrical conductivity anomaly coincident with the geothermal anomaly reported by Lam et al, (1982). Ingham et al, (1983) suggested an alternate explanation for the Hinton/Edson geothermal anomaly in that it may be due to a region of partial melt with its top some 5-10 km below the surface and extending to considerable depth. However, further analysis of BHT data by Majorowicz et al, (1983a) and Majorowicz et al, (1983b) shows that the location and general shape of the geothermal anomaly varies with depth, which is inconsistent with an anomaly associated with a deep source of partial melt.

The present work is a detailed study of BHT data from the Hinton/Edson area in order to gain better knowledge of the temperature regime there. Also, detailed heat flow

estimates are made in this work.

### 1.1.3 Geology of the Area

The area of interest lies between latitude 52.7 degrees north to latitude 54.0 degrees north and between longitude 115.8 degrees west to longitude 118.0 degrees west, and is part of the interior plains of western Canada.

Western Canada may be divided into three geological and physiological provinces. From west to east these are

(i) the Cordillera

(ii) the interior plains

(iii) the Canadian shield.

The Cordillera has extreme topographic relief and forms the western boundary of the interior plains. The rocks are mostly miogeoclinal and were deformed during the Cretaceous and early Cenozoic orogenies.

The interior plains, or western Canadian sedimentary basin, is a broad gently rolling plain from the Rocky Mountain foothills in the west to the Precambrian shield of central Canada. The thickness of the sedimentary column is about 7,000m in the west and gradually thins until it disappears some 1000km or so to the east. The rocks are Paleozoic, Mesozoic, and Tertiary. The Mesozoic is separated unconformably from the Paleozoic. The middle Cambrian extends far out from the mountains across the basin. The Devonian rocks are reasonably continuous throughout the basin, and are terminated in the easterly and northeasterly directions by post-Paleozoic erosion. The Paleozoic finally crops out along a narrow eastern edge of the plains

bordering the shield.

The Cretaceous rocks cover the entire basin, and dip in south west direction. The Paleozoic, Triassic and Jurassic strata are basically marine. The Cretaceous is both continental and marine, while the Cenozoic is completely continental, (McCrossan and Glaister, 1970).

# 2. DATA COLLECTION AND ANALYSIS

## 2.1 Sources of Data

Three sources of data were used for this work:

(1) Bottom-hole temperatures (BHT) from petroleum exploration well logs kept at the Alberta Energy Resources Conservation Board in Calgary. These temperatures are recorded at well bottoms by maximum recording thermometers attached to logging equipment. These data are taken from about eight hundred wells whose locations range from latitude 52.7 degrees north to latitude 54.0 degrees north and from longitude 115.8 degrees west to longitude 118.0 degrees west. On the township-range grid, this area includes townships 43 to 57 and ranges 13 to 27, west of the 5th meridian. The entire area is about 21,072 square kilometers, and is shown on the map of Fig. 2.1 where the plotted positions indicate well locations. The temperature data have not been corrected for effects associated with fluid circulation during drilling.

(2) The second set of data is taken from the Alberta Energy Resources Conservation Board tops file. It consists of lists of geological formation tops with their respective depths for each well. The ages of these formations range from Tertiary to Precambrian period, with about 95% occurring in Mesozoic to Paleozoic strata. The wells used were the same as those from which BHT data were taken.

(3) The third set of data consists of thermal conductivity

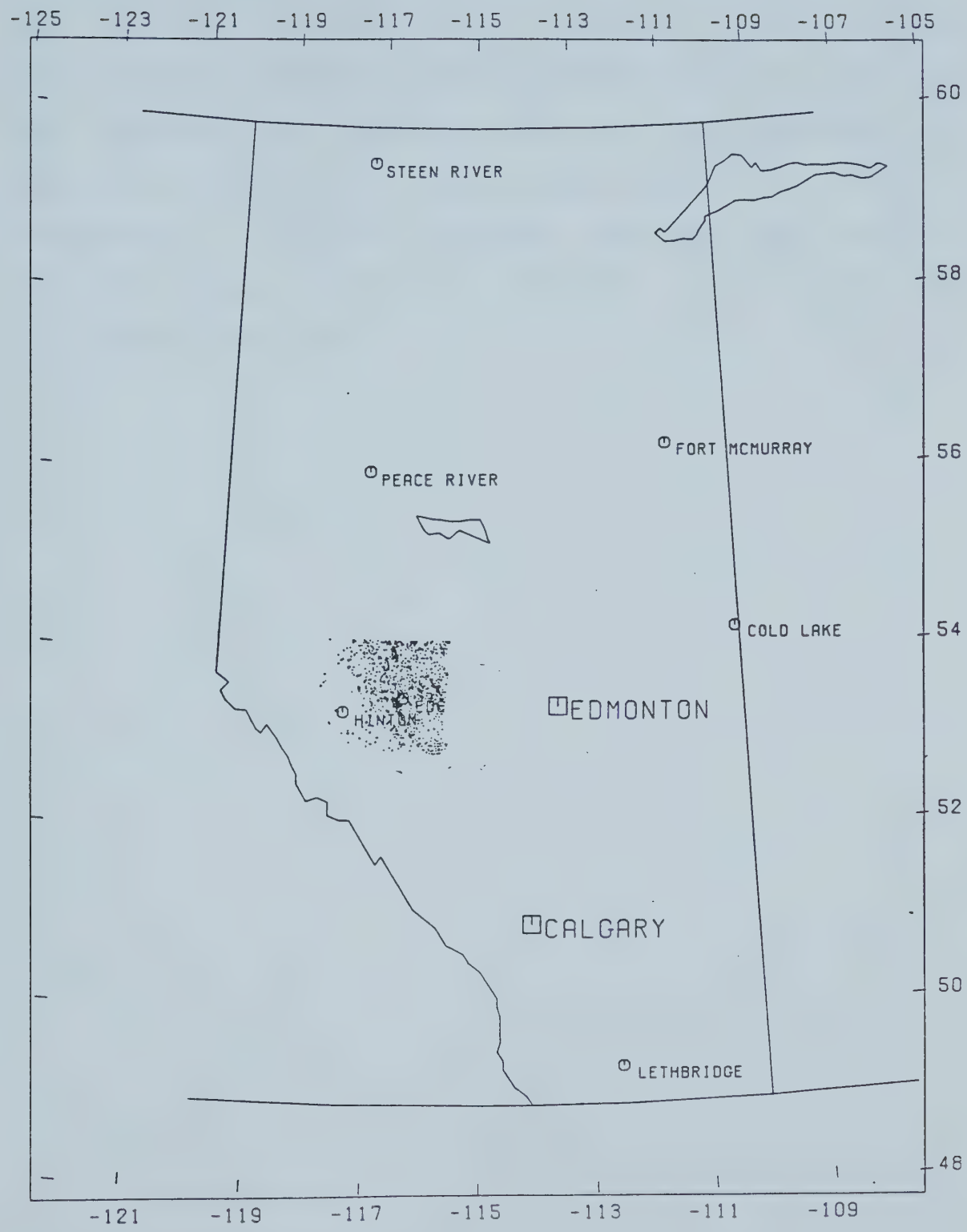


Figure 2.1 The plotted positions on this map indicate the locations of the wells from which BHT data were taken.

measurements made from core samples. The samples were taken from industry acquired cores from wells in south central Alberta, and the measurements were performed on a divided bar apparatus by the heat flow group at the University of Alberta. In addition to the thermal conductivity values, information on density, porosity and rock type has been recorded. Figure 2.2 shows the positions of the wells from which these data came.

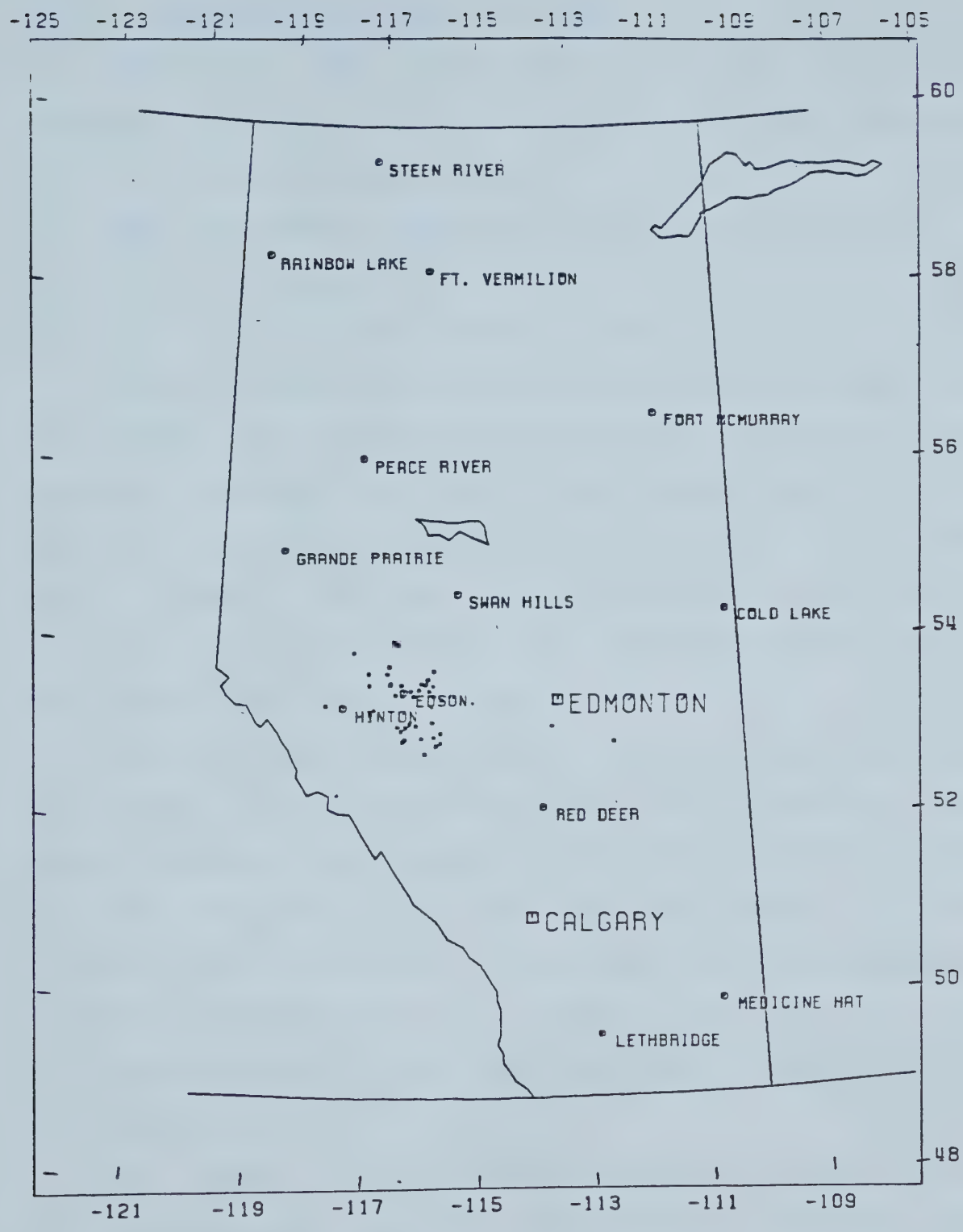


Figure 2.2 The plotted positions show the locations of wells from which core samples were taken for conductivity measurements.

### 2.1.1 Mapping of Geological Surfaces

Analysis of the three data sets began by mapping important geological surfaces. Three surfaces were selected:

(a) top of the Colorado formation,

(b) the unconformity separating Cretaceous formations from the Jurassic-Triassic formations,

(c) the top of the upper Devonian formation.

These surfaces were selected because a large number of the bottom-hole temperatures occurs in the Cretaceous and Devonian formations. The unconformity surface was considered because it represents a surface where different lithologies are in contact, and heat flow estimates across such a surface should yield insight into the pattern and nature of the general heat flow of the area.

To map the surfaces using the geological formation depth data, the area was divided into 225 1x1 township/range areas. To obtain the representative depths to the top of the Colorado formation for each 1x1 area, the depths to this formation for all the wells within each area were summed and averaged. These averages were assigned to the centres of the 1x1 township-range areas and from these a contour map was drawn and is shown in Fig. 2.3.

The depths to the unconformity surface in each of the 1x1 township-range areas were determined in a different way from those to the top of the Colorado formation. The unconformity surface separates formations of the lower Cretaceous from those of the Jurassic-Triassic or the

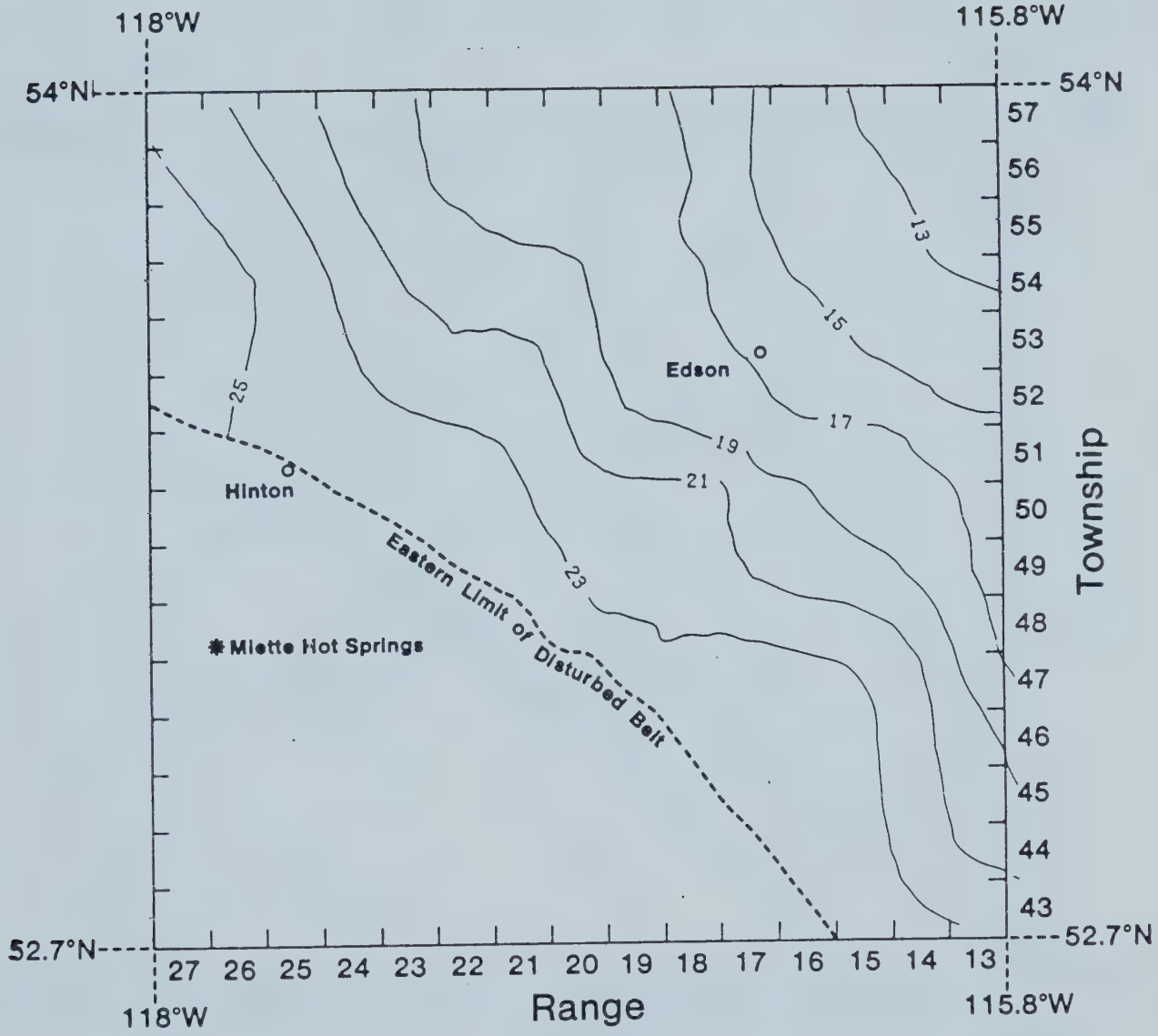


Figure 2.3 Depths from the surface of the Earth to the top of Colorado formation (contour values in hundreds of meters). The limit of the disturbed belt is indicated.

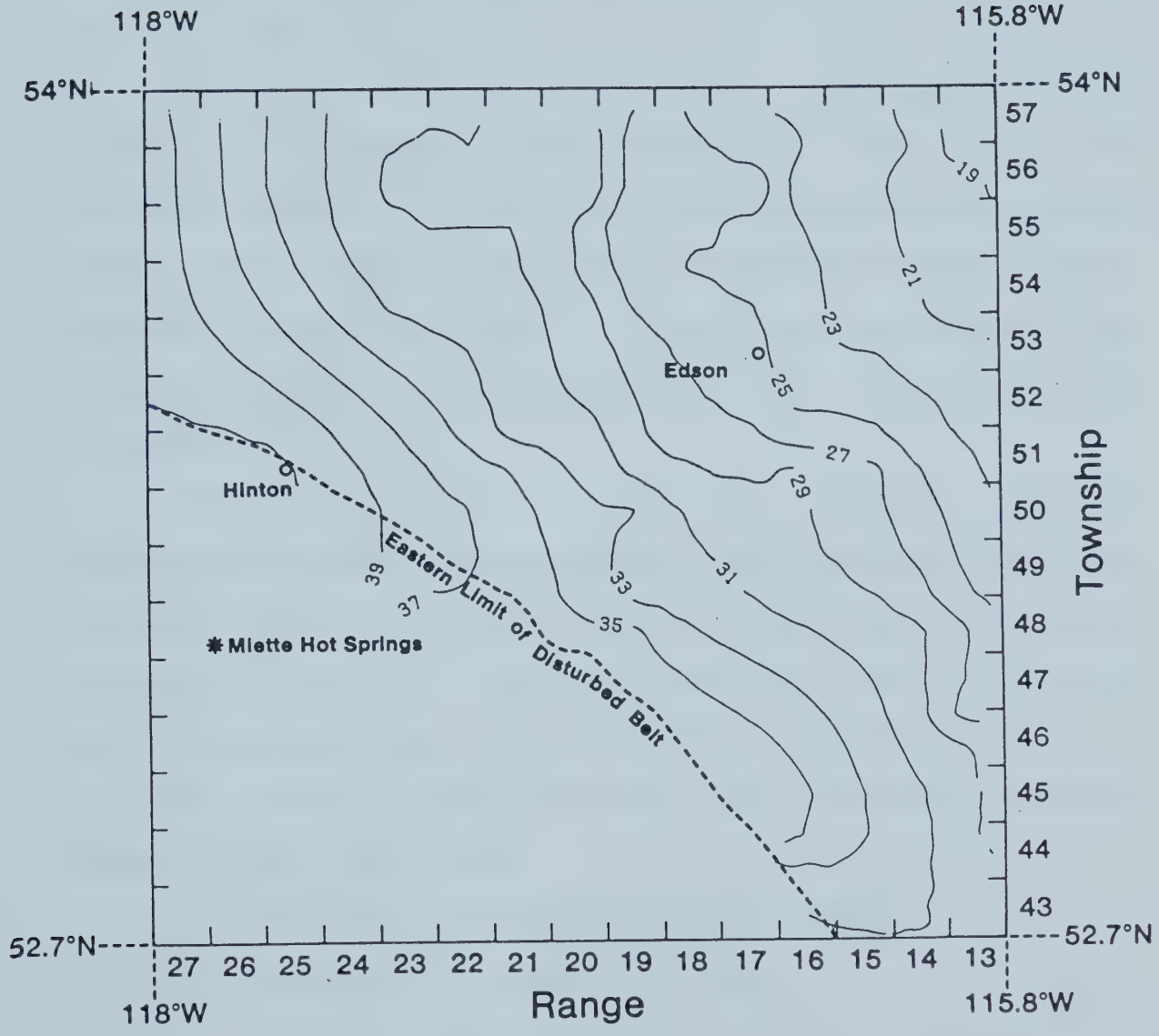


Figure 2.4 Depths (in hundreds of meters) from the surface of the Earth to the unconformity surface which separates the lower Cretaceous formation from the rest of the Mesozoic formations.

Mississippian. Therefore, in each of the 1x1 township/range areas, the depths to the top of the latest formation of the Jurassic were averaged. When no Jurassic formation occurred, the most recent formation of the Triassic or Mississippian was considered. The resulting unconformity surface map is shown in Fig. 2.4.

The third surface, the top of the upper Devonian formation, was mapped in the same way as the top of the Colorado formation. In this case the surface was taken to be the contact between the Exshaw or the Exshaw Wabamun and the Devonian formations. Figure 2.5 illustrates the depth to the contact between the Wabamun and the upper Devonian formations.

Observations from these three maps indicate that the sediments dip in approximately the southwest direction. However, there are not sufficent data in the extreme southwest corner to completely describe how the sediments dip as the Rocky Mountain foothills are approached.

The slopes of the surfaces in the southwest direction as far as data exist are:

(1) the top of the Colorado formation ≃12m/km.

(2) the unconformity surface ≃ 16.1m/km.

(3) the top of the upper Devonian surface ≃ 17.3m/km.

The contour interval for the three maps is 200m and the contour values are in hundreds of meters.

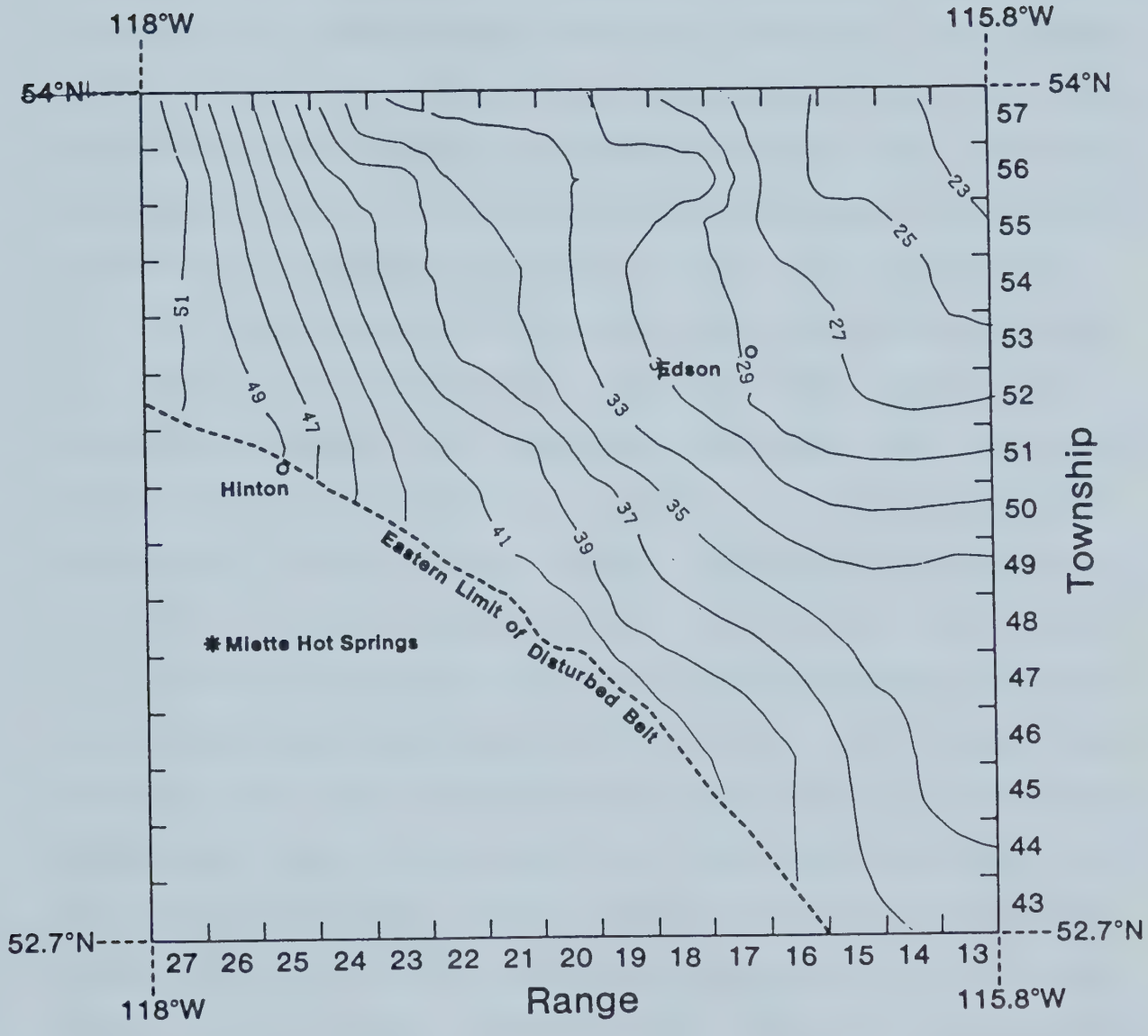


Figure 2.5 Depths from the surface of the Earth to the contact between the Wabamun and the upper Devonian formations. (Contour values are given in hundreds of meters).

### 2.1.2 Calculation of Geothermal Gradients

In order to calculate the conductive heat flow in a given direction across a column of rock material, the rate of change of temperature with depth (geothermal gradient) is required as well as the average thermal conductivity for the column. For a homogeneous isotropic material with steady heat flow, two temperature measurements at different positions in the column are needed to define the geothermal gradient. The heat flow can then be estimated by taking the product of the thermal gradient and the rock conductivity.

It is important to realize that a considerable amount of scatter is introduced into the BHT values due to mechanical errors in recording and also due to fluid circulation during drilling. In order to estimate geothermal gradients using these data, statistical methods are employed. A computer program based on a linear least squares fit technique was used to calculate the geothermal gradients from temperature depth plots of the data. The region was divided into 3x3 township/range areas. Each of these areas was moved every two ranges to the west starting from townships 43,44,45, ranges 13,14,15 to townships 43,44,45, ranges 25,26,27 and then every two townships to the north. This moving window procedure was adopted to enhance the geothermal gradients and also to average out any abnormal temperatures which might otherwise lead to spurious values for the calculated gradients for any particular 3x3 township/range.

By this procedure, average geothermal gradients were calculated for each 3x3 township/range area for the entire area. Figures 2.6-2.8 show temperature/depth plots for three 3x3 township/range areas. The data represented in Fig. 2.6 are from an area which falls within the Hinton/Edson geothermal gradient anomaly reported by Lam et al, (1982). Figure 2.7 is taken from the area covering townships 45,46 and 47 and ranges 19,20 and 21 and falls within the disturbed belt. Figure 2.8 gives data from townships 55,56 and 57, and ranges 15, 16 and 17 which are located within the northeast region of the study area. The geothermal gradients obtained in this manner were assigned to the centres of each of the corresponding 3x3 township/range areas for contouring. Figure 2.9 is the resulting geothermal gradient contour map. The contour interval for this map is 2°C/km.

Even though the Earth's heat source is fairly constant and the heat flow is upward, the vertical heat flow varies both laterally and vertically. In sedimentary basins, fluid motions and rock inhomogeneities are the main causes for such variations. It is therefore necessary to calculate geothermal gradients over various depth intervals, the same way as is done for sonic velocities in seismic interpretation. Four lithological sections are considered here. Their surfaces correspond to those mapped in Figs. 2.3-2.5. These intervals include formations from

(1) the top of the Colorado formation to the unconformity

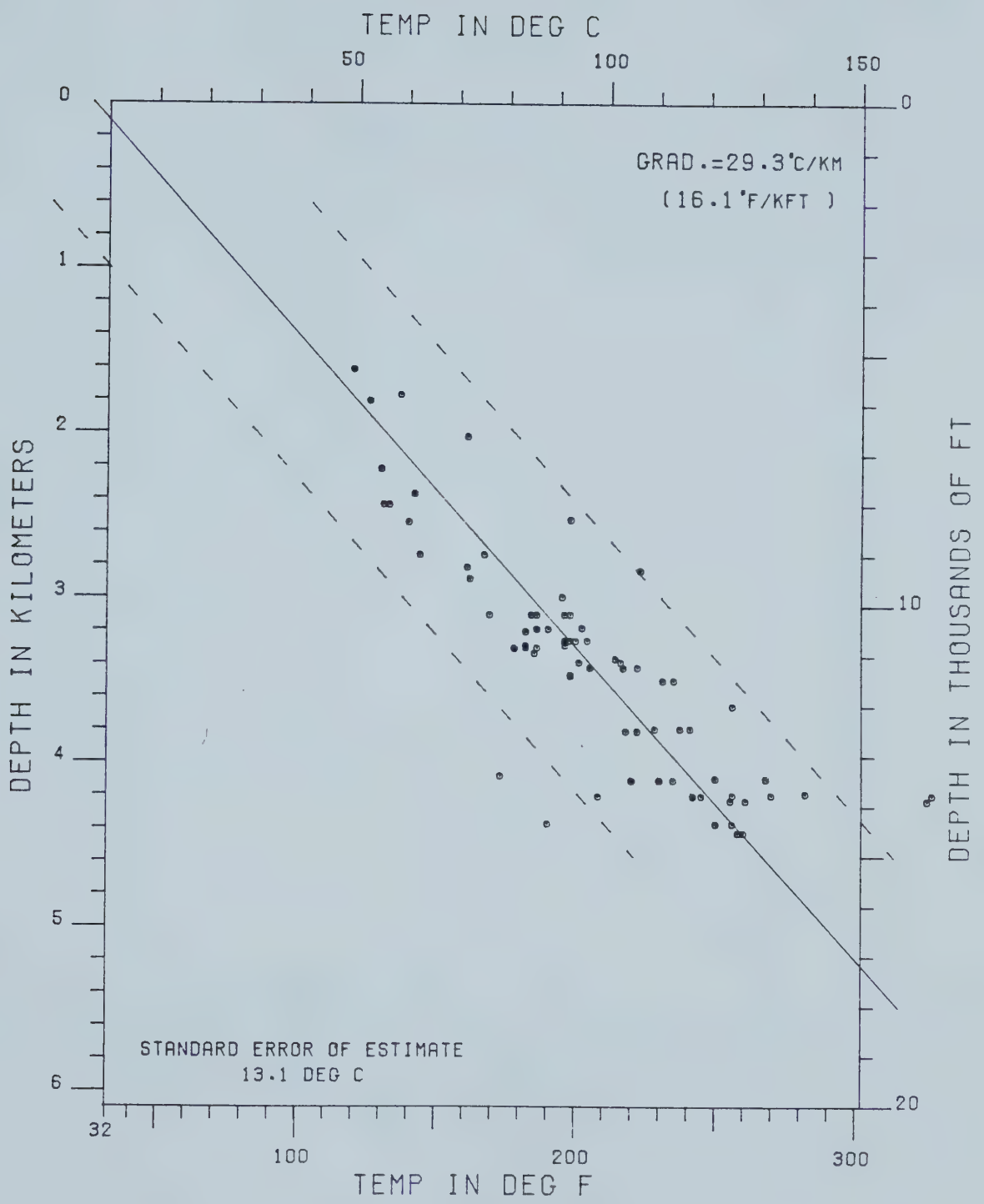


Figure 2.6 Temperature/depth plot for townships 51,52,53 and ranges 19,20,21 showing the linear least squares fitted line. The broken lines define the 95% confidence limits.

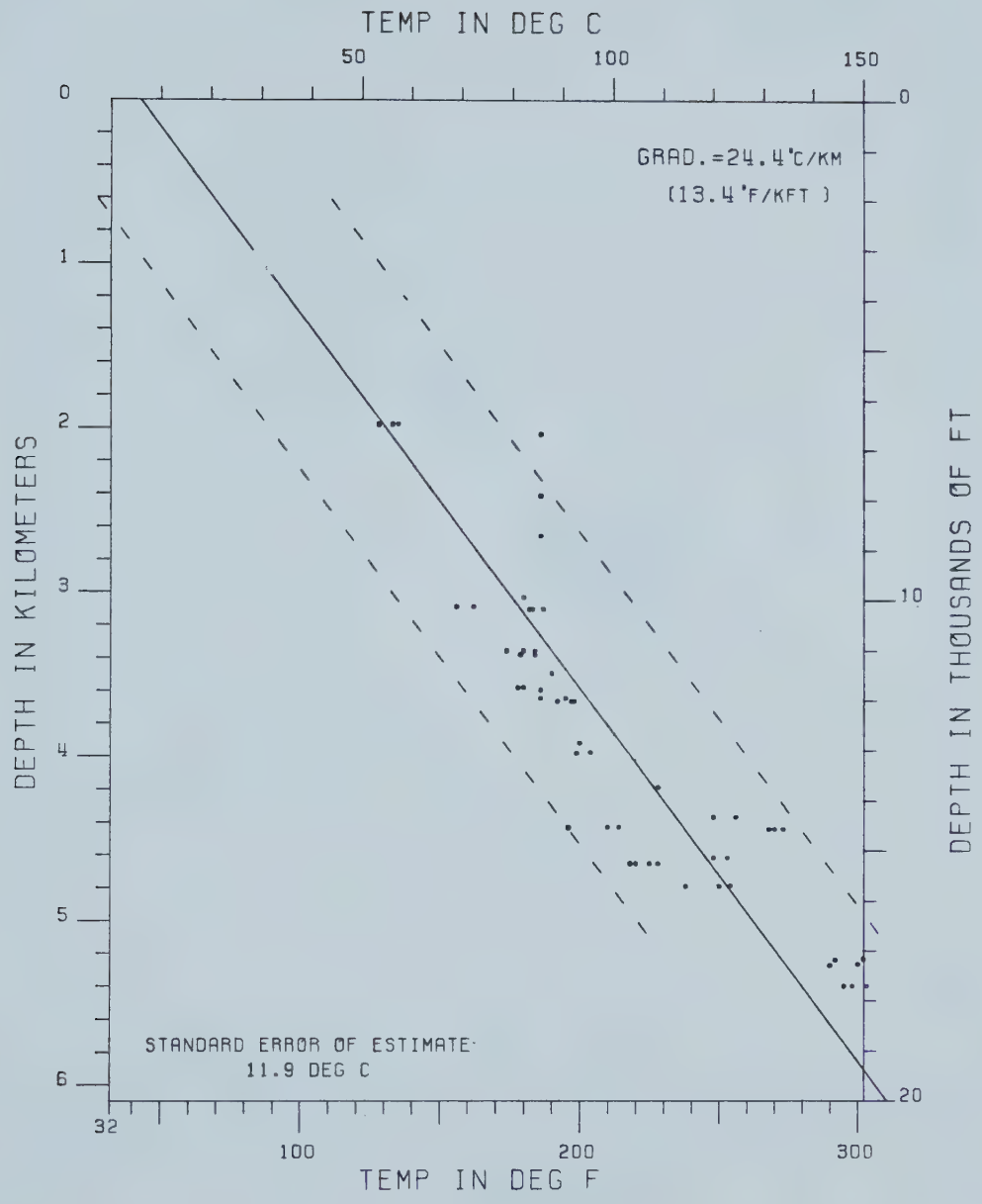


Figure 2.7 Temperature/depth plot for townships 45,46,47 and ranges 19,20,21 showing the linear least squares fitted line. The broken lines define the 95% confidence limits.

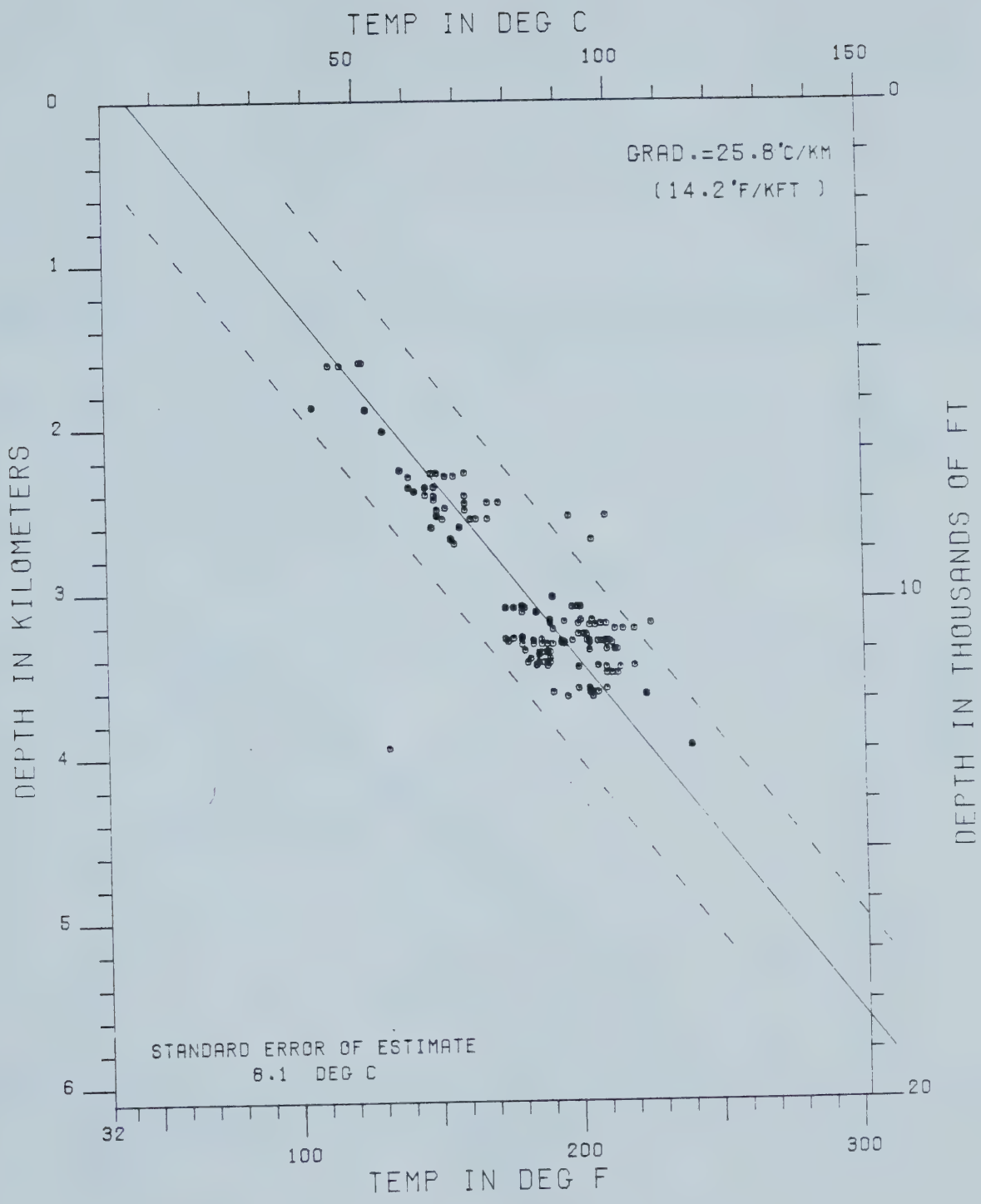


Figure 2.8 Temperature/depth plot for townships 55,56,57 and ranges 15,16,17 showing the linear least squares fitted line. The broken lines define the 95% confidence limits.

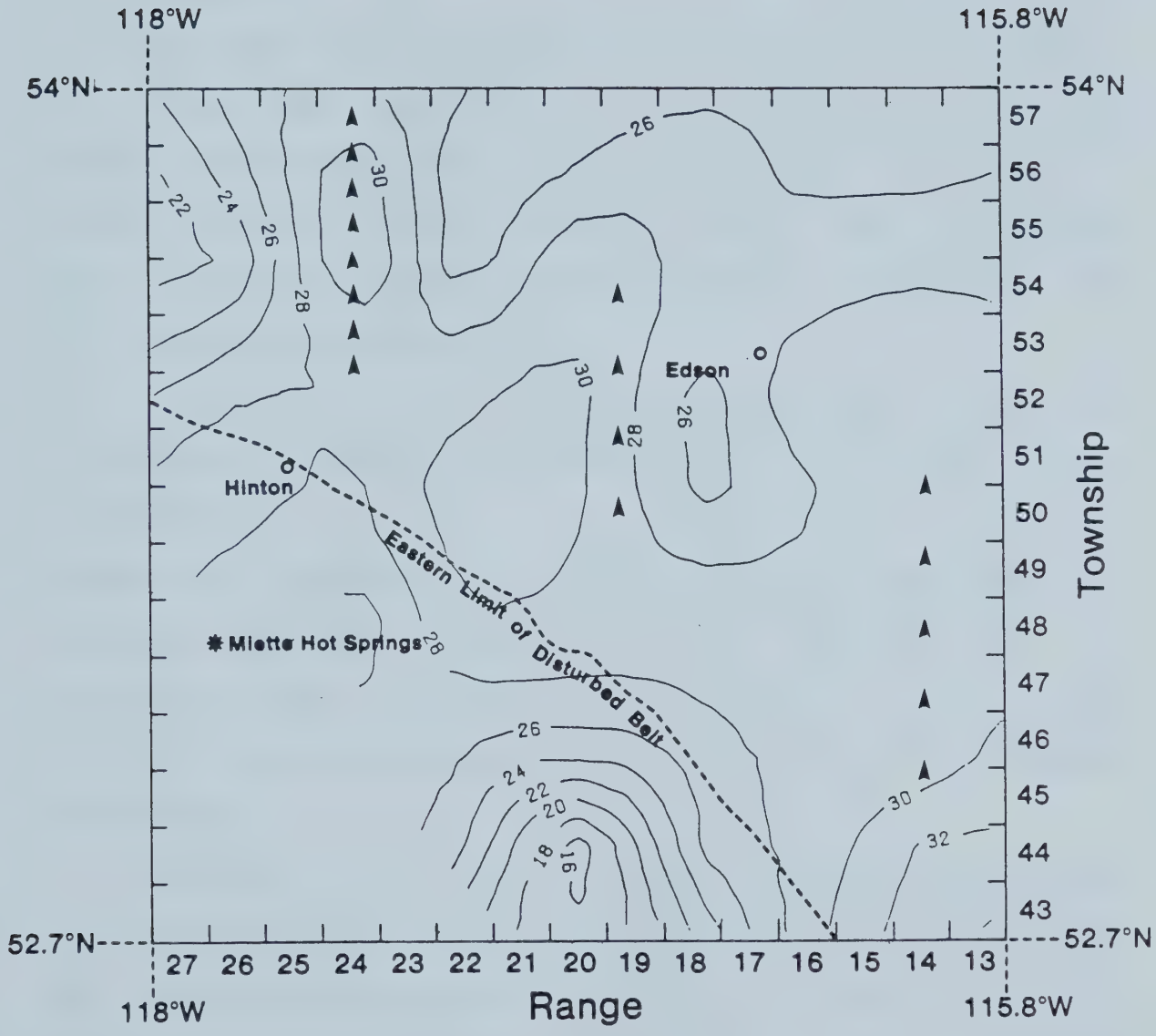


Figure 2.9 Geothermal gradient contour map from the 3x3 township/range moving window estimates.

surface,

(2) the top of the Colorado formation to the upper Devonian surface,

(3) the surface of the unconformity to the Precambrian basement,

(4) the upper Devonian surface to the Precambrian basement.

Using the same linear least squares technique as before, geothermal gradients were calculated for each of these intervals. In all cases the 'spread' was calculated as well. It is the standard error of estimate associated with the least squares fitted line.

Figures 2.10 and 2.11 show temperature/depth plots and calculated geothermal gradients for the 3x3 areas given by townships 51, 52 and 53 and ranges 19, 20 and 21. Temperature gradients were estimated for the intervals above and below the upper Devonian in Fig. 2.10, and for the intervals above and below the unconformity surface in Fig. 2.11. Different gradients were observed for the intervals considered.

Figures 2.12 and 2.13 are temperature/depth plots and calculated thermal gradients for the area covering townships 45, 46 and 47 and ranges 19, 20 and 21. This area falls within the disturbed belt, and the plots show the geothermal gradients obtained when the slopes were calculated for different lithological intervals.

Figures 2.14 and 2.15 illustrate two further such plots for the area which includes townships 55, 56 and 57 and

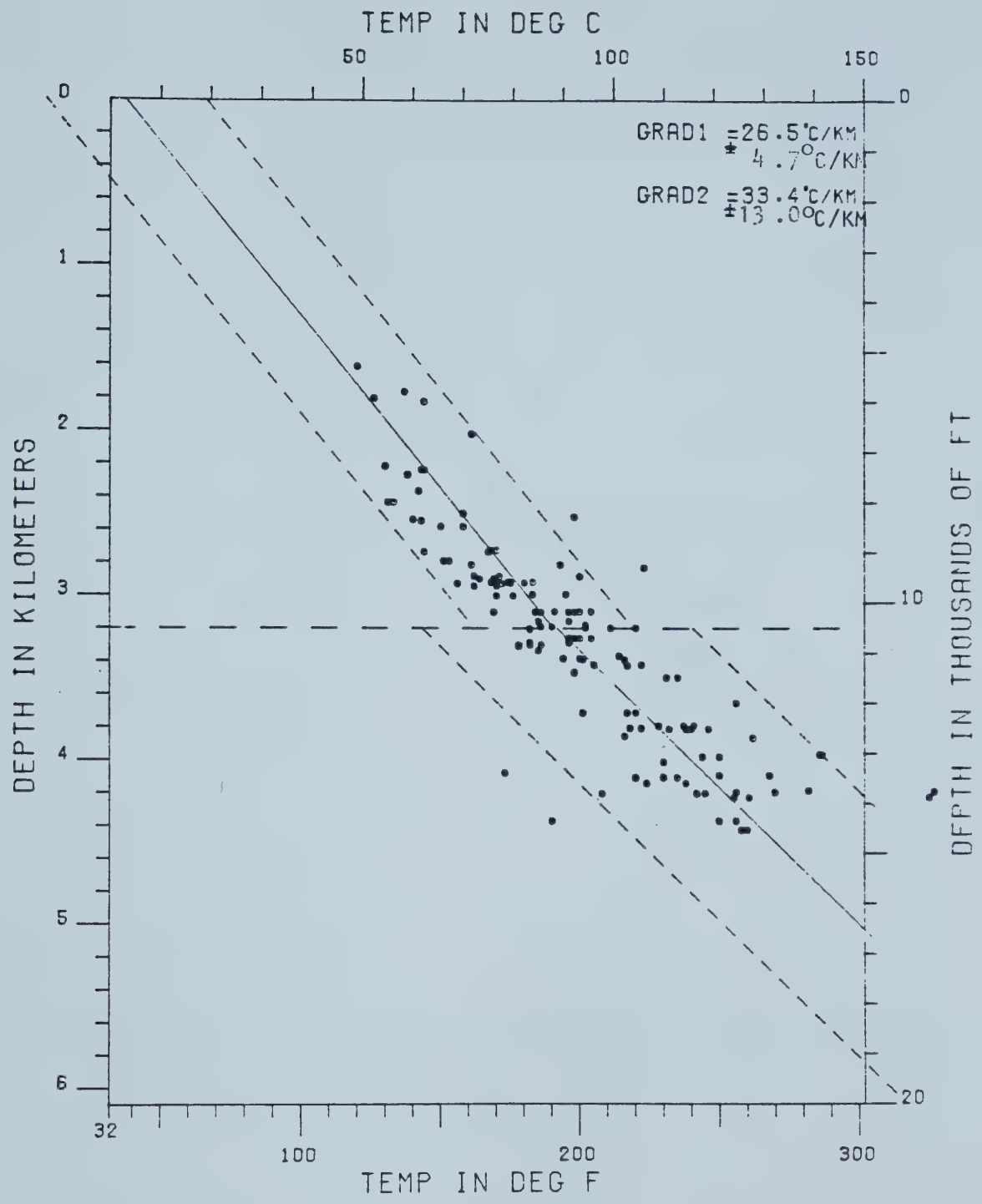


Figure 2.10 Temperature/depth plot for lithological intervals (2) and (4), separated by the upper Devonian surface at 3200m. (Townships 51, 52, 53; ranges 19, 20, 21.)

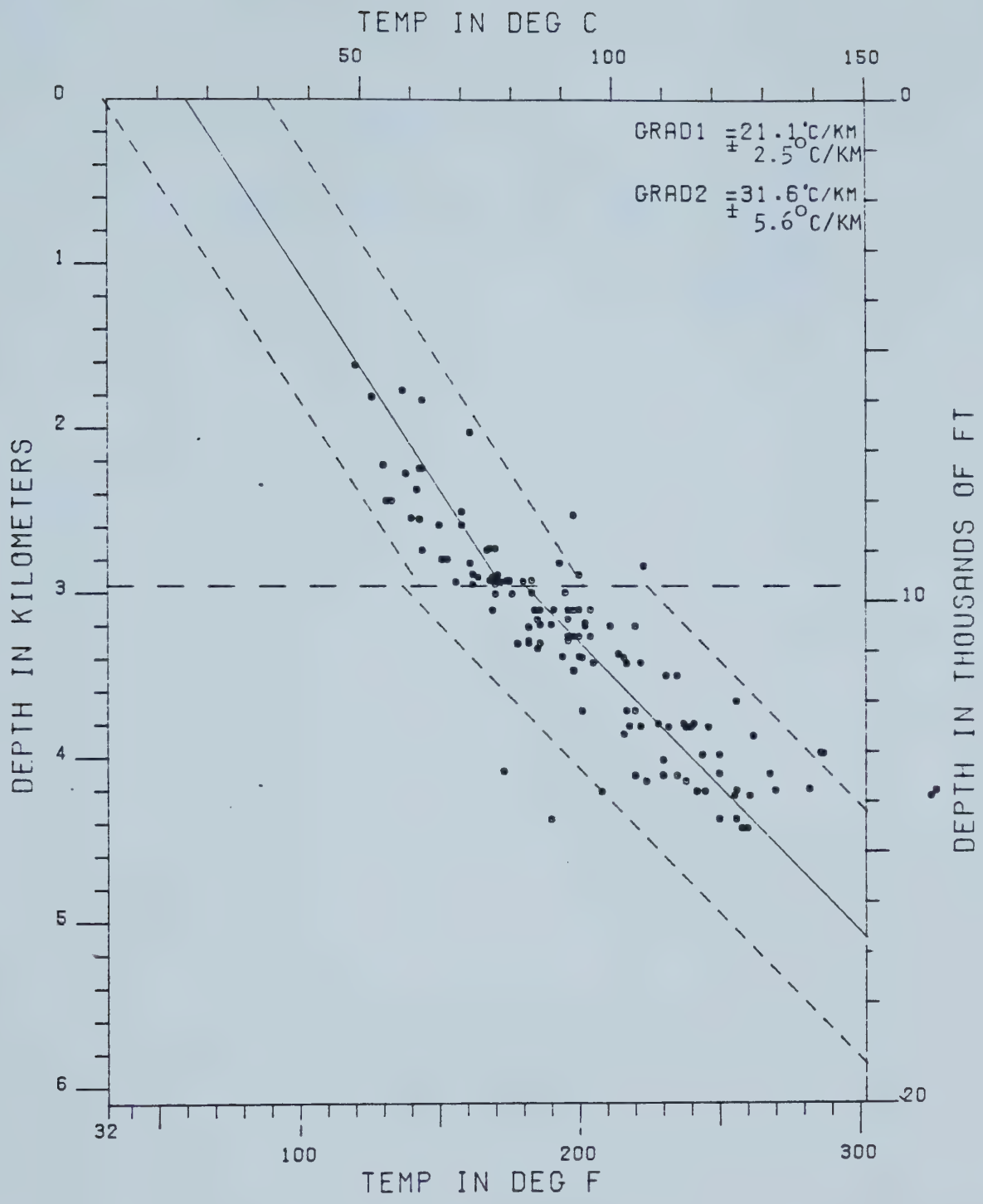


Figure 2.11 Temperature/depth plot for lithological intervals (2) and (3), separated by the unconformity surface at 2957m. (Townships 51, 52, 53; ranges 19, 20, 21.)

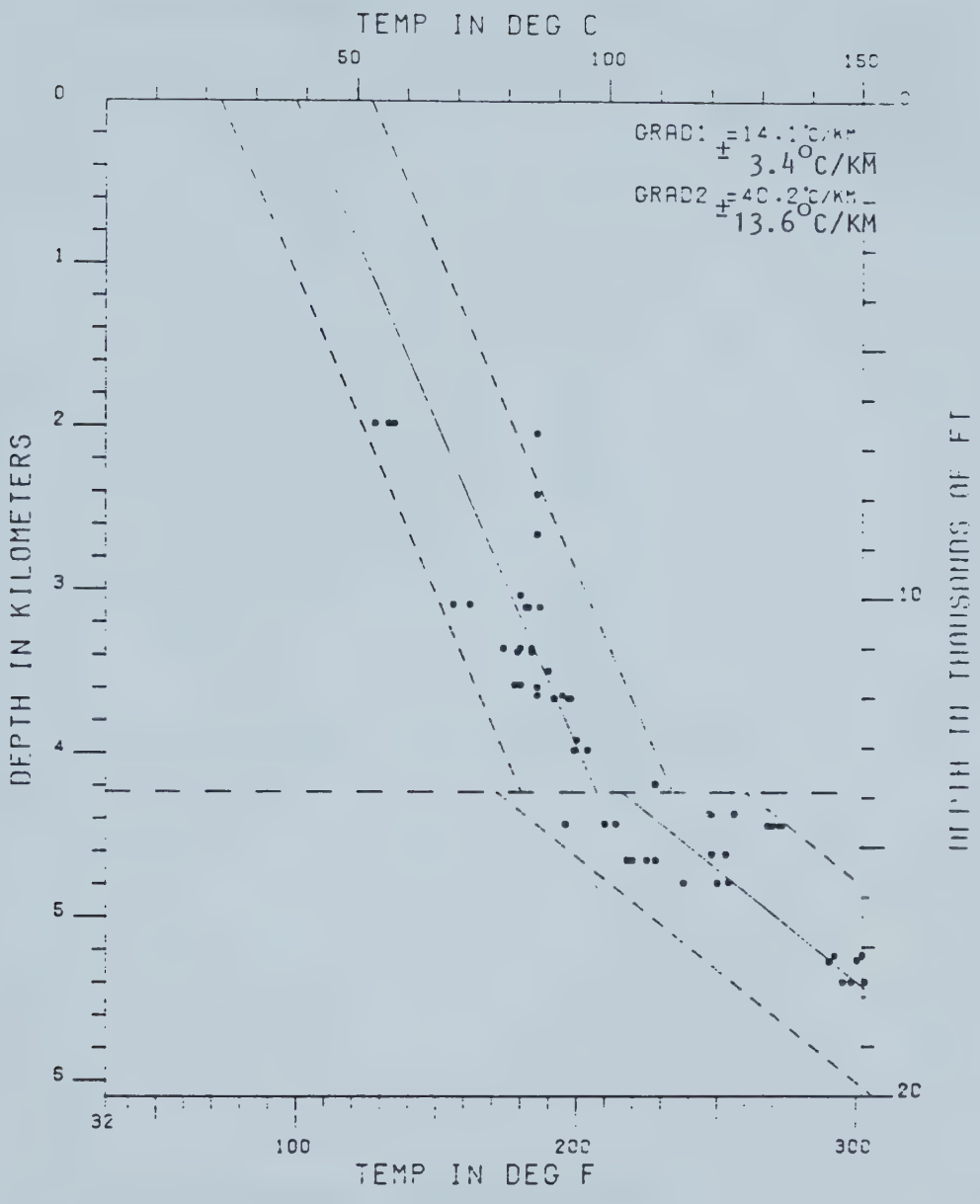


Figure 2.12 Temperature/depth plot for lithological intervals (2) and (4), separated by the upper Devonian surface at 4247m. (Townships 45,46 47; ranges 19, 20, 21.)

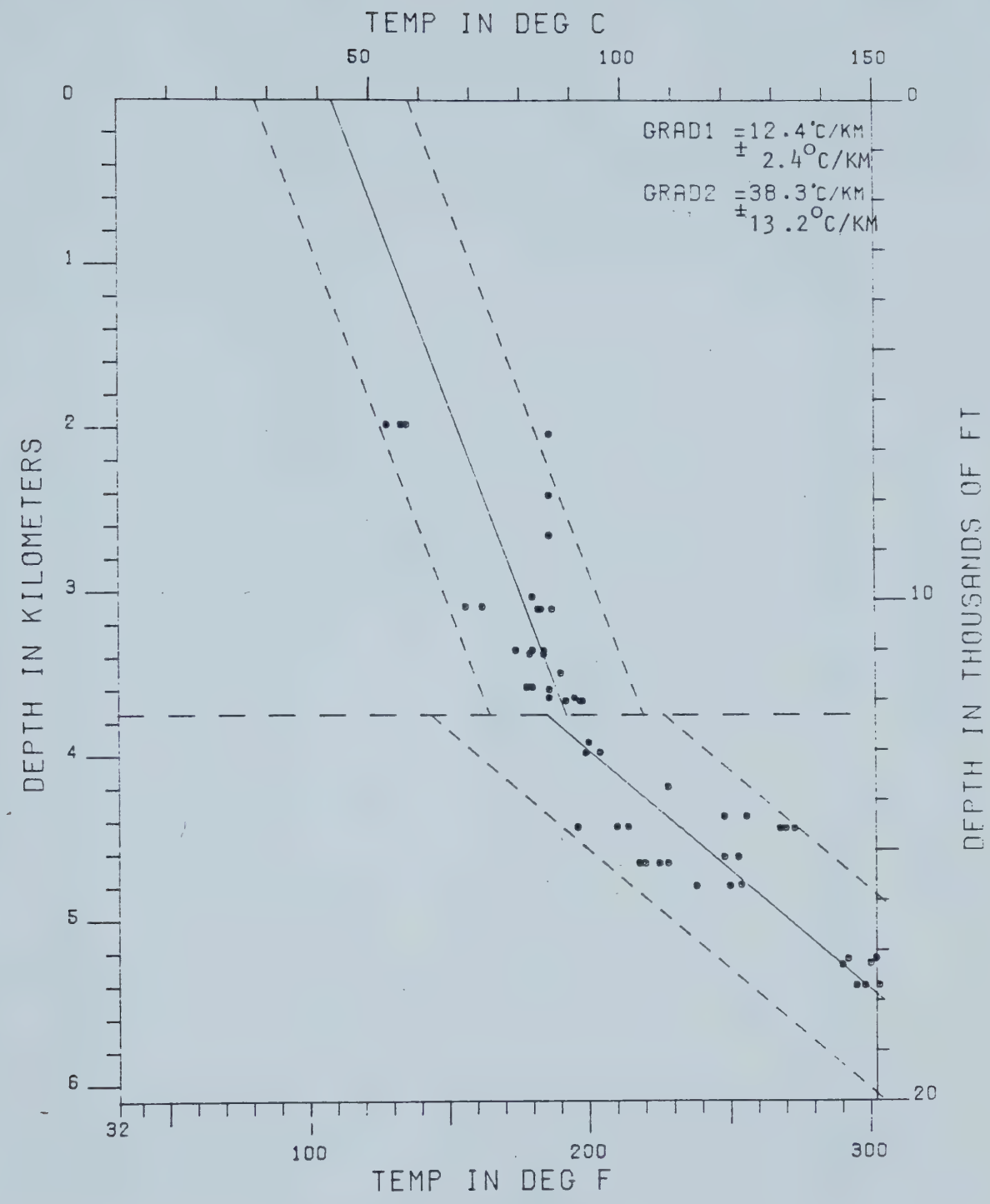


Figure 2.13 Temperature/depth plot for lithological intervals (1) and (3), separated by the unconformity surface at 3749m. (Townships 45, 46, 47; ranges 19, 20, 21.)

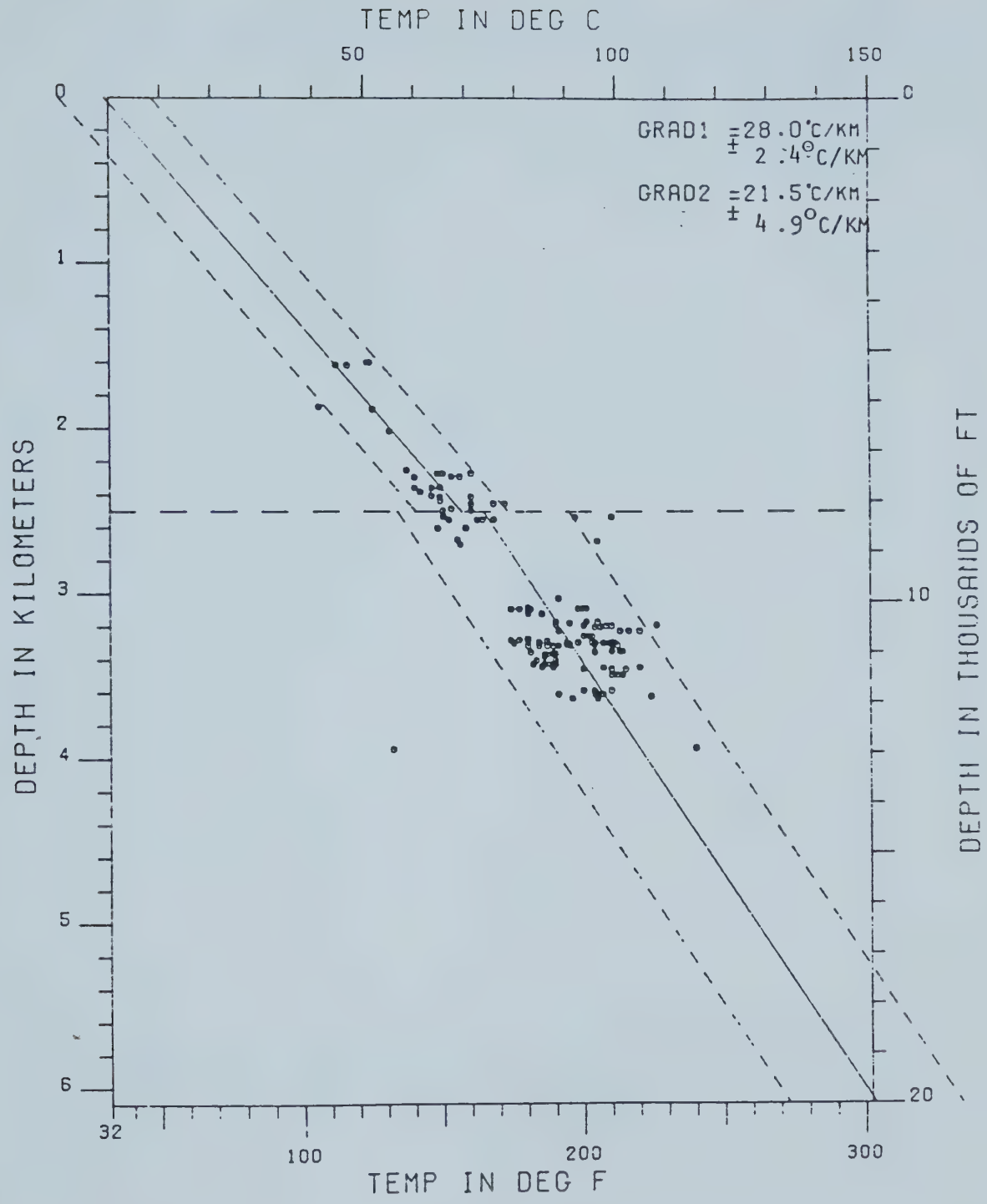


Figure 2.14 Temperature/depth plot for lithological intervals (2) and (4), separated by the upper Devonian surface at 2500m. (Townships 55, 56, 57; ranges 15, 16, 17.)

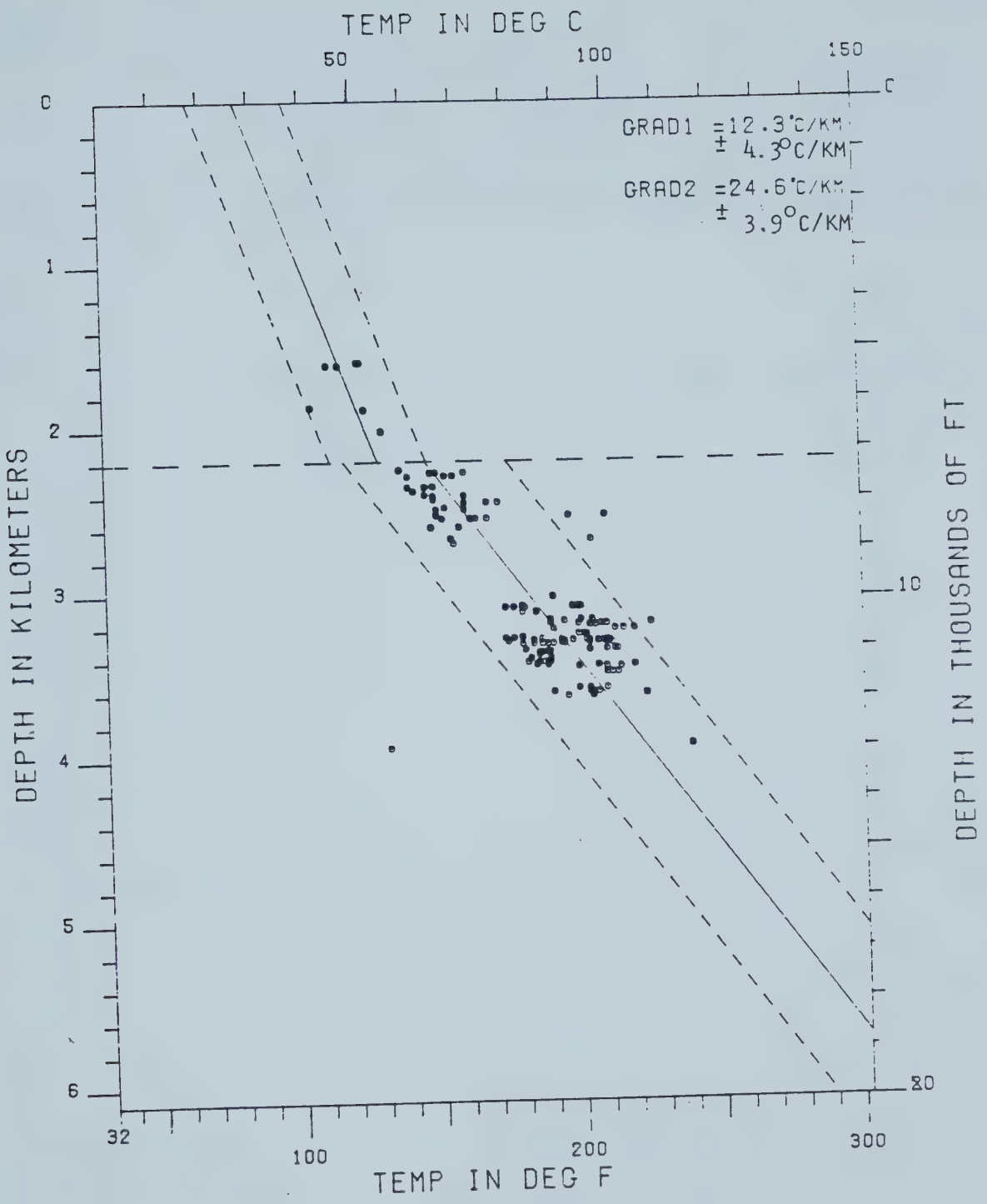


Figure 2.15 Temperature/depth plot for lithological intervals (1) and (2) separated by the unconformity surface at 2200m. (Townships 55, 56, 57; ranges 15, 16, 17.)

ranges 15, 16 and 17.

The calculated gradients were used to plot geothermal contour maps for the four selected intervals. These gradient maps are given in Figs. 2.16-2.19. The contour interval is (2°C/km).

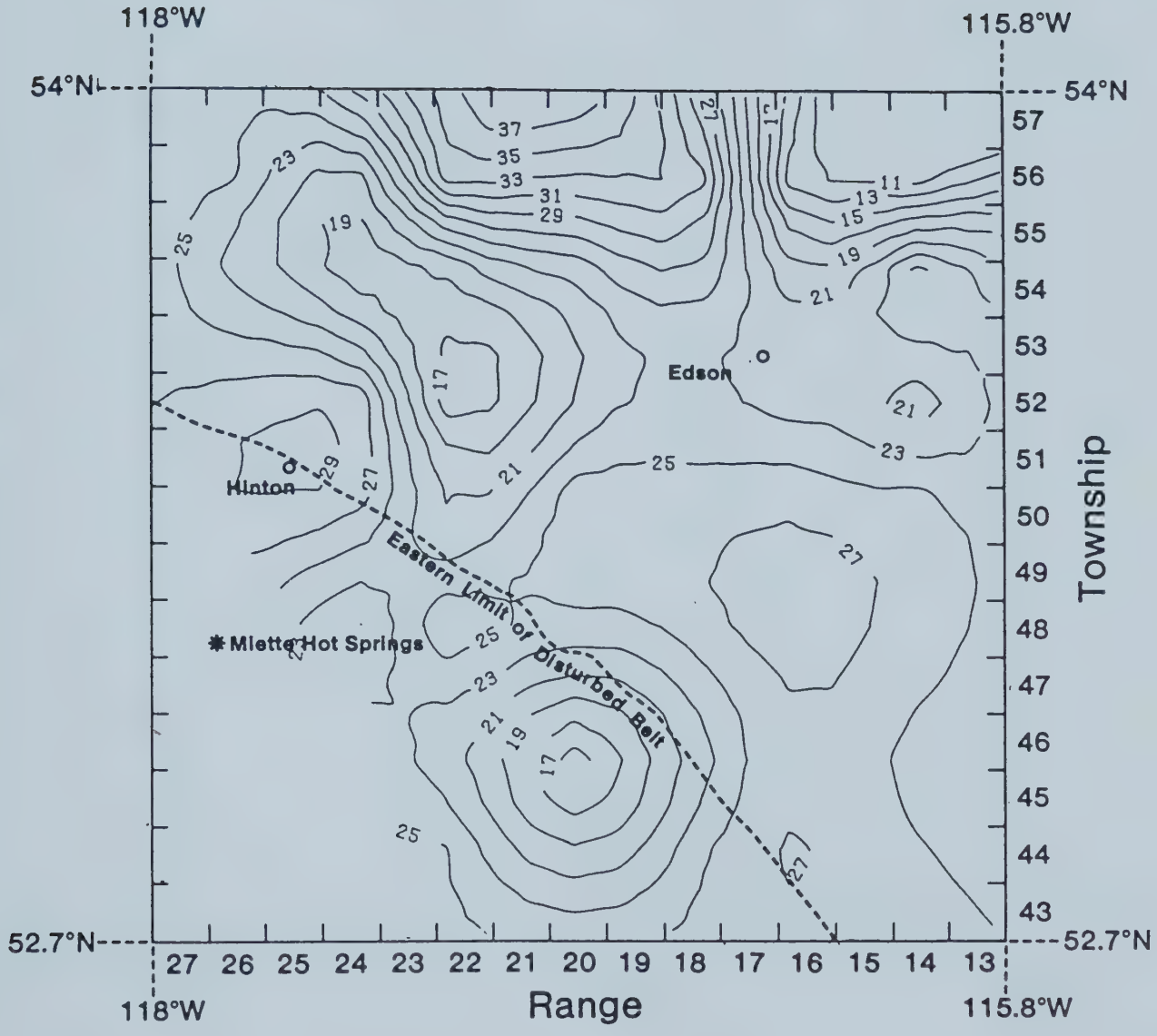


Figure 2.16 Geothermal gradient contour map for the lithological interval (1): top of the Colorado formation to the unconformity surface.

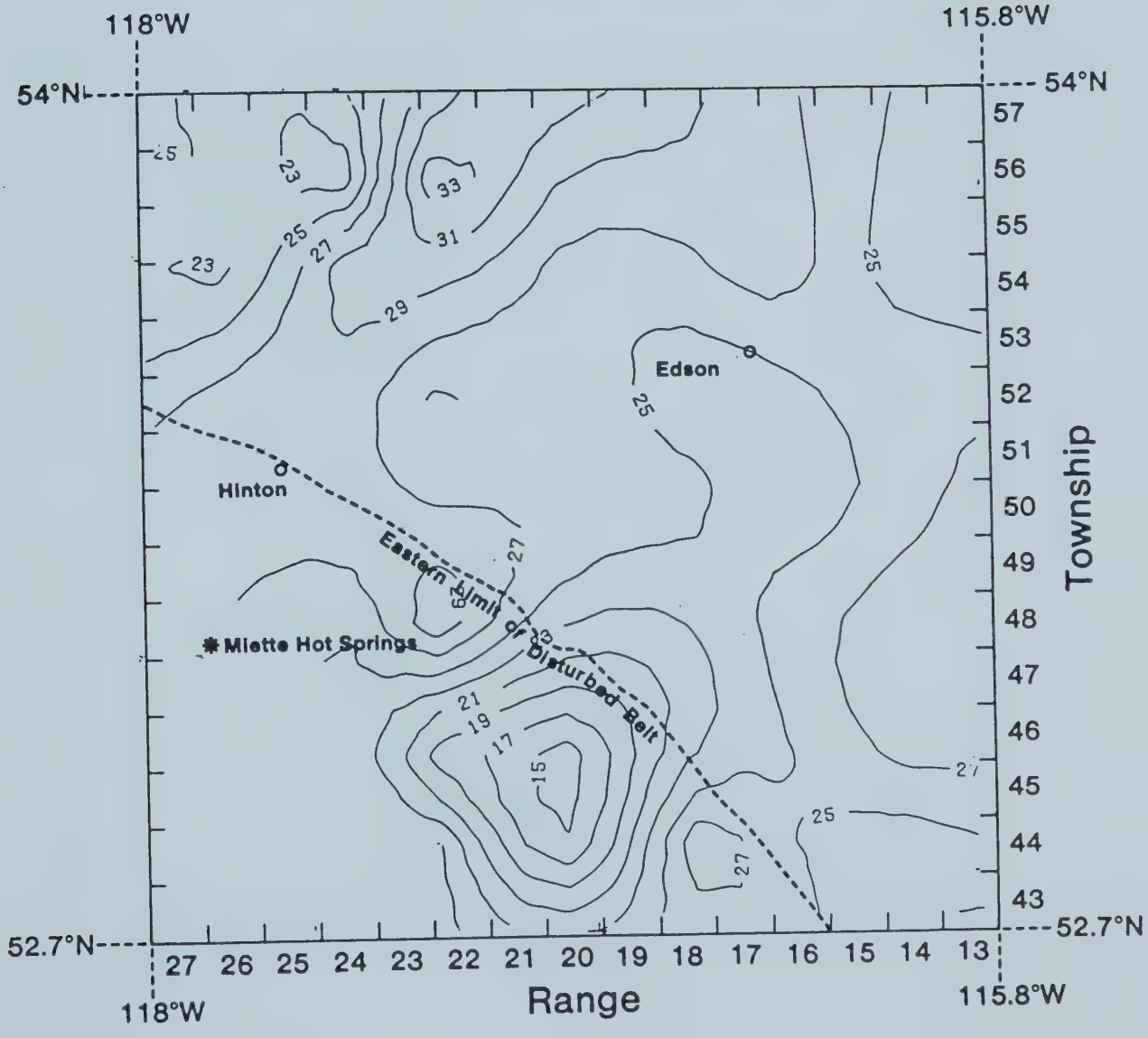


Figure 2.17 Geothermal gradient contour map for the lithological interval (2): top of the Colorado formation to the upper Devonian surface.

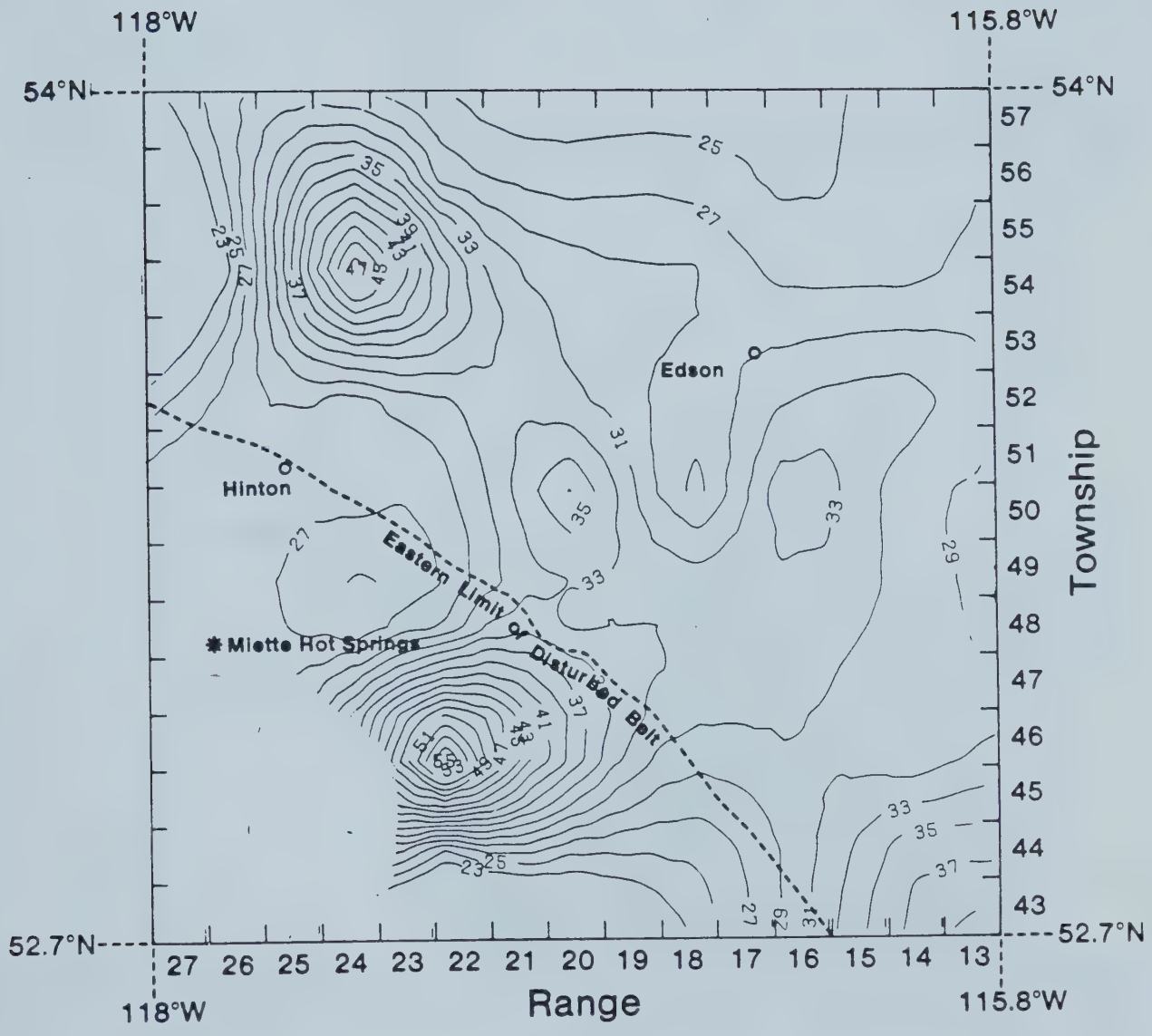


Figure 2.18 Geothermal gradient contour map for the lithological interval (3): the unconformity surface to the Precambrian.

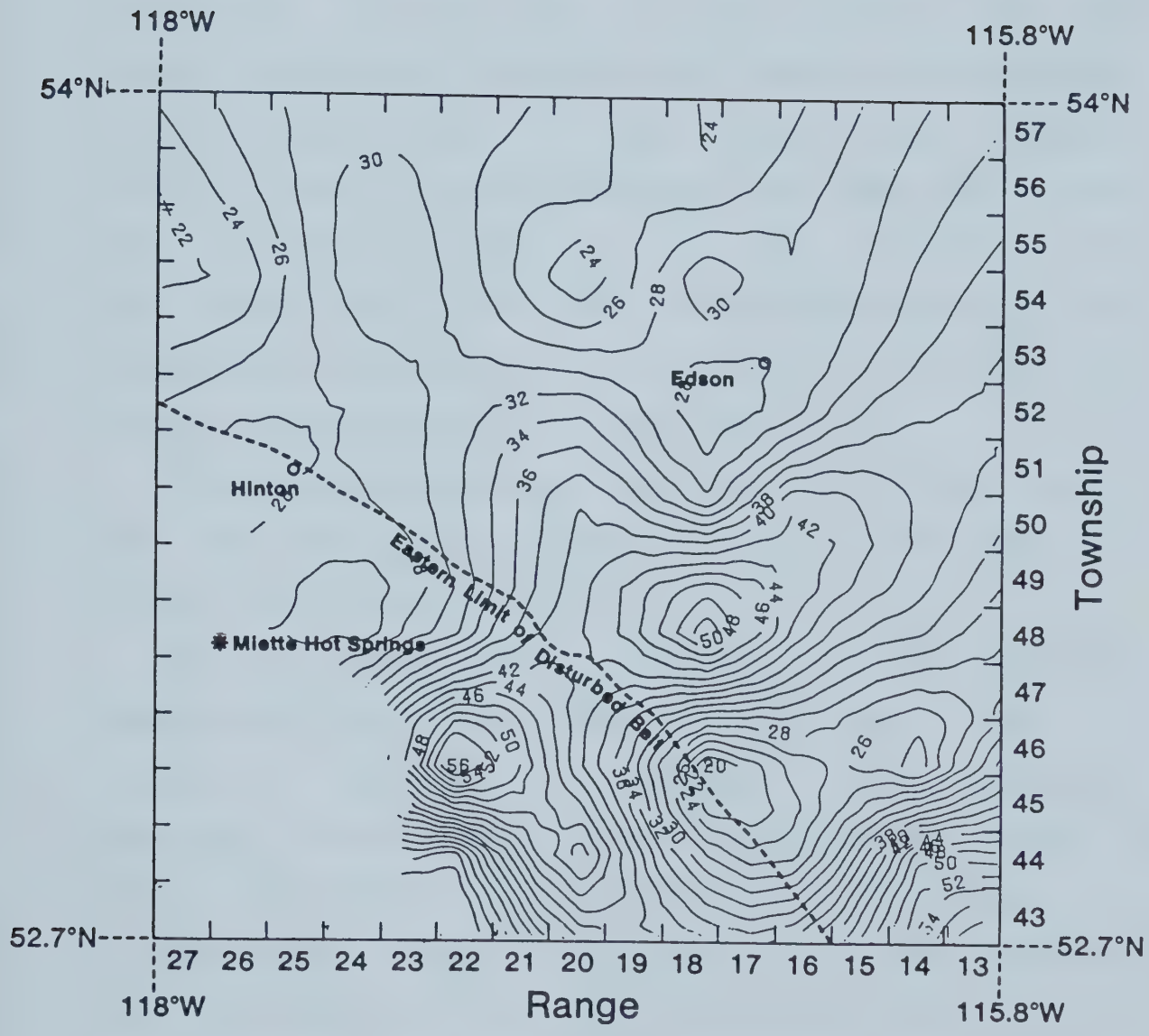


Figure 2.19 Geothermal gradient contour map for the lithological interval (4): the upper Devonian surface to the Precambrian.

### 2.1.3 Detailed Temperature Analysis

Detailed temperature analysis was carried out in order to investigate the subsurface temperature distribution. Seven levels were considered starting from 2000m to a maximum depth of 5000m in steps of 500m. To obtain formation temperatures at each depth and for each of the 3x3 township/range areas, the geothermal gradient plots obtained in 2.1.2 were used. For each depth, the formation temperature which occurred exactly at that depth was chosen. Where no actual measured temperature value existed at the exact depth for a particular 3x3 township/range area, the temperature as defined by the linear least squares fit line of the temperature/depth plot was taken.

These temperature values were used to construct contour maps of the seven levels considered. The maps are illustrated in Figs. 2.20 to 2.26.

It is informative to determine how the subsurface temperatures vary across each of the seven levels. By correlating changes in temperature with geological formations, deductions can be made regarding the nature of the heat flow pattern and its relationship to geology.

Four profiles were drawn across the seven surfaces. Three of these profiles are in the SW to NE direction, and are labelled AA, BB, and FF. (These profiles are shown in Fig. 2.20). The profile labelled BB cuts diagonally across the entire area while AA and FF are about 50 km from BB toward the northwest and the southeast directions

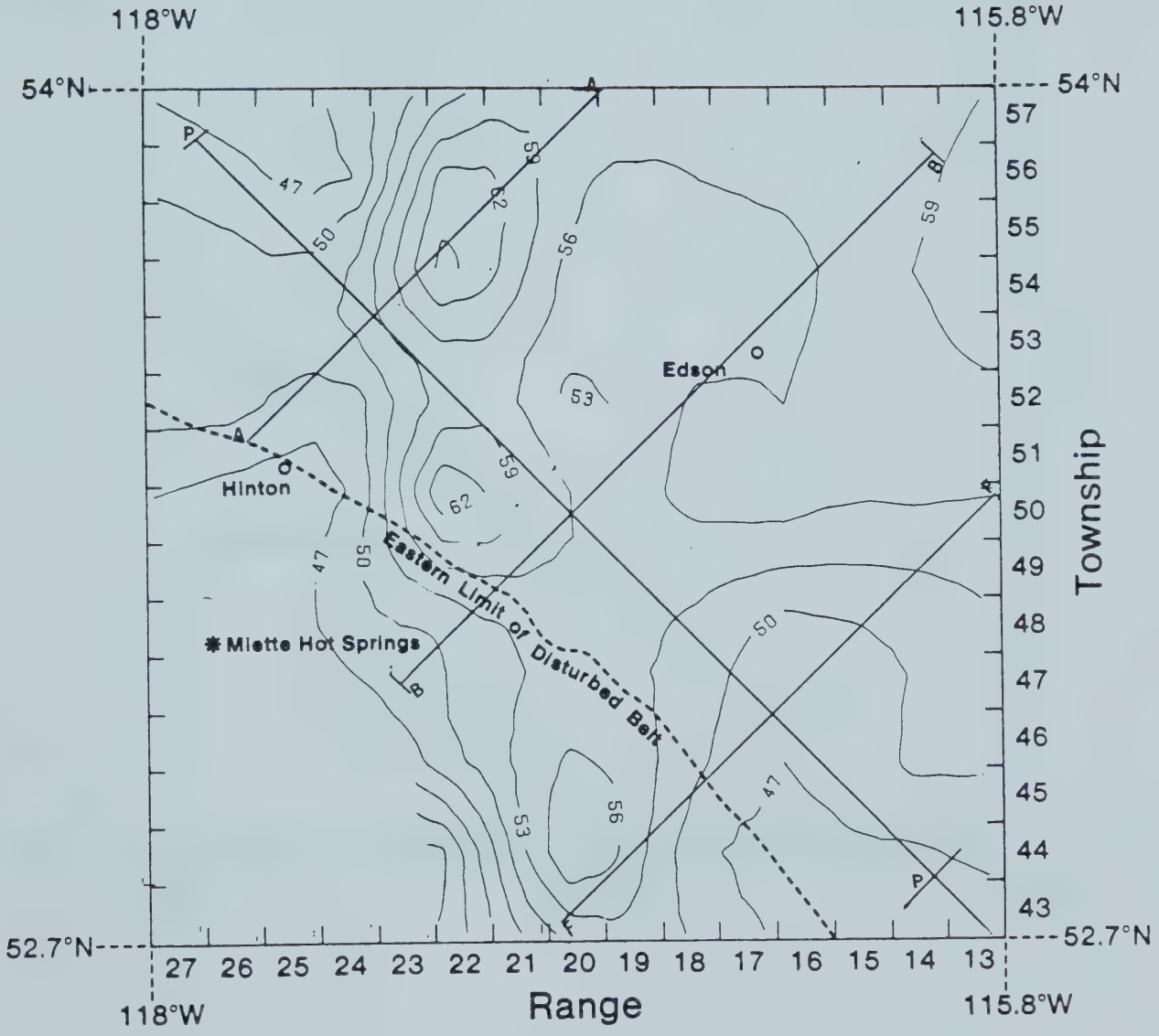


Figure 2.20 Contour map of the subsurface temperature distribution at 2000m.

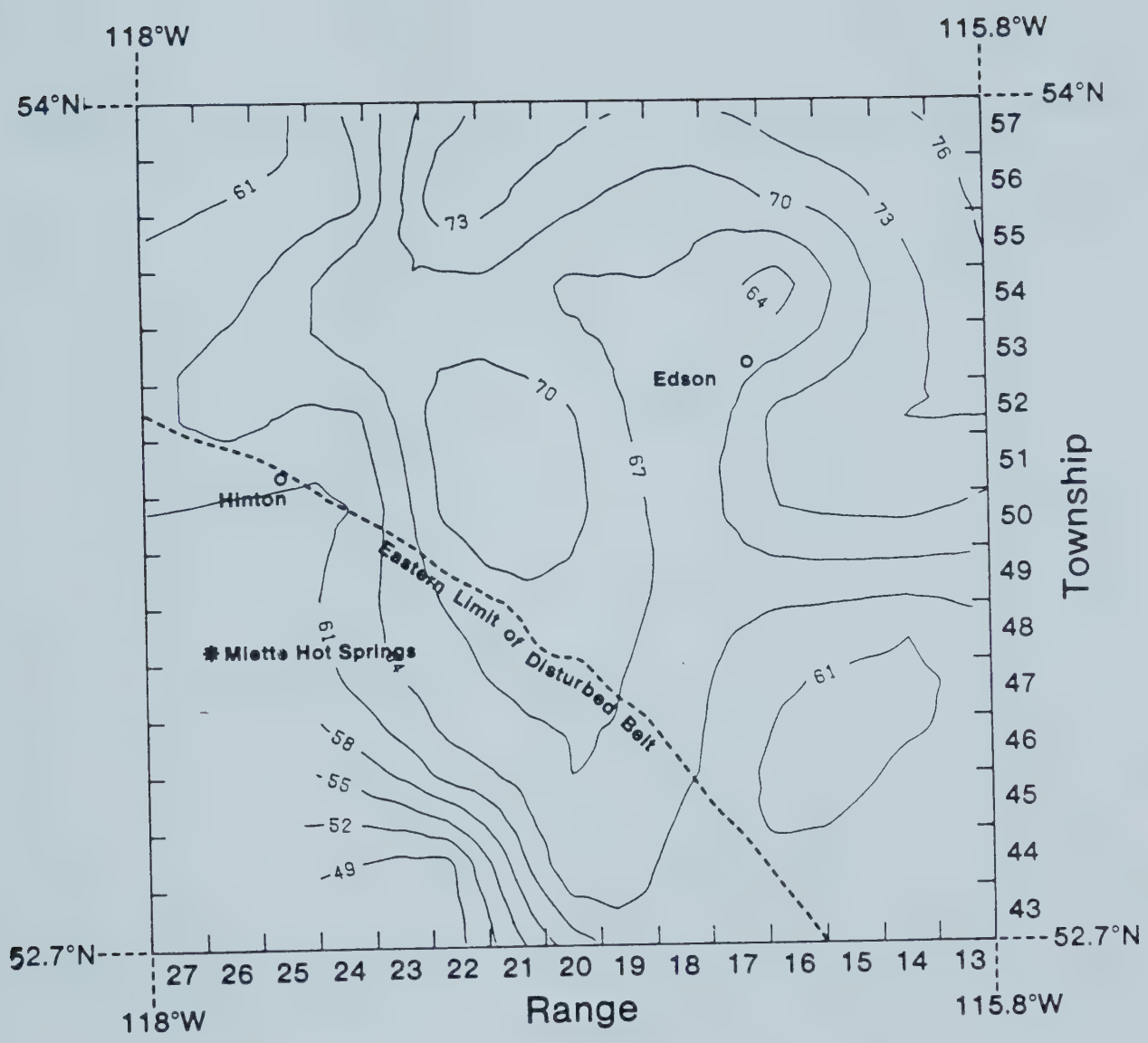


Figure 2.21 Contour map of the subsurface temperature distribution at 2500m.

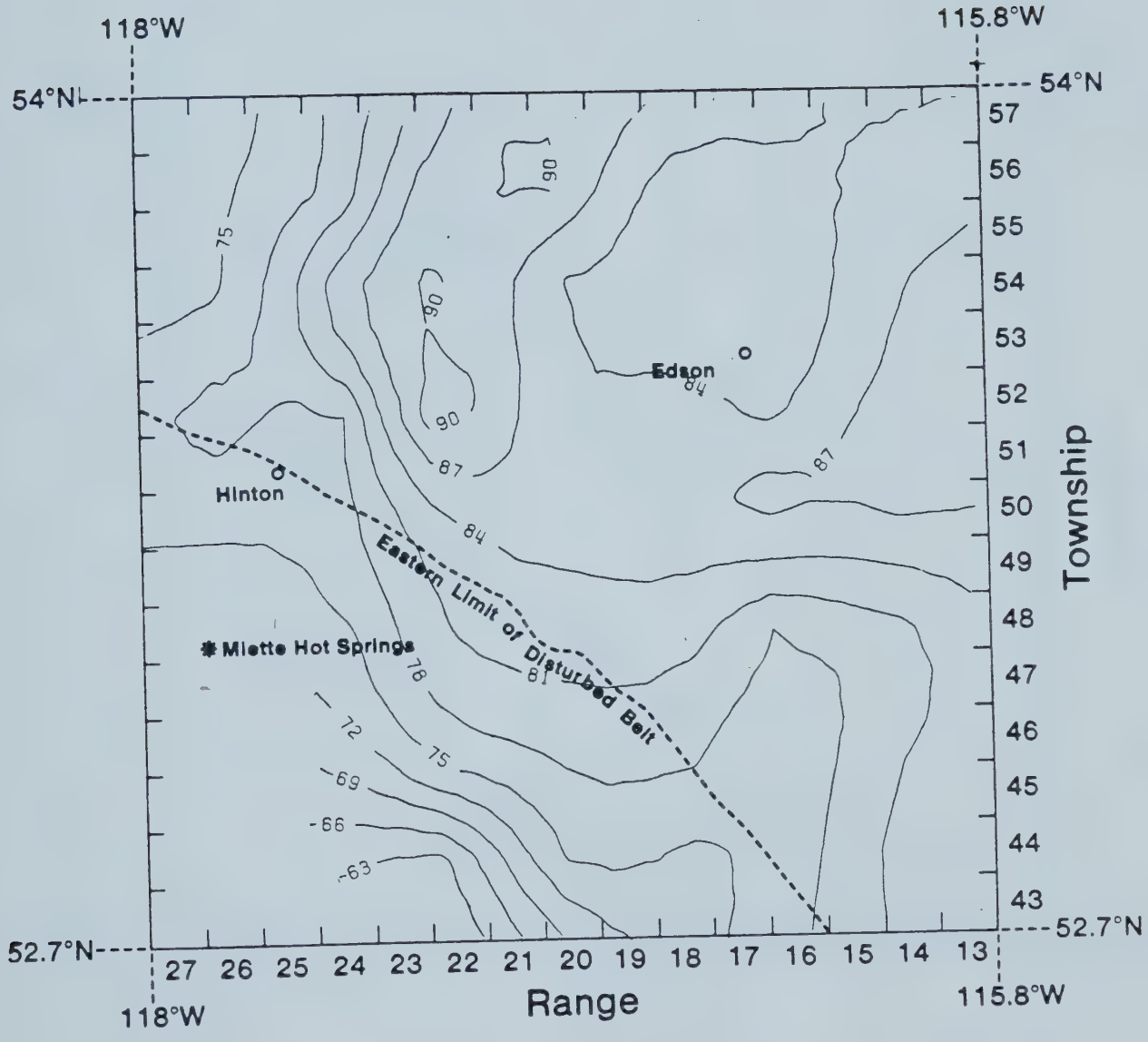


Figure 2.22 Contour map of the subsurface temperature distribution at 3000m.

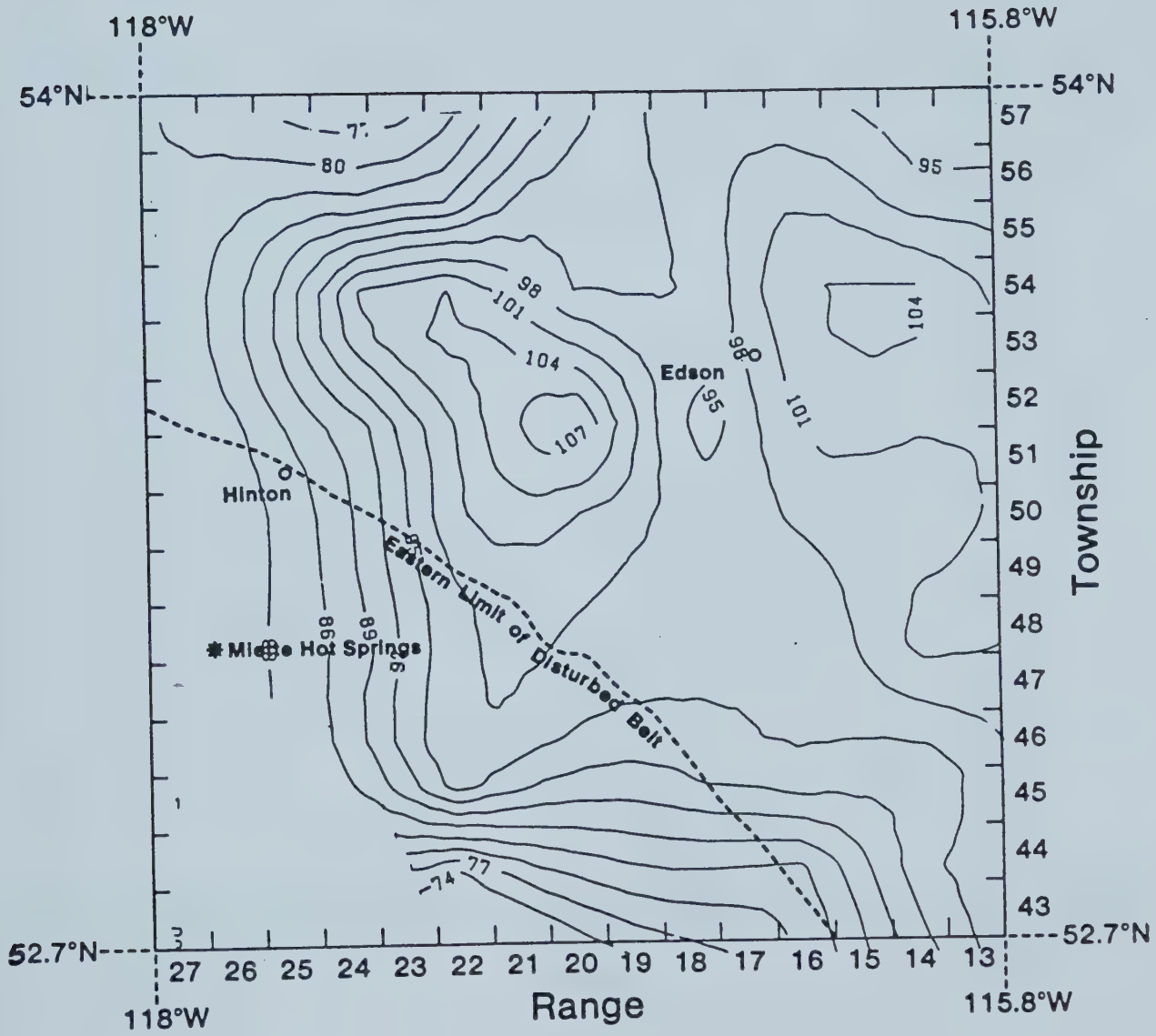


Figure 2.23 Contour map of the subsurface temperature distribution at 3500m.

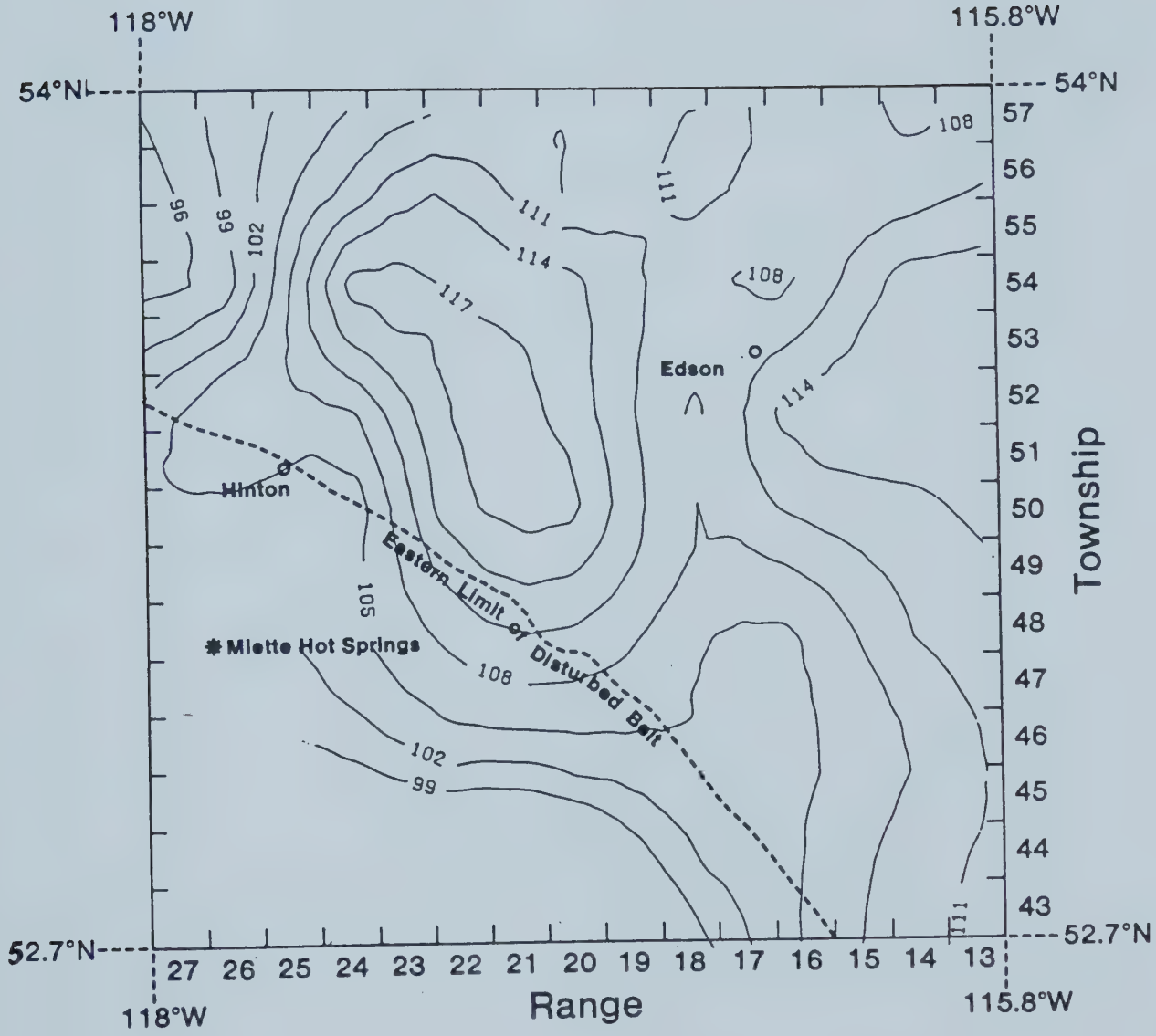


Figure 2.24 Contour map of the subsurface temperature distribution at 4000m.

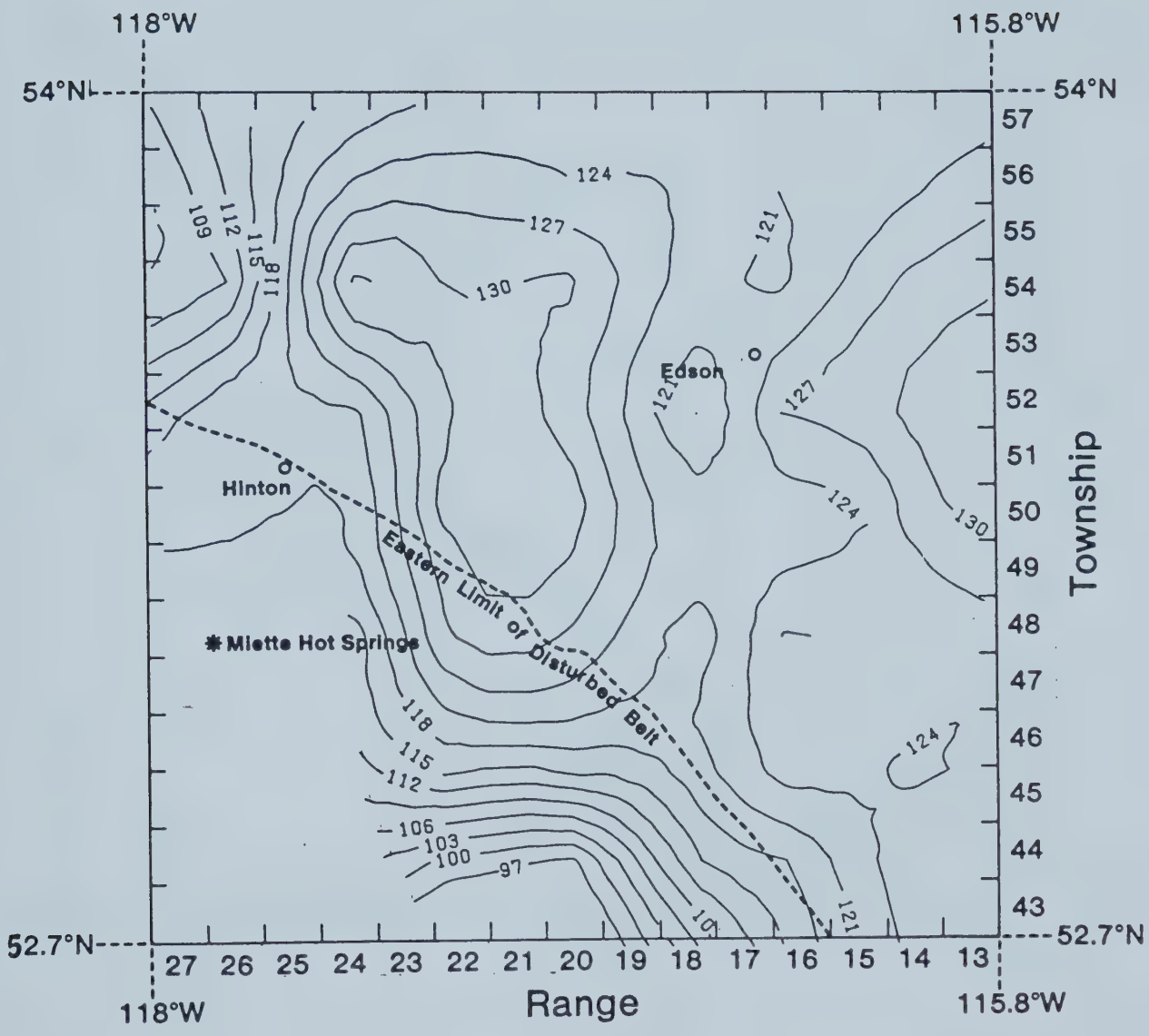


Figure 2.25 Contour map of the subsurface temperature distribution at 4500m.

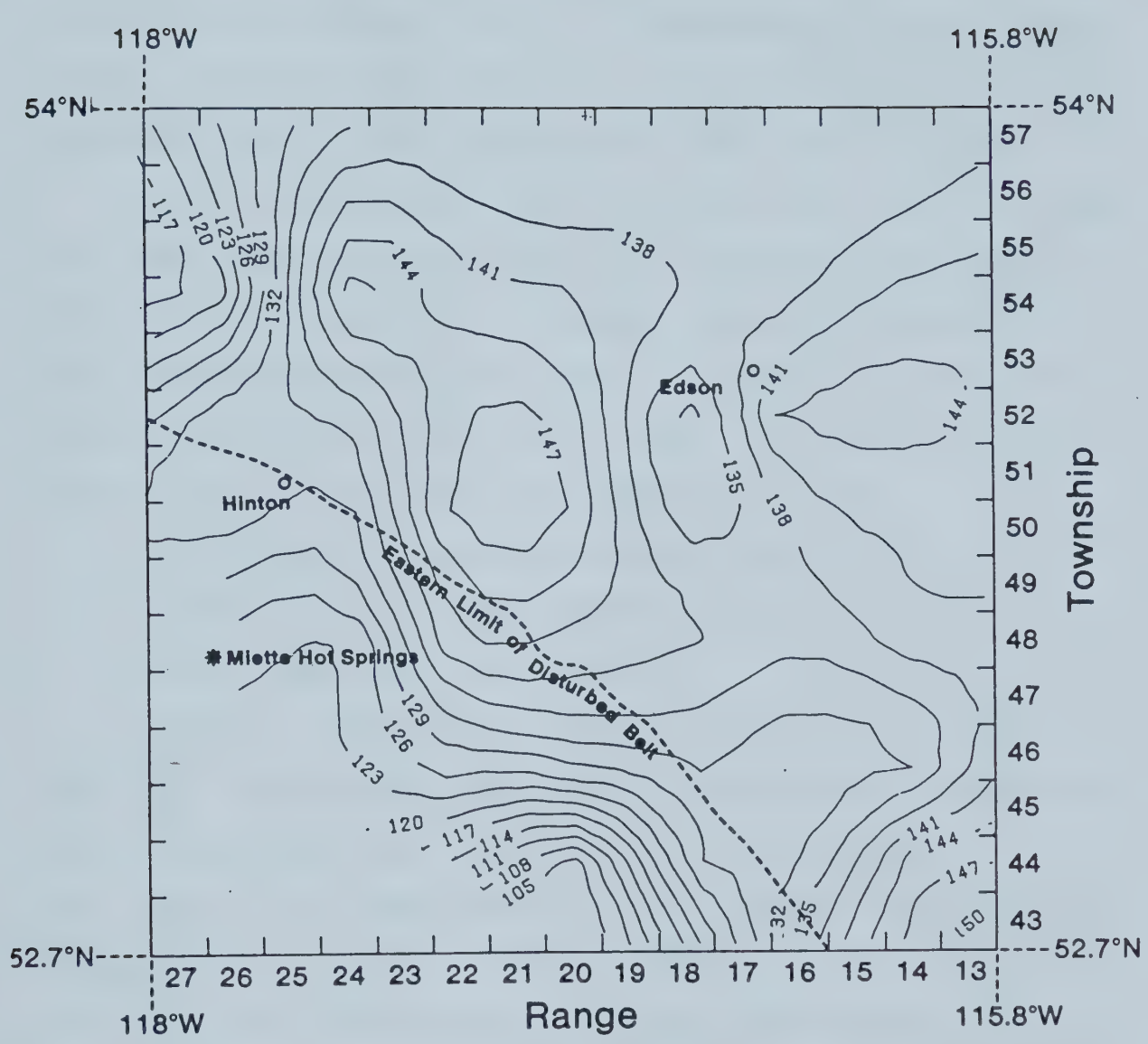


Figure 2.26 Contour map of the subsurface temperature distribution at 5000m.

respectively. The limits of the profiles were chosen so that only areas where data exist were included.

The profile labelled PP cuts diagonally across the area in the NW-SE direction, and it is perpendicular to the other three profiles. The location of the eastern limit of the disturbed belt is also indicated on Figs. 2.20 to 2.26.

Along each of the profiles, and for each of the surfaces, temperature and formation information were used to construct contour plots on vertical planes corresponding to each profile. Figures 2.27, 2.29, 2.31 and 2.33 show these contour maps and Fig. 2.28, 2.30, 2.32 and 2.34 show profiles of the three surfaces mapped in 2.1.2:

(A) The top of the Colorado formation.

(B) The surface of the Unconformity.

(C) The upper Devonian surface.

Since the temperatures used here are not corrected in any way, an attempt was made to determine the expected error. The Horner-type correction (Fertl & Wichmann, 1977) was applied to temperatures for which there was sufficient information. An example of the temperature stabilization, and graphical method used to find the equilibrium formation temperatures, is shown in Fig. 2.35. Figure 2.35a gives BHT versus time from when circulation ceased to the time at which the temperature measurement was made. Figure 2.35b gives temperature versus $\Delta T/(\Delta T+T)$ where T is the circulation time and $\Delta T$ is the time from when circulation stopped until the particular measurement was made. The

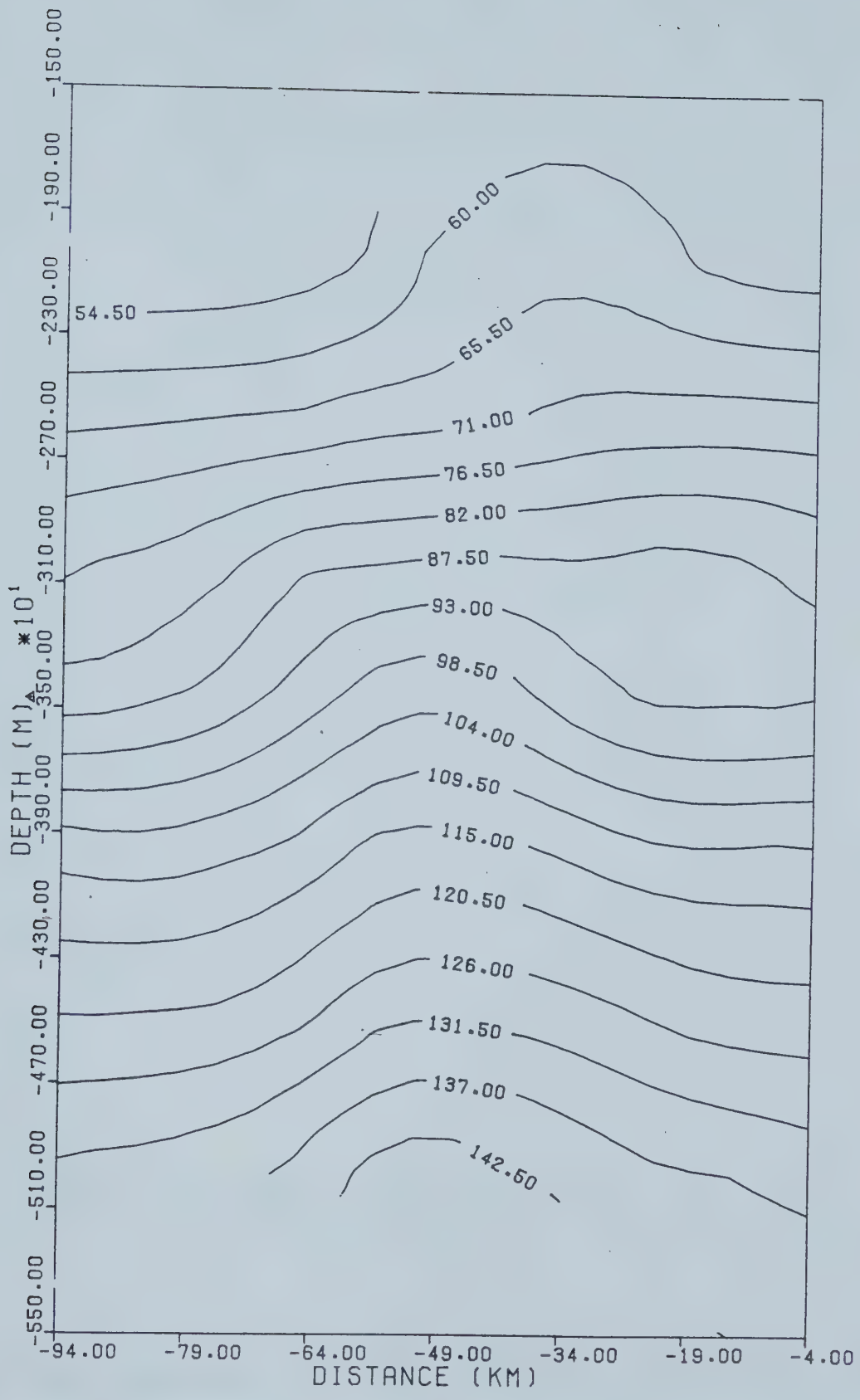


Figure 2.27 Temperature contour map in the vertical plane along profile (AA). Temperature in degrees centigrade.

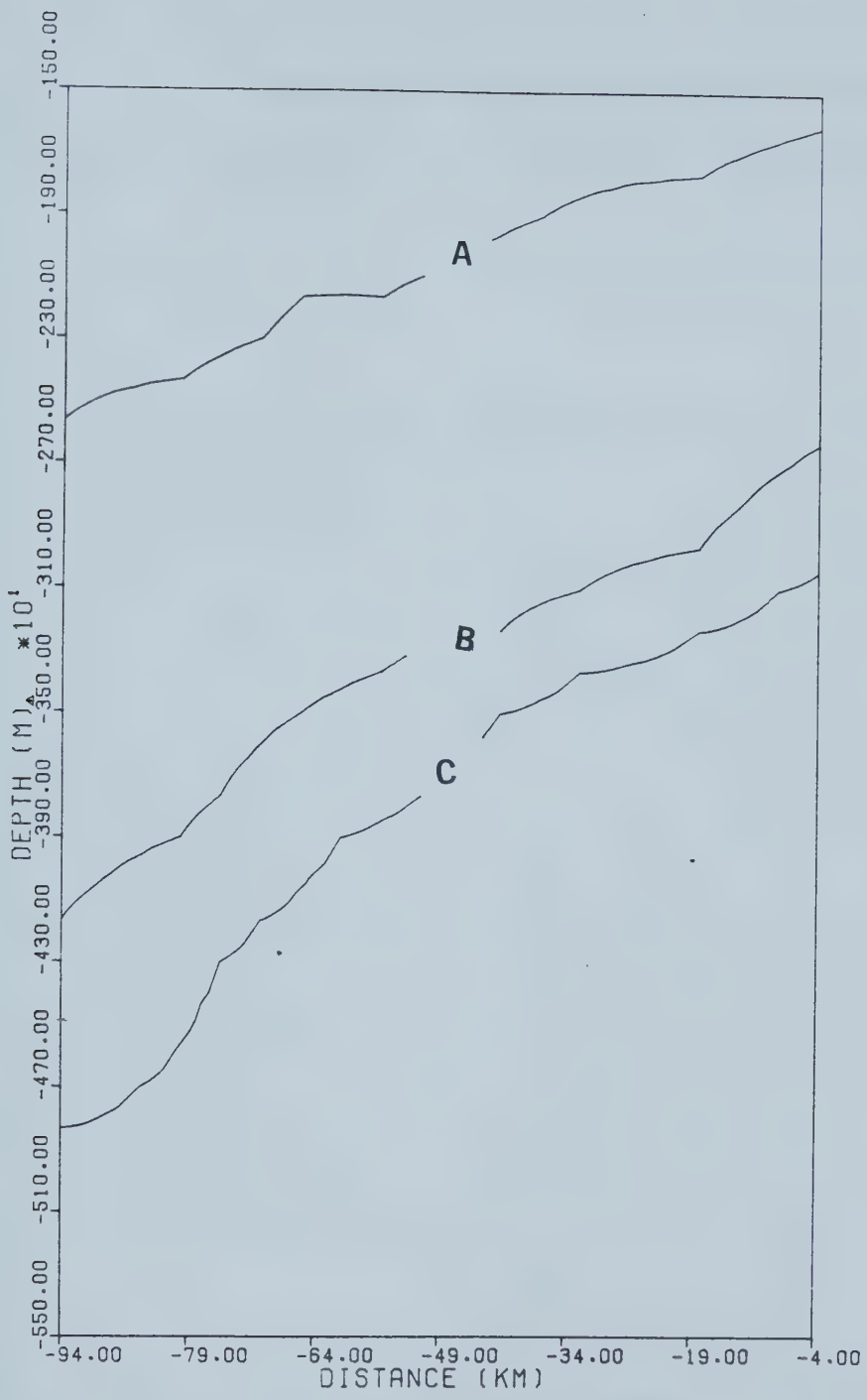


Figure 2.28 Topography of the surfaces (A) top of the Colorado (B) unconformity surface (C) upper Devonian surface along profile (AA).

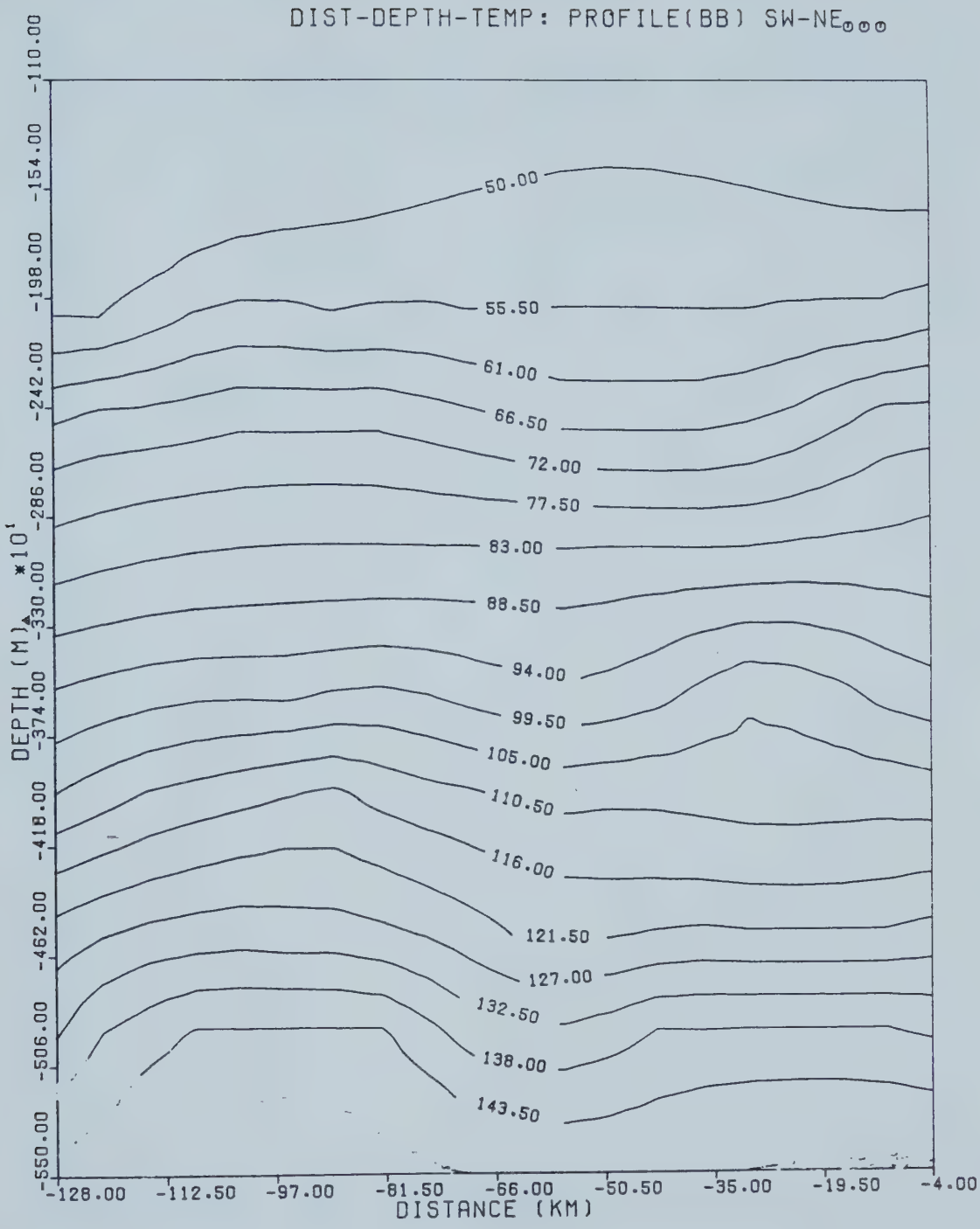


Figure 2.29 Temperature contour map in the vertical plane along profile (BB). Temperature in degrees centigrade.

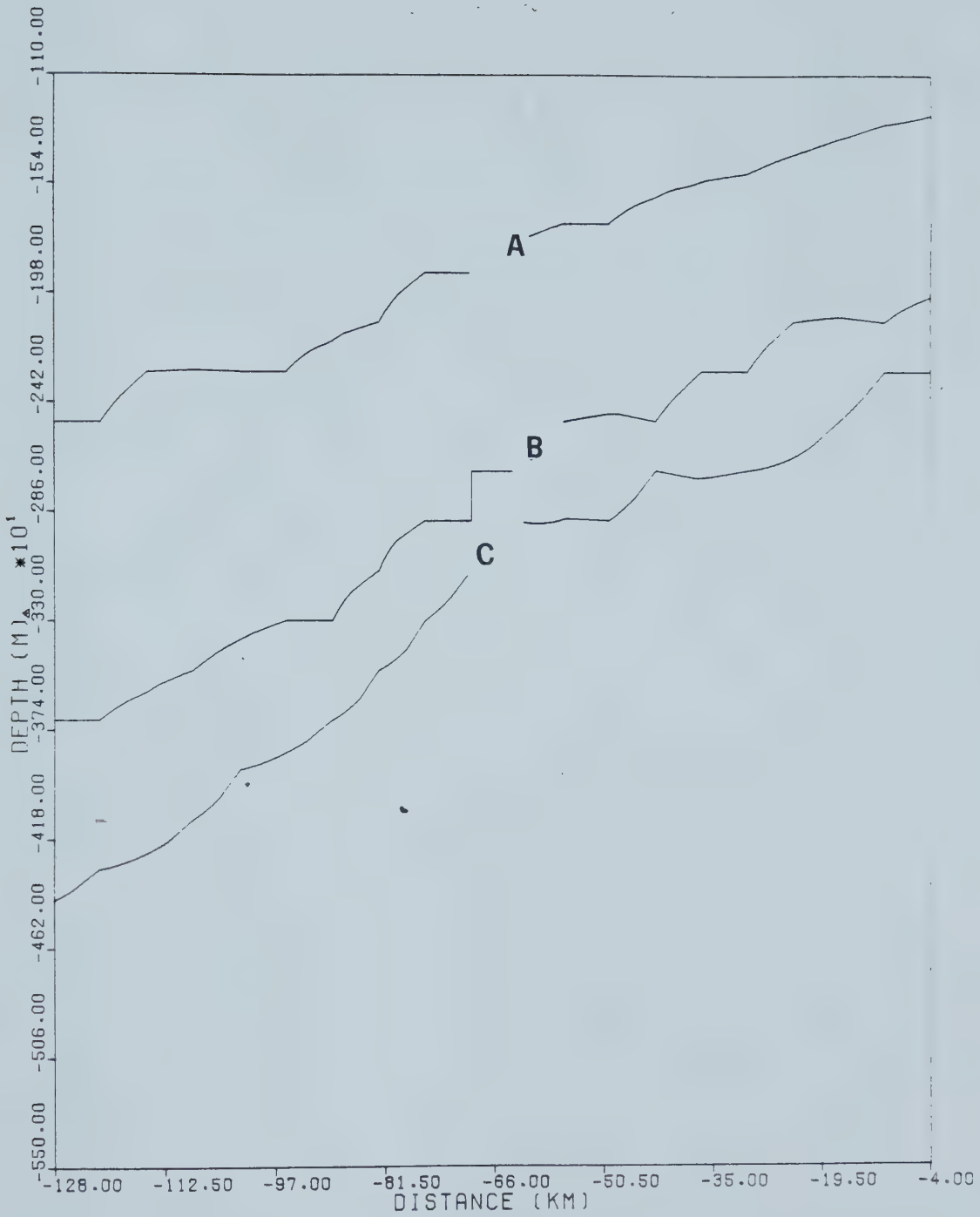


Figure 2.30 Topography of the surfaces (A) top of the Colorado (B) unconformity surface (C) upper Devonian surface along profile (BB).

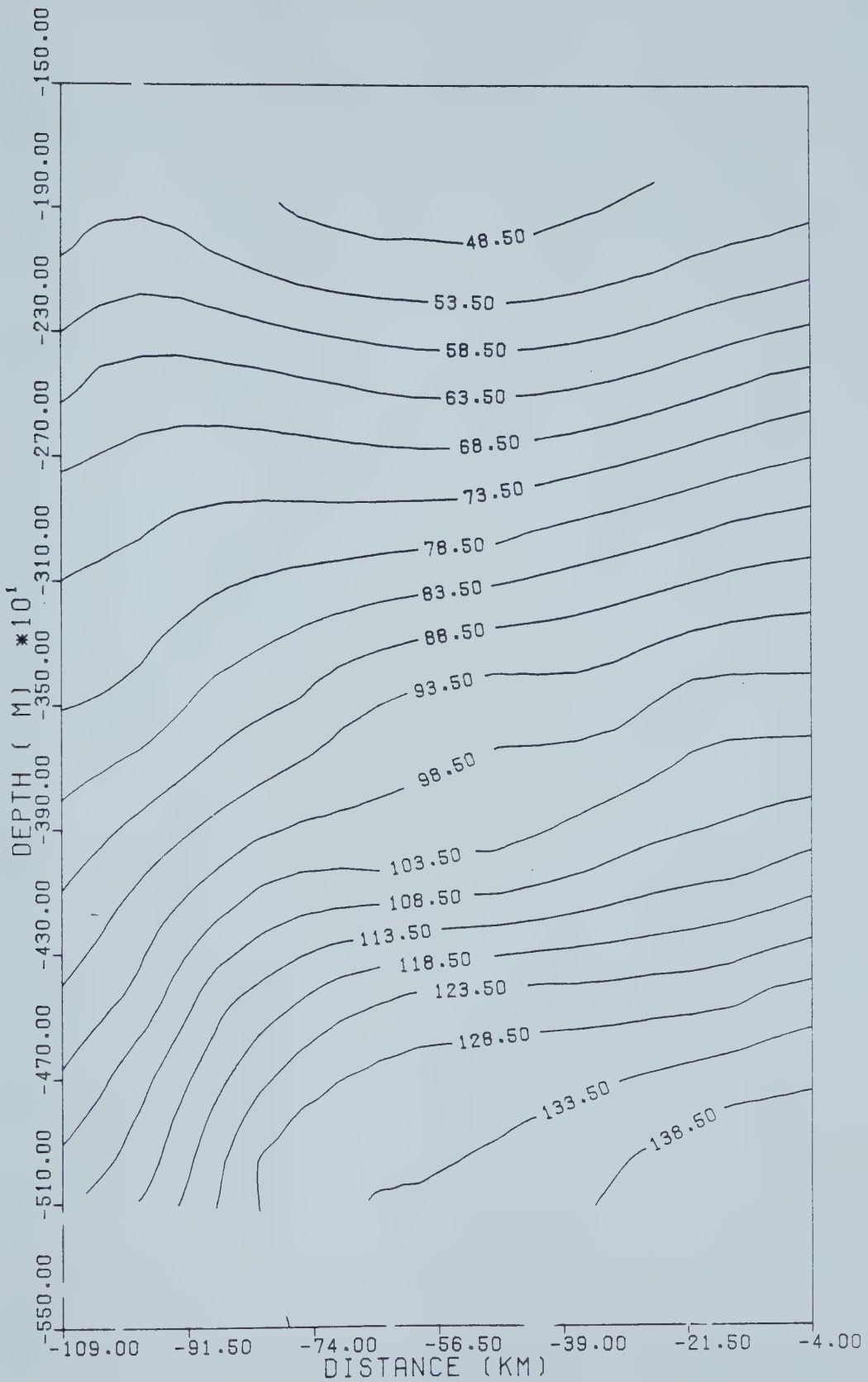


Figure 2.31 Temperature contour map in the vertical plane along profile (FF). Temperature in degrees centigrade.

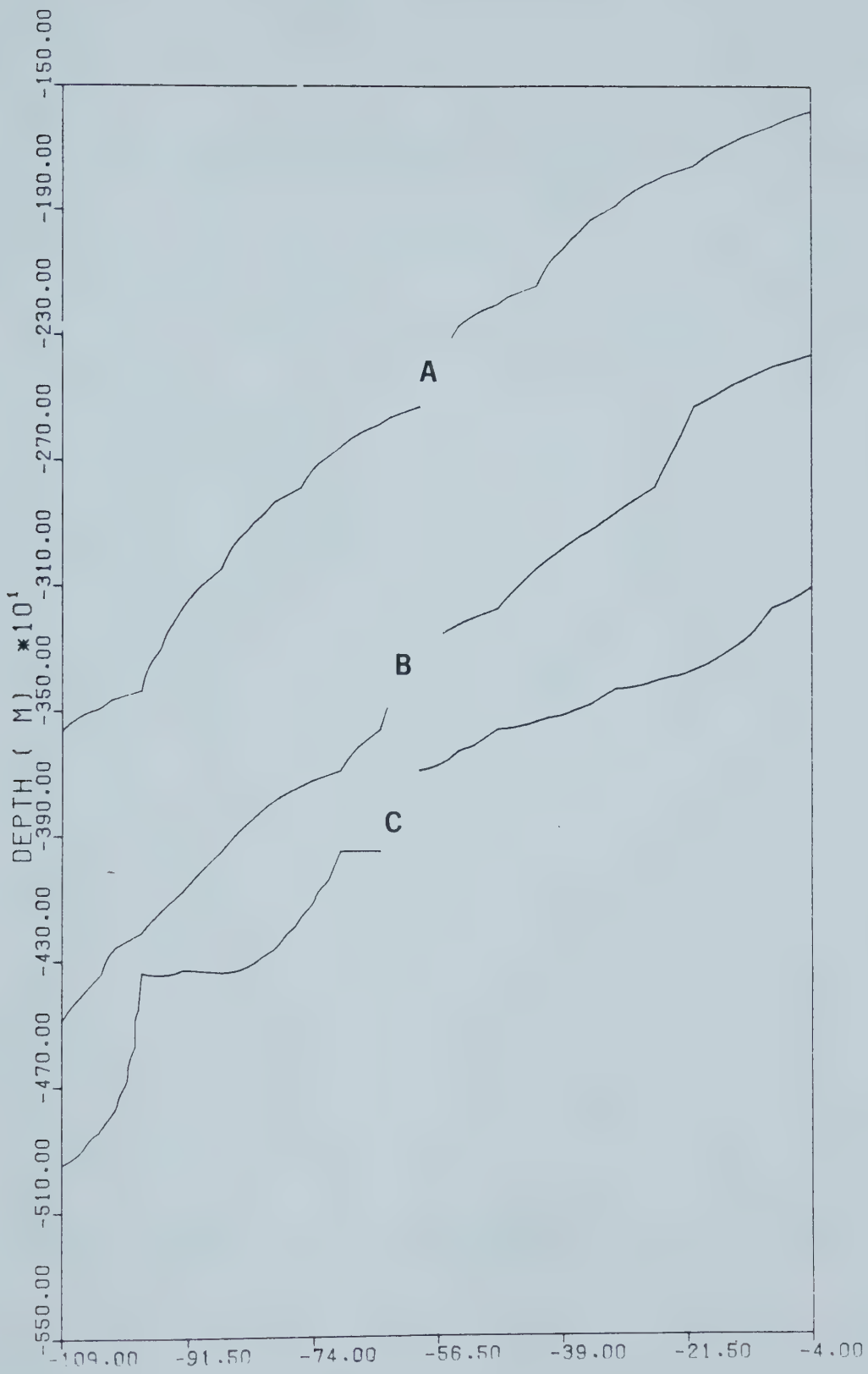


Figure 2.32 Topography of the surfaces (A) top of the Colorado (B) unconformity surface (C) upper Devonian surface along profile (FF).

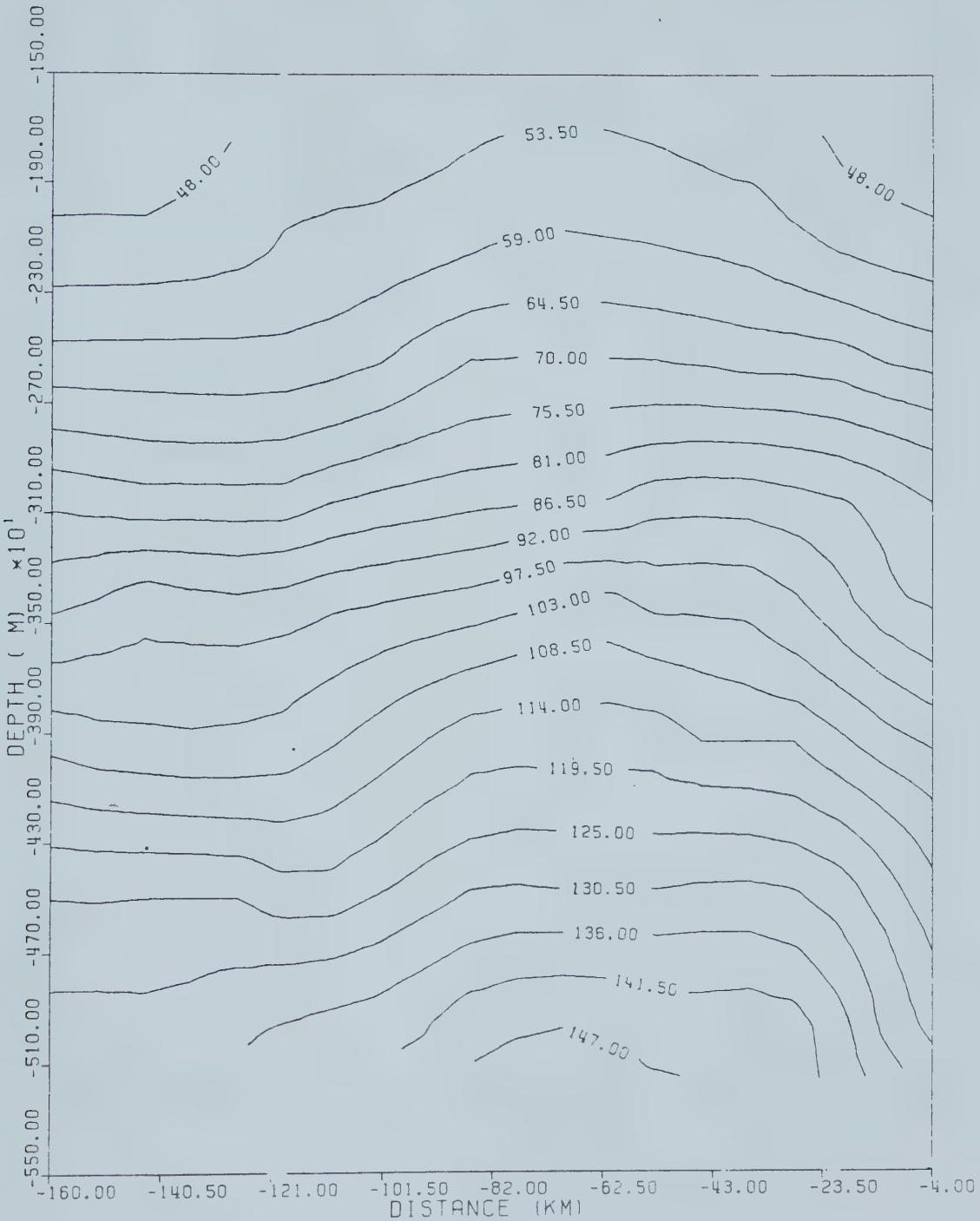


Figure 2.33 Temperature contour map in the vertical plane along profile(PP). Temperature in degrees centigrade.

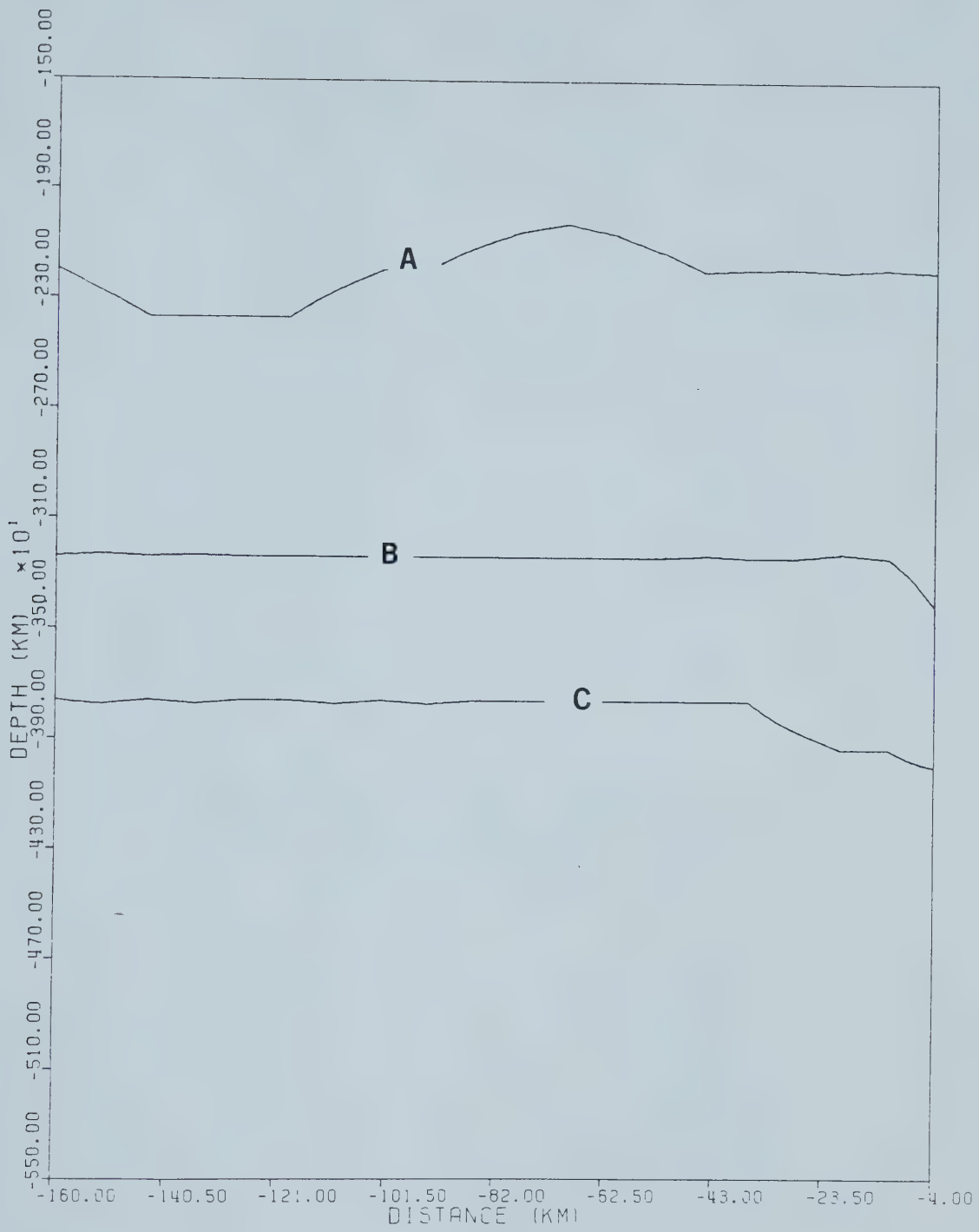


Figure 2.34 Topography of the surfaces (A) top of the Colorado (B) unconformity surface (C) upper Devonian surface along profile (PP).

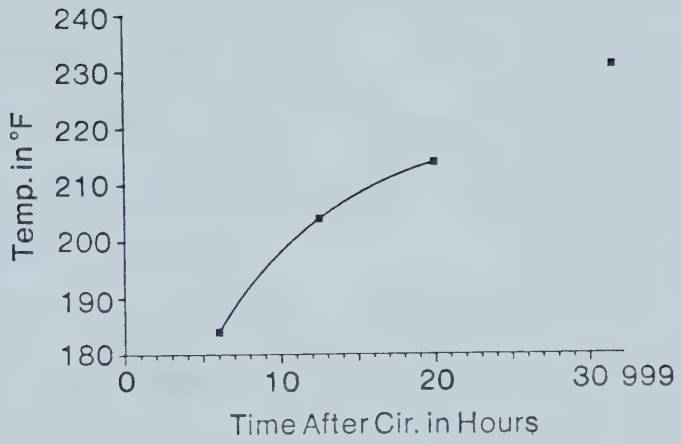


2.35a

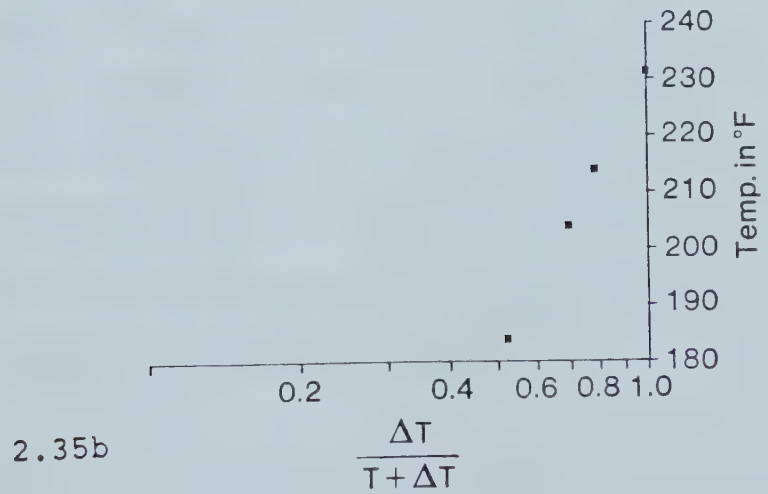


2.35b

Figure 2.35 An example of the Horner-type correction. (From Lam et al. 1981).

equilibrium formation temperature is then obtained by extrapolating a least squares fitted line to the vertical axis which corresponds to infinite elapsed time.

This procedure was applied to the wells for which there was sufficient information, and the values were used to generate the corrected temperature/depth plot which is shown in Fig. 2.36. The least squares fitted line for the corrected data gives a greater slope than that obtained from the uncorrected data. To determine the temperature change to be expected at any depth, the uncorrected and corrected temperature/depth plots were overlaid and the indicated correction for the temperature as a function of depth was determined.

Table 2.1 gives the temperature correction that can be expected for each depth considered. From this table it can be inferred that equilibrium temperatures are higher than measured temperatures. Also, the table indicates that the temperature differences between corrected and uncorrected values increases with depth. In this regard, the calculated temperature gradients may be viewed as minimum values. Also, from the calculated average relative errors, it is found that the uncorrected temperatures are about 12.5% lower than the equilibrium formation temperatures.

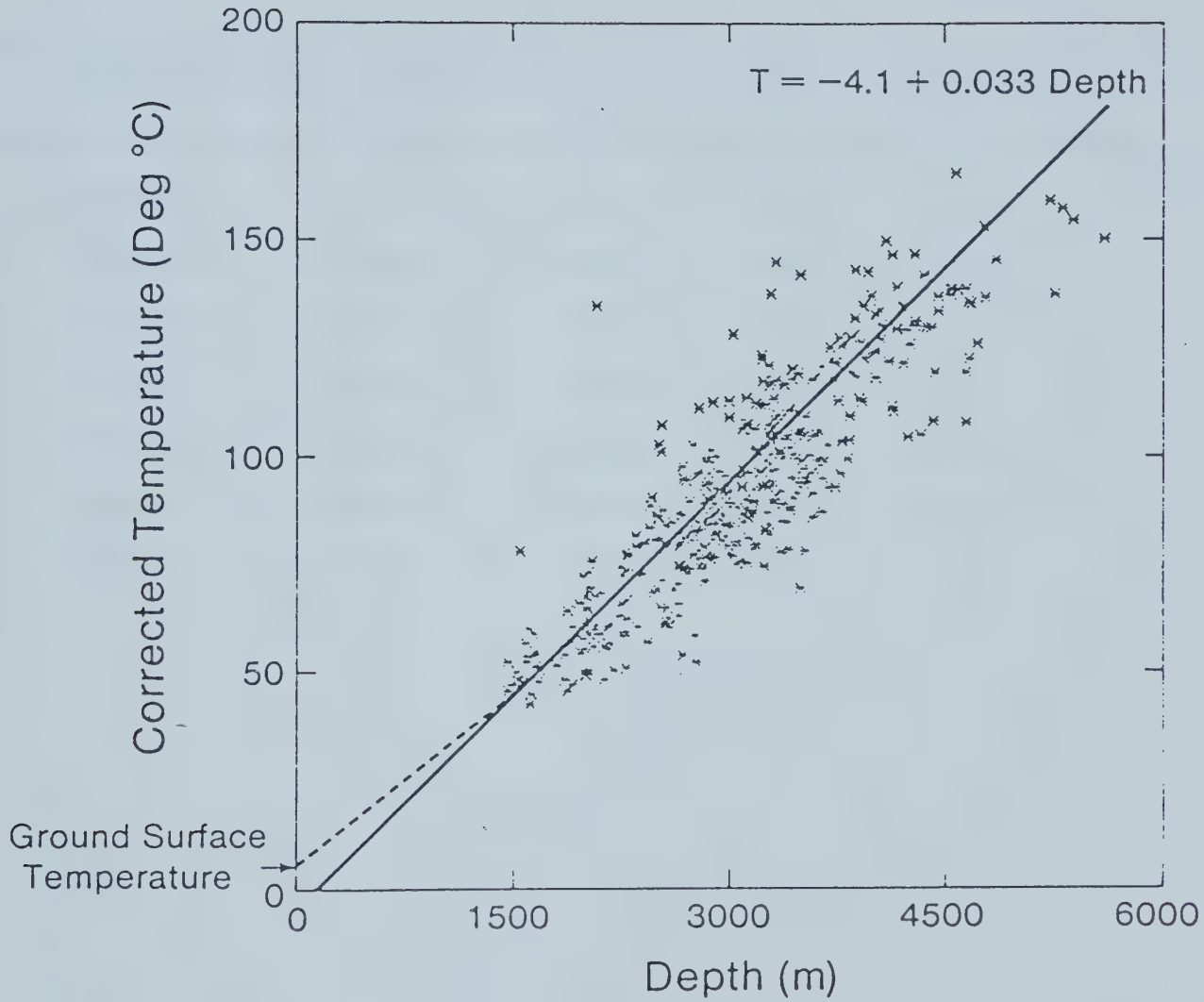


Figure 2.36 Temperature/depth plot from the corrected temperature values. (From Jones et al, 1983).

Table 2.1

Temperature correction as function of depth based on Horner temperature correction.

| Depth(m) | Corrected T°C | Uncorrected T°C | +ΔT°C | % Error |
|---|---|---|---|---|
| 2000.0 | 63.0 | 57.0 | 6.0 | 10.5 |
| 2500.0 | 78.0 | 70.0 | 8.0 | 11.4 |
| 3000.0 | 94.0 | 83.5 | 10.5 | 12.6 |
| 3500.0 | 109.5 | 97.5 | 12.0 | 12.3 |
| 4000.0 | 124.0 | 109.5 | 14.5 | 13.2 |
| 4500.0 | 140.0 | 124.0 | 16.0 | 12.9 |
| 5000.0 | 155.0 | 136.5 | 18.5 | 13.6 |

### 2.1.4 Thermal Conductivity Estimates

In order to estimate terrestrial heat flow it is necessary to know the thermal conductivity of the strata through which the heat flows as well as the temperature gradient across the interval of interest.

Many strata of different rock types occur in the sedimentary column in the west central Alberta region. Thus, an effective thermal conductivity for the column must be estimated for each interval across which heat flow is to be computed.

If thermal conductivity values $K_1$, $K_2$, $K_3$, ..., $K_n$ can be assigned to discrete layers of thicknesses $L_1$, $L_2$, $L_3$, ..., $L_n$ respectively, then the effective conductivity for the total interval is given by

$$K = \Sigma_1^n L_i / (L_i / K_i) \qquad 2.1$$

and is equivalent to the weighted mean thermal conductivity across the total thickness.

Jones et al, (1983) measured thermal conductivities of 936 samples from 48 wells in the study area. The locations of the wells are shown in Fig. 2.37. The samples are from different formations. The measurements were made on core plugs in a divided-bar apparatus.

In order to obtain effective conductivity estimates, these measured values were investigated in detail. Initially, the samples were grouped as to rock type, and the

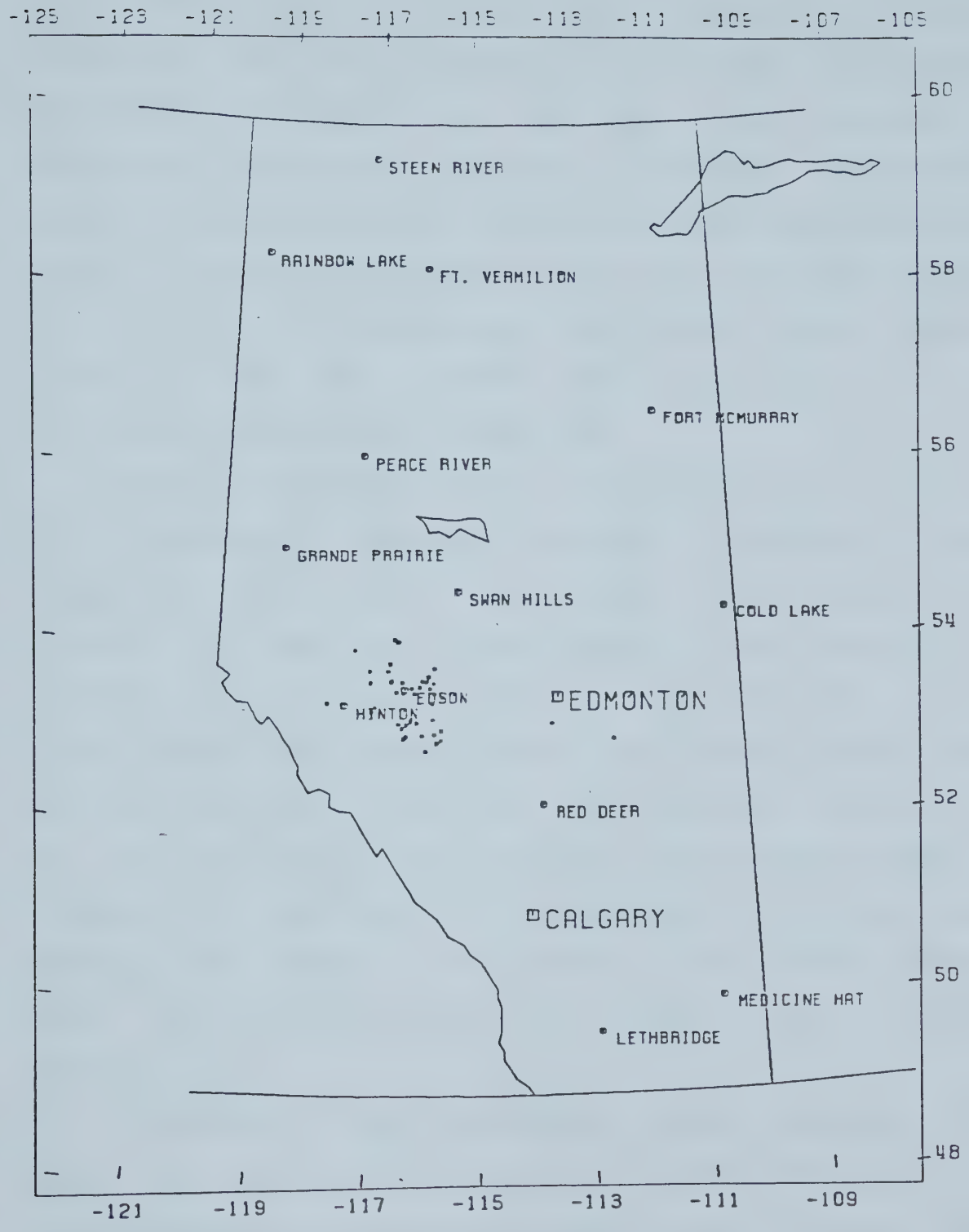


Figure 2.37 Locations of wells from which measurements of thermal conductivity were made on core plugs.

mean thermal conductivities and the standard deviations were calculated. The results are shown in the graph of Fig. 2.38. The number of samples of each rock type is also indicated in this figure. Dolomites, limestones, siltstones, sandstones, dolomite-limestones, shales, and shaly-siltstones constitute about 89% of the rock samples. Among these major rock types, the dolomites and sandstones have thermal conductivites a little greater than 3.0W/m/K. The limestones are of generally lower thermal conductivity.

Thermal conductivity values representative of each of the lithological intervals described in section 2.3 were sought. In this regard, the thermal conductivity as a function of depth was investigated for each lithological interval. Scatter plots are shown in Figs. 2.39-2.42. Also, these figures show average conductivity values together with standard deviations calculated from individual values for all the rock types in each interval. These diagrams show in a general way the depths of the formations from which the samples came. Based on these figures, there does not appear to be a direct relationship between thermal conductivity and depth.

In addition, the relationship between porosity and depth was investigated by plotting the measured porosities of the samples as a function of depth for all samples. The resulting plot is illustrated in Fig. 2.43, and indicates that there is a decrease of porosity with depth.

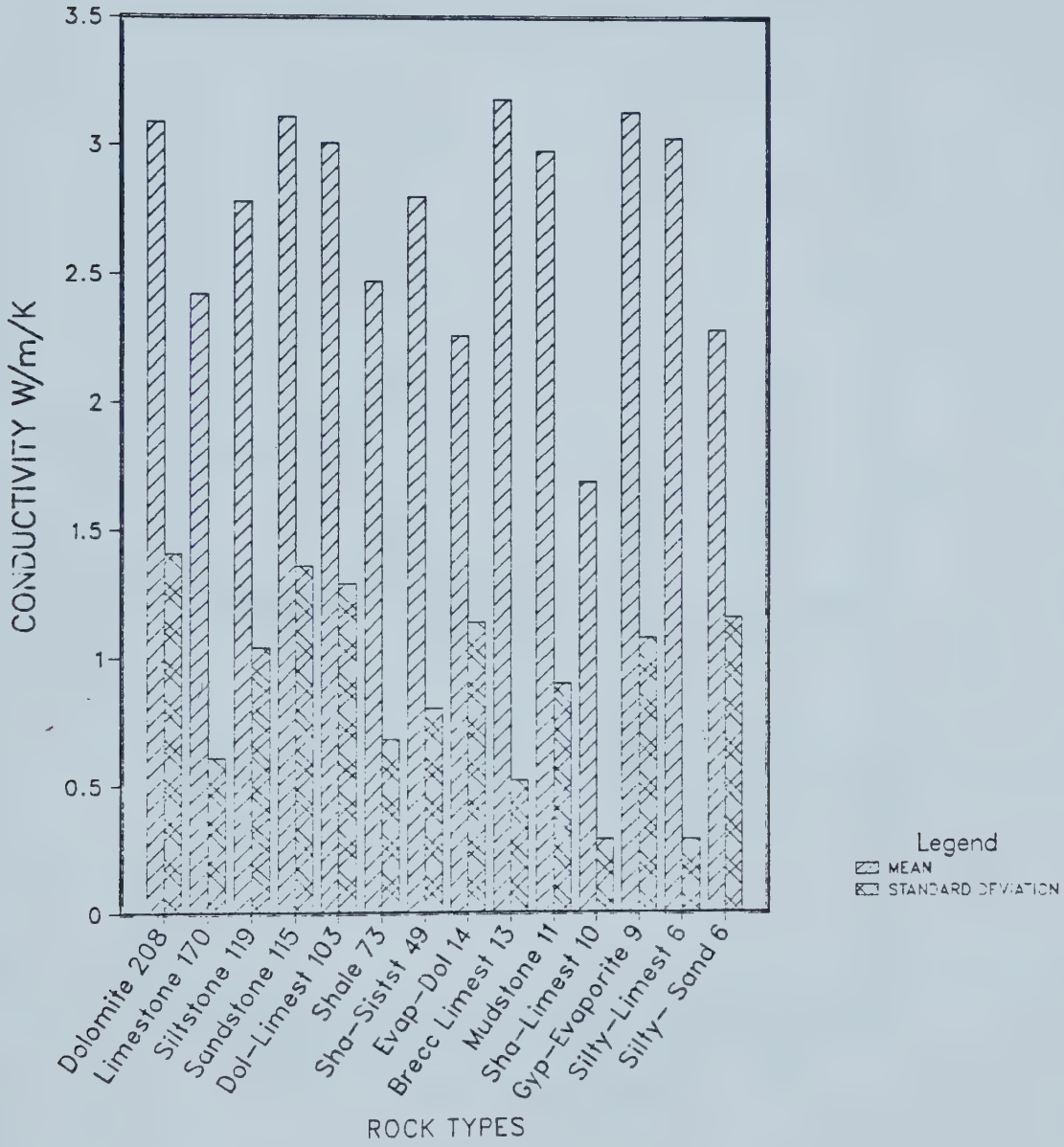


Figure 2.38 Graph of conductivity values for the various rock types.

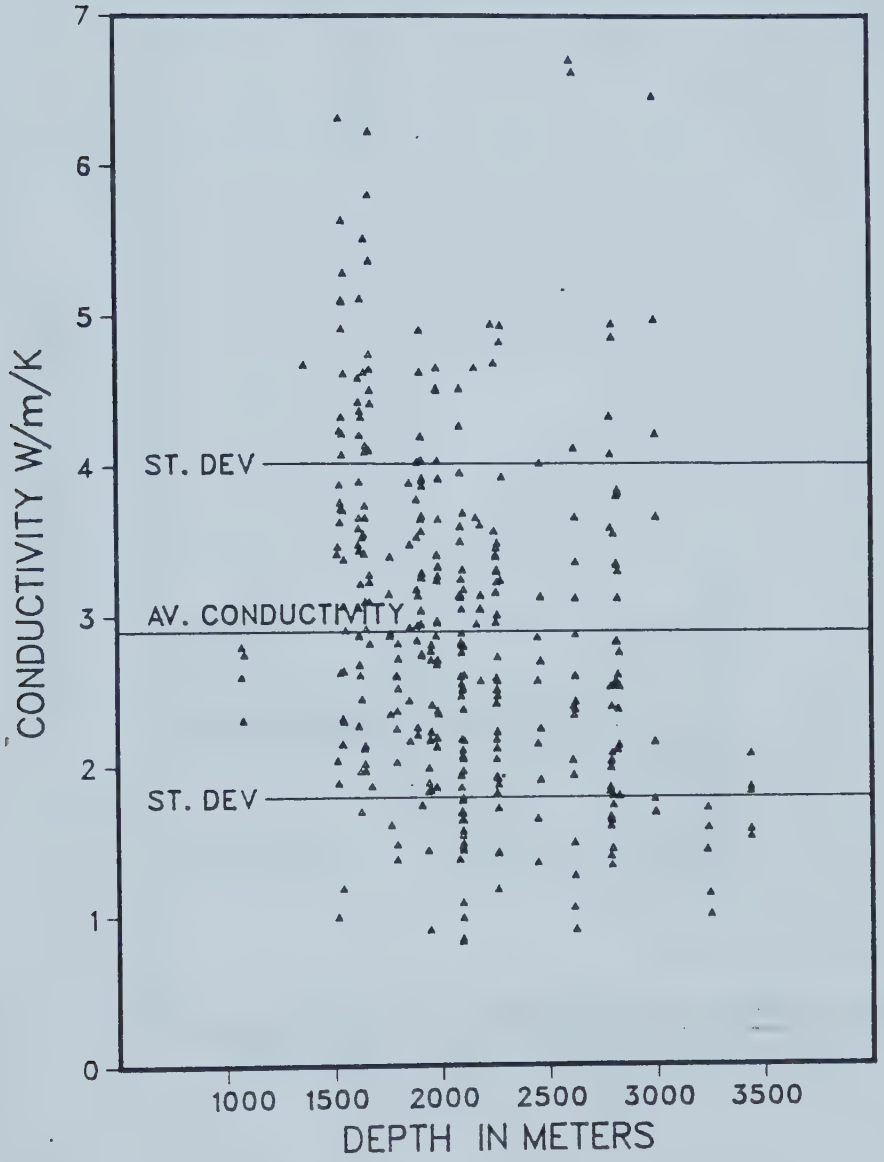


Figure 2.39 Scatter diagram illustrating thermal conductivity as a function of depth for lithological interval (1), the top of the Colorado formation to the unconformity surface.

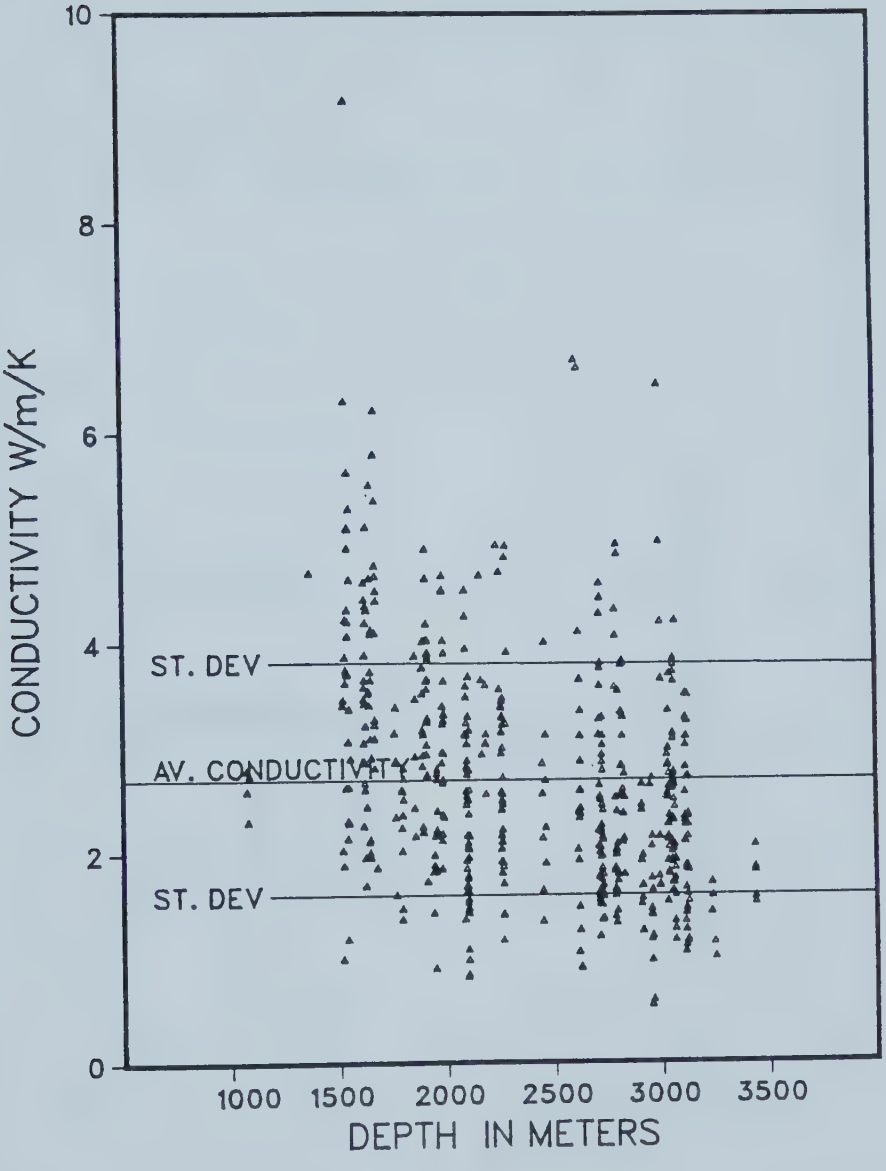


Figure 2.40 Scatter diagram illustrating thermal conductivity as a function of depth for lithological interval (2), the top of the Colorado formation to the upper Devonian formation.

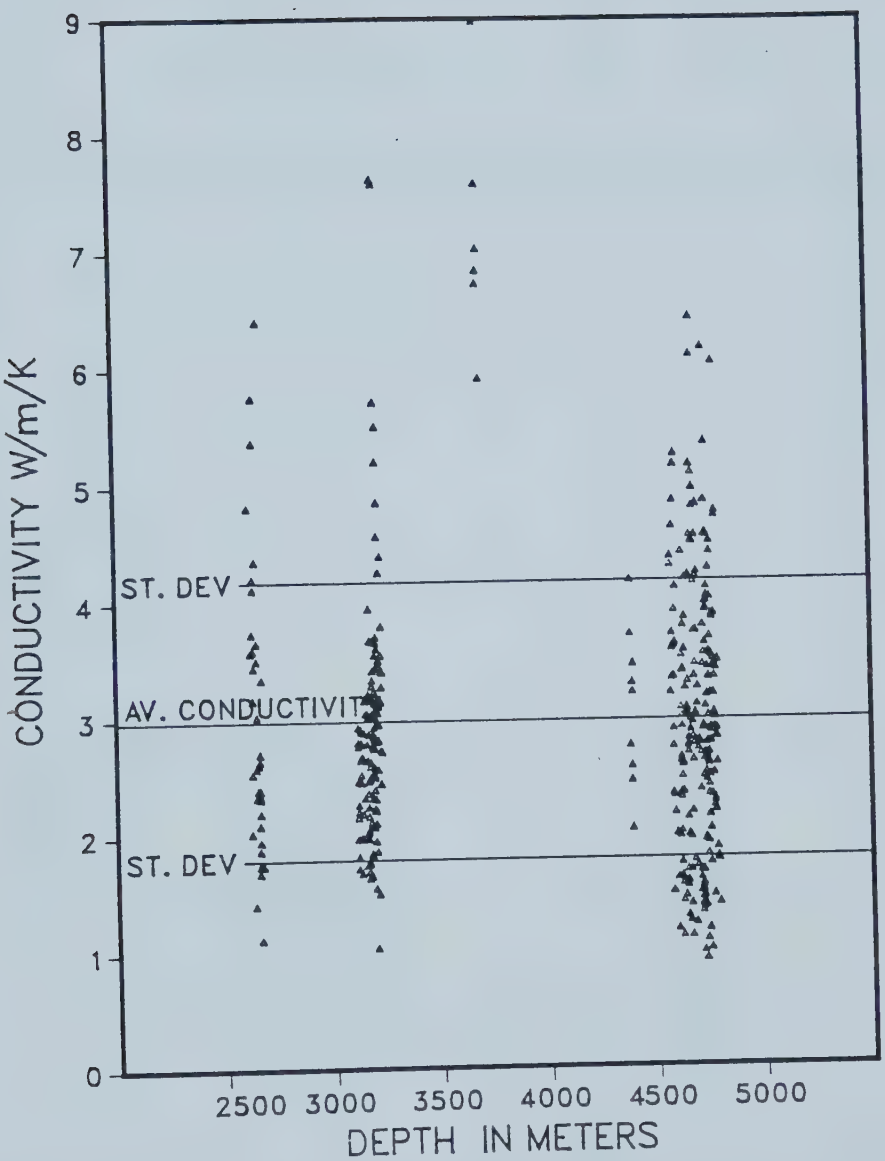


Figure 2.41 Scatter diagram illustrating thermal conductivity as a function of depth for lithological interval (3), the surface of the unconformity to the Precambrian.

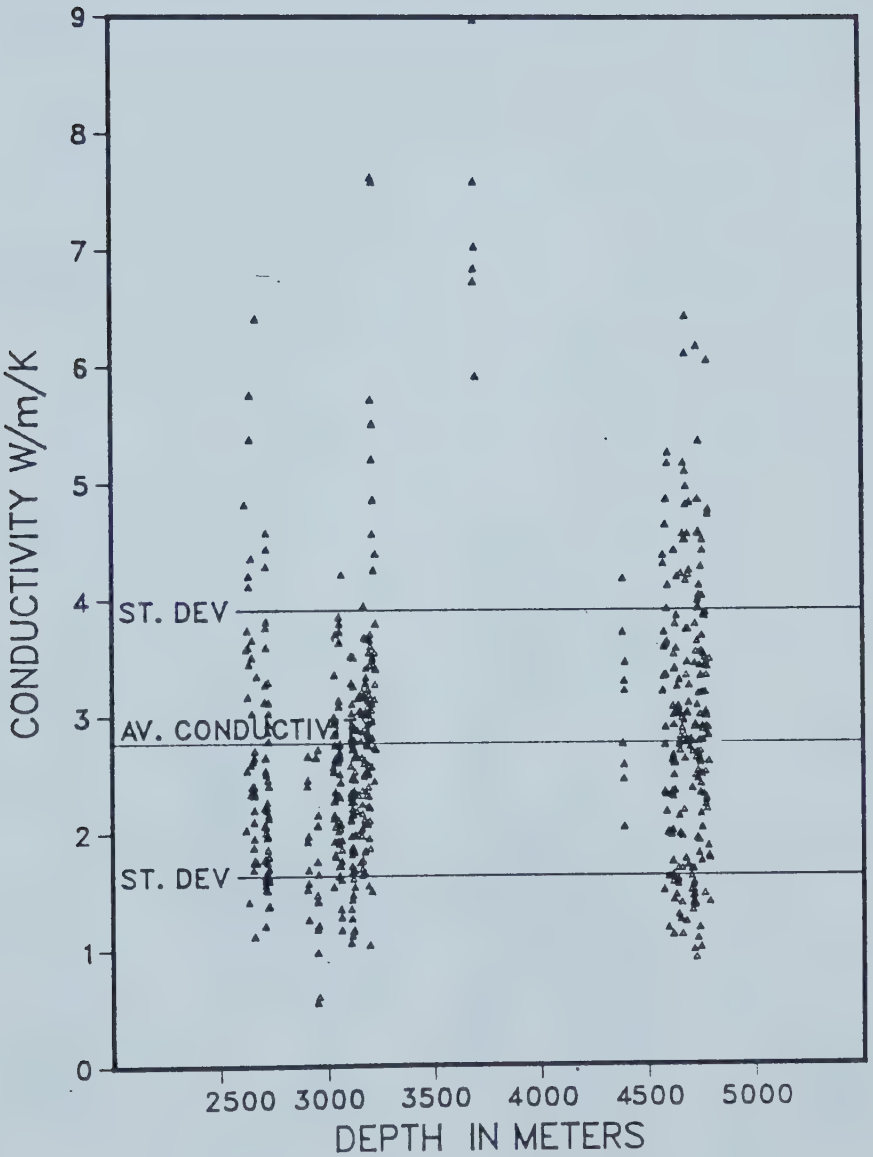


Figure 2.42 Scatter diagram illustrating thermal conductivity as a function of depth for lithological interval (4), the upper Devonian surface to the Precambrian.

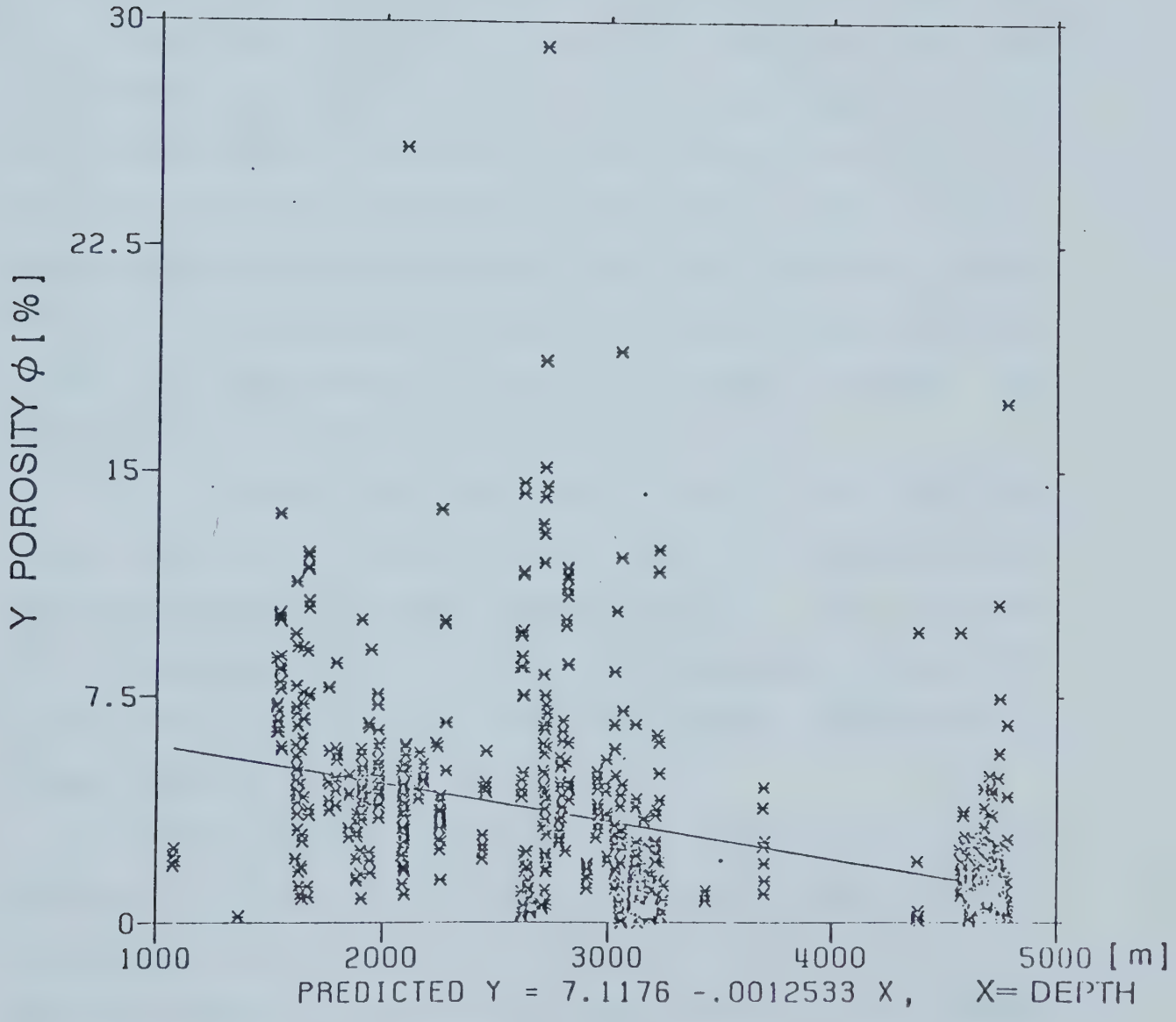


Figure 2.43 Porosity/depth plot for rock samples taken from wells in west-central Alberta. (From Jones et al. 1983).

With these general results in mind, and to better understand the thermal conductivity distribution, each lithological interval was considered separately and graphs of thermal conductivities and calculated standard deviations of the measurements for the main rock types in each interval were constructed. These graphs are given in Figs. 2.44-2.47

Comparison of Figs. 2.44 and 2.45 indicates that the siltstones from the Colorado to the unconformity surface have higher thermal conductivity than those from the top of the Colorado to the upper Devonian. This is also true for sandstones and shaly-siltstones. For these three rock types, there is an apparent decrease in thermal conductivity with depth for the samples from the interval between the unconformity surface and the Devonian.

On the other hand, comparison of Figs. 2.46 and 2.47 shows that the thermal conductivity of the dolomites is slightly greater at greater depths. This is also apparent for dolomite-limestones, though the limestone conductivity itself does not differ for the two intervals considered in these figures.

Further efforts were made to find representative thermal conductivity values for the lithological intervals by grouping the measured values for each interval into various conductivity intervals without regard to rock types. All measured values were assigned to thermal conductivity intervals of 0.20W/m/K wide over the whole range of conductivities. From this classification, a set of

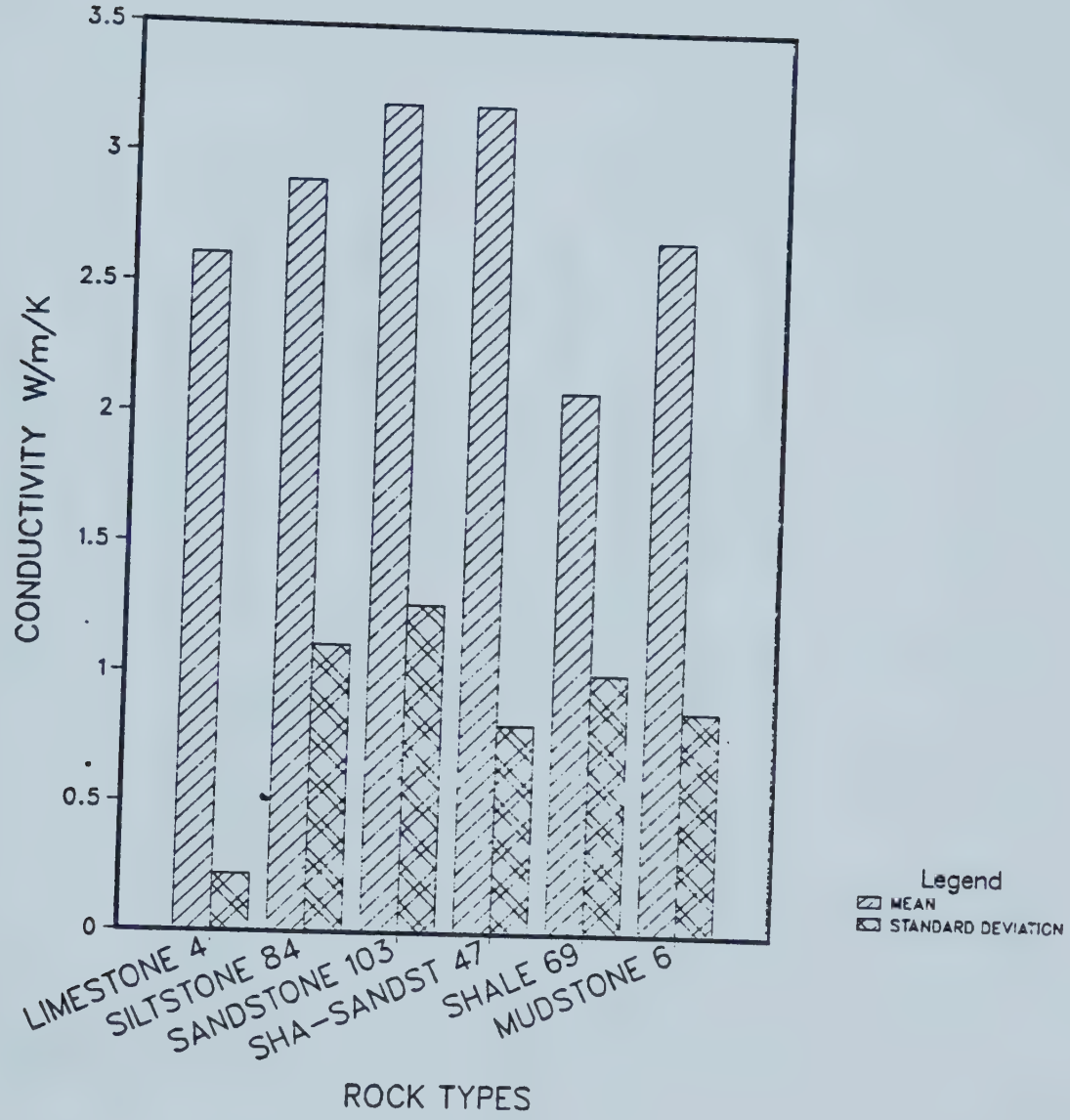


Figure 2.44 Graph of thermal conductivity for the main rock types within the lithological interval (1), the top of the Colorado to the unconformity surface.

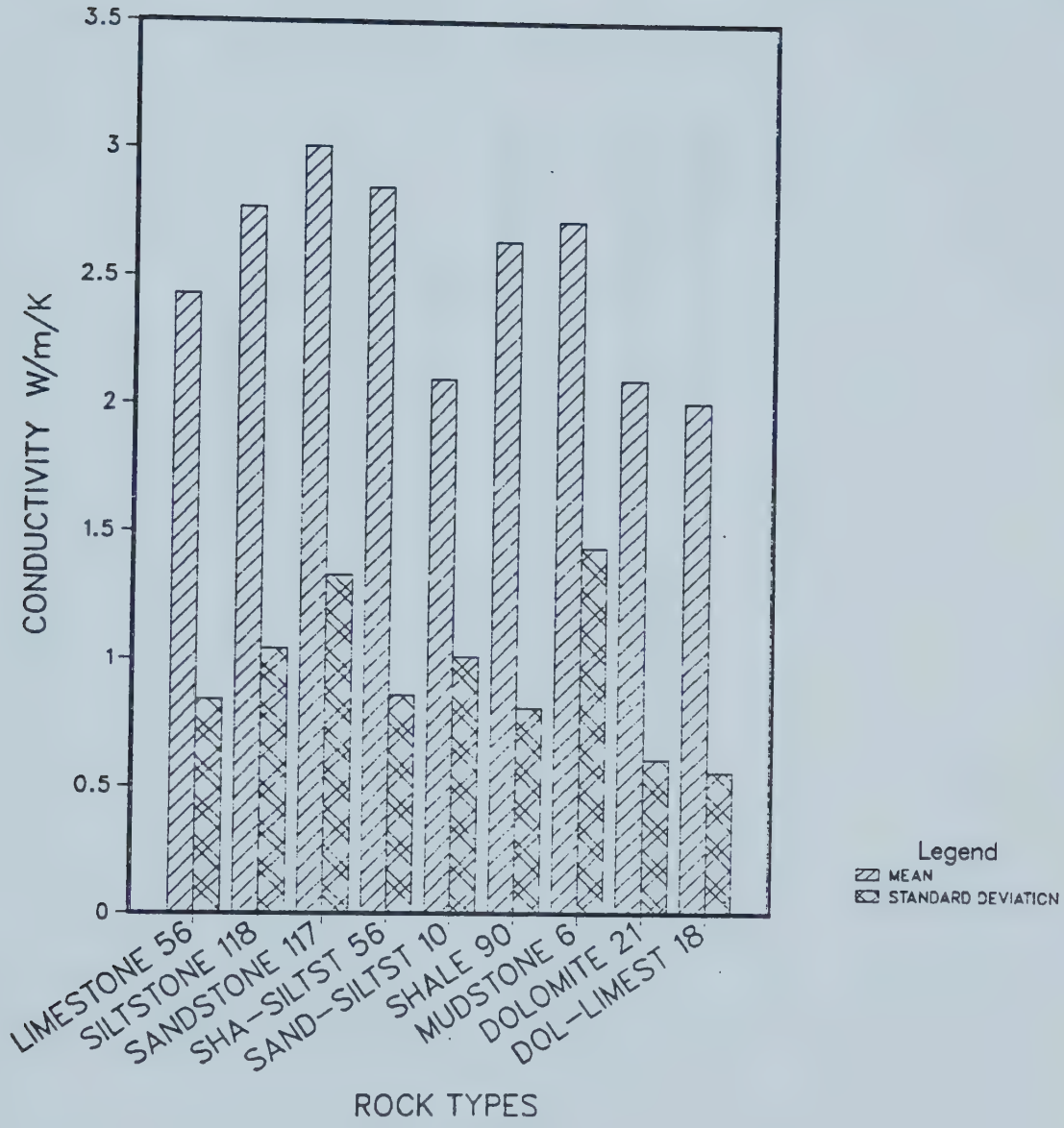


Figure 2.45 Graph of thermal conductivity for the main rock types within the lithological interval (2), the top of the Colorado to the upper Devonian.

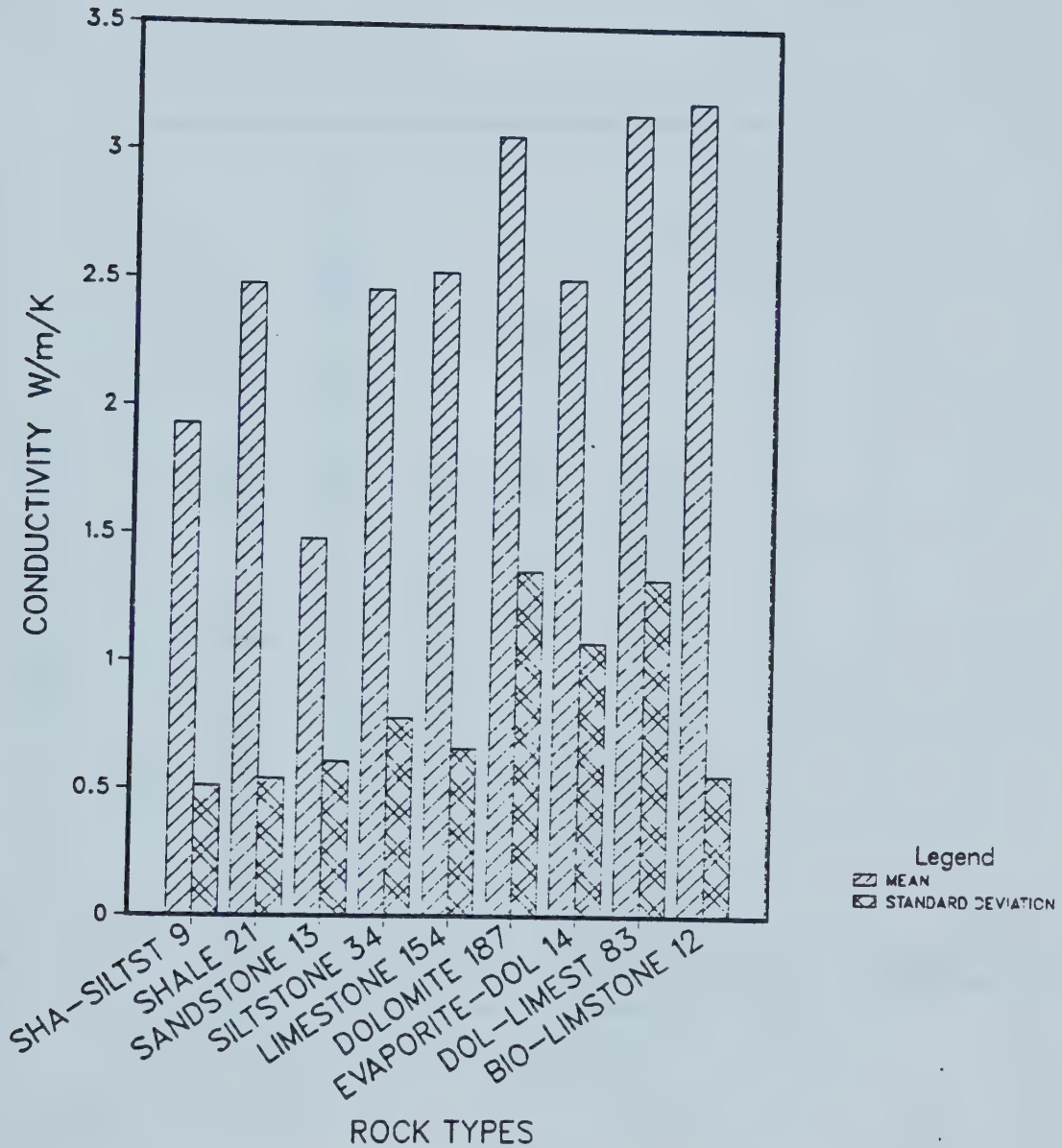


Figure 2.46 Graph of thermal conductivity for the main rock types within the lithological interval (3), the unconformity surface to the Precambrian.

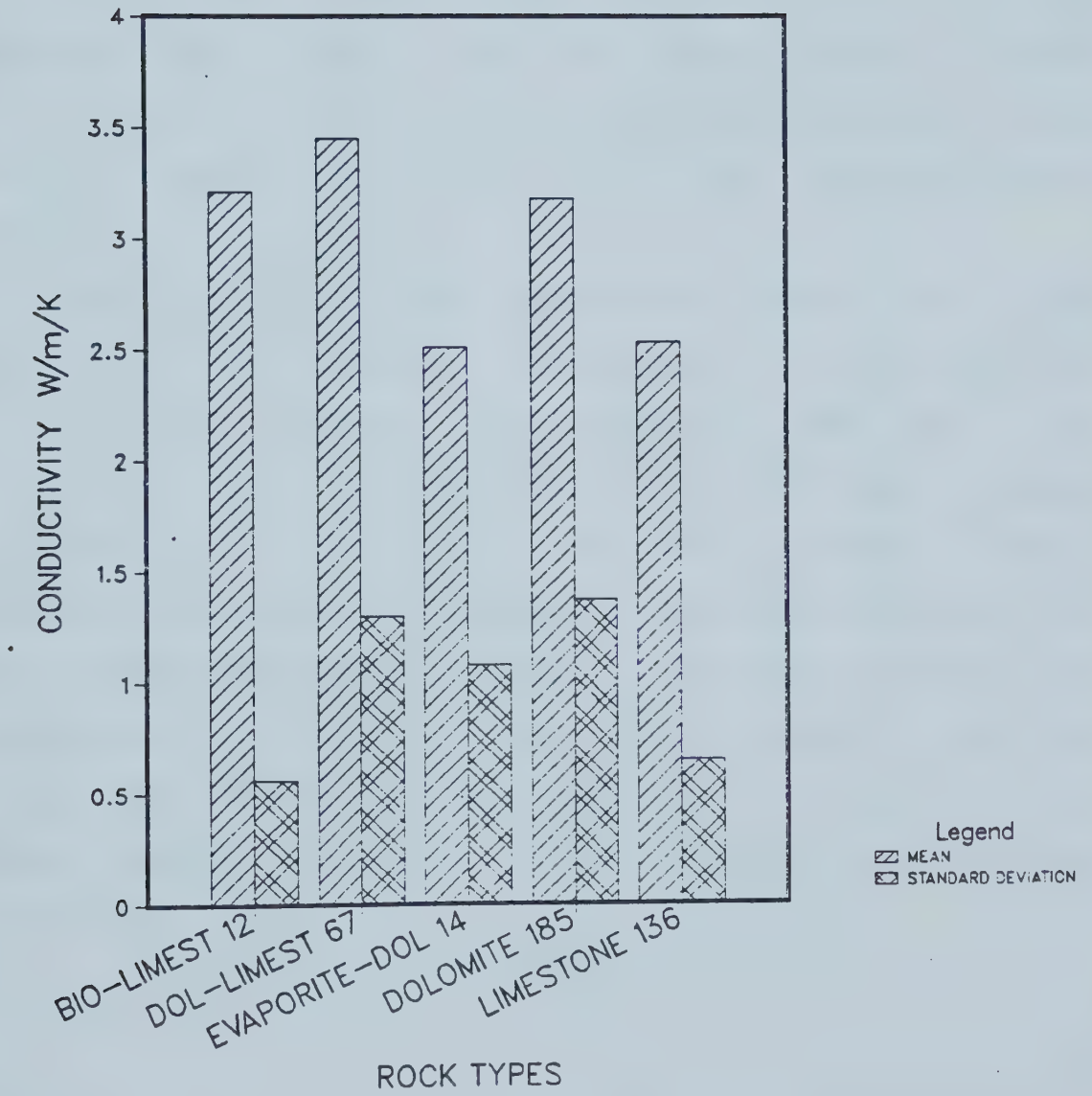


Figure 2.47 Graph of thermal conductivity for the main rock types within the lithological interval (4), the upper Devonian to the Precambrian.

histograms was constructed for the lithological intervals, and these histograms are given in Figs. 2.48-2.51. As before, the mean and standard deviation for each interval were calculated from the individual values for all the rock types in the interval.

The mean conductivities calculated by this last approach were taken as the representative thermal conductivity values for the lithological intervals. These values, together with the main rock types, are summarized in Table 2.2.

Table 2.3 gives the conductivity values which were taken for the different rock types for the effective conductivity estimates. The sources of data are also indicated in this table. The estimated thermal conductivities are lower than the average thermal conductivities based on measured values. The results, based on effective conductivity estimates, take into account the proportion of the sedimentary column occupied by each rock type, and therefore such estimates are probably better than those based on measured values from selected formations within the intervals.

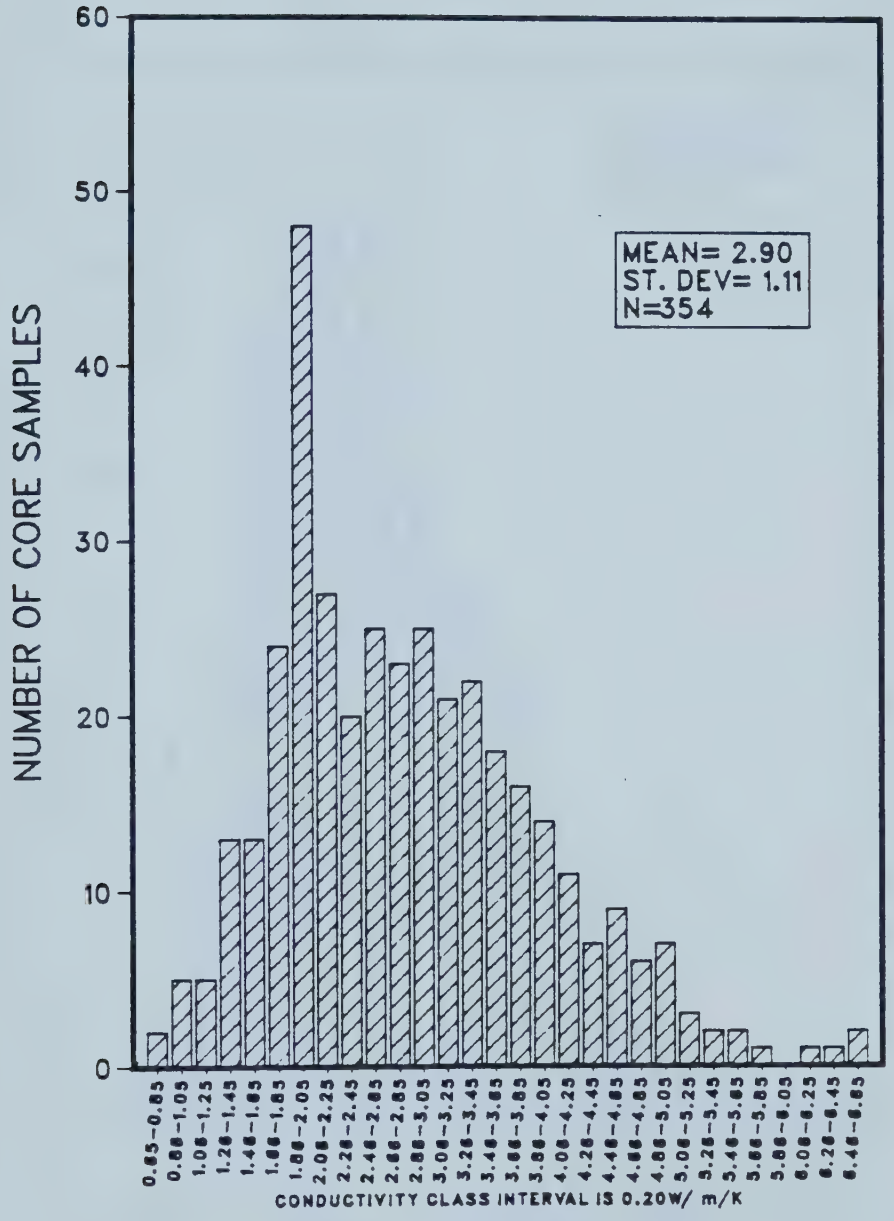


Figure 2.48 Histogram of thermal conductivity for all rock types with a class interval of 0.20W/m/K for lithological interval (1), top of the Colorado to the unconformity surface.

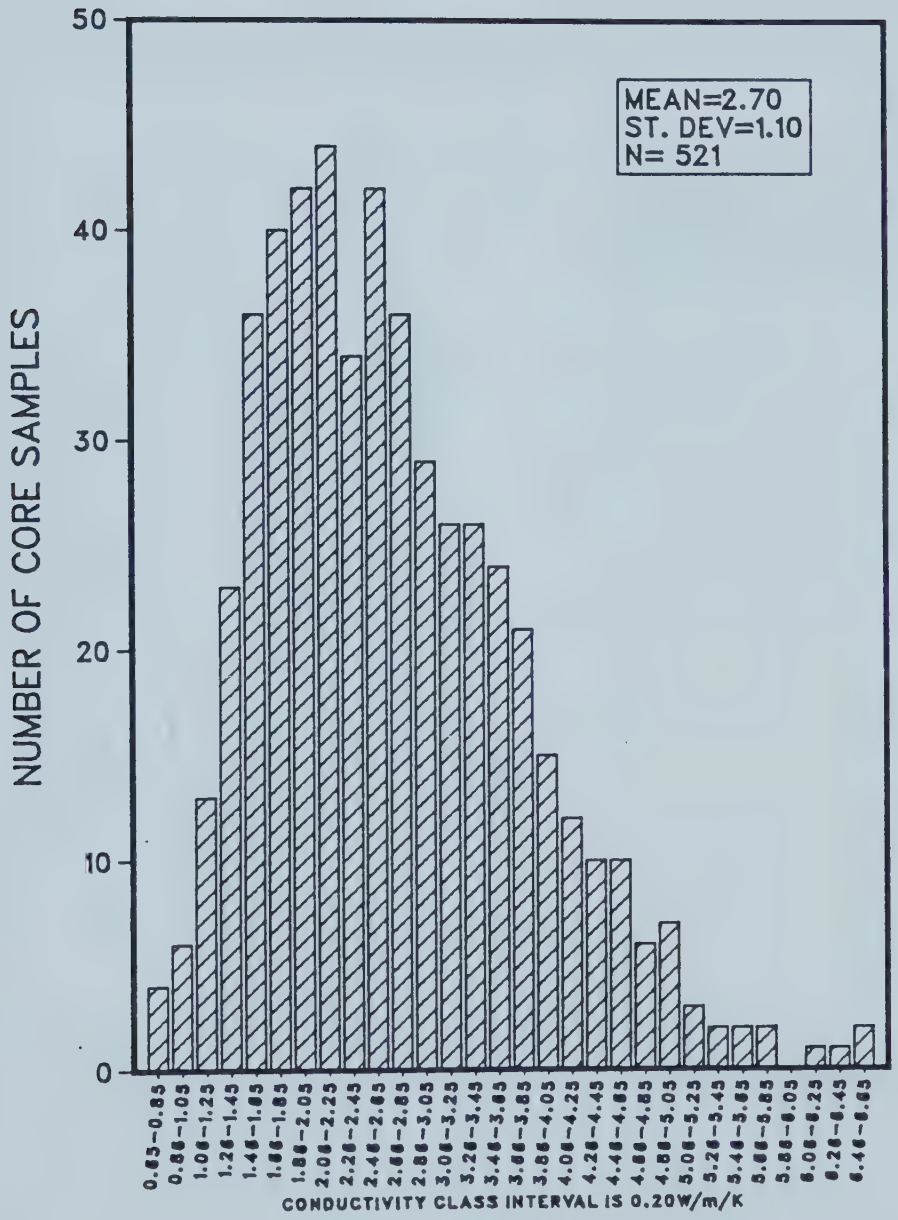


Figure 2.49 Histogram of thermal conductivity for all rock types with a class interval of 0.20W/m/K for lithological interval (2), top of the Colorado to the upper Devonian.

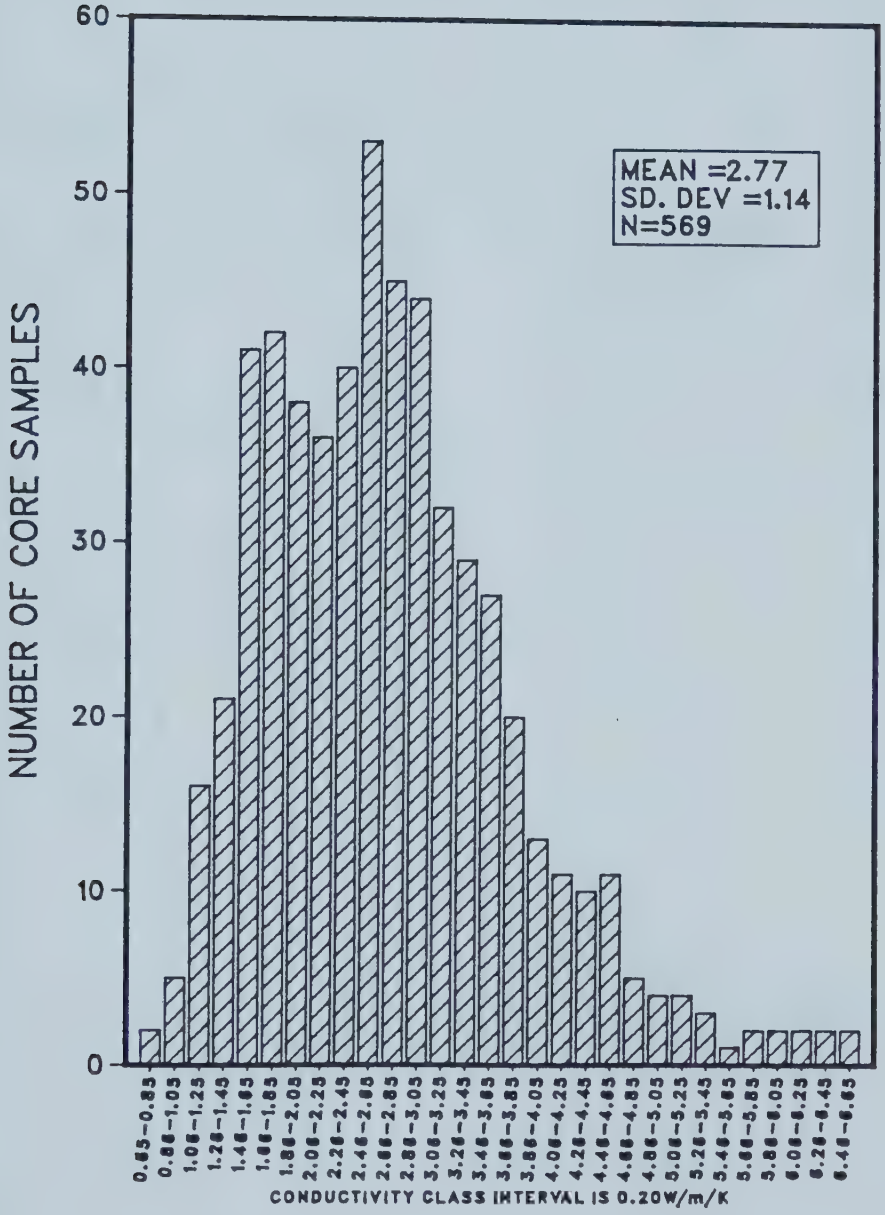


Figure 2.50 Histogram of thermal conductivity for all rock types with class interval of 0.20W/m/K for lithological interval (3), the unconformity surface to the Precambrian.

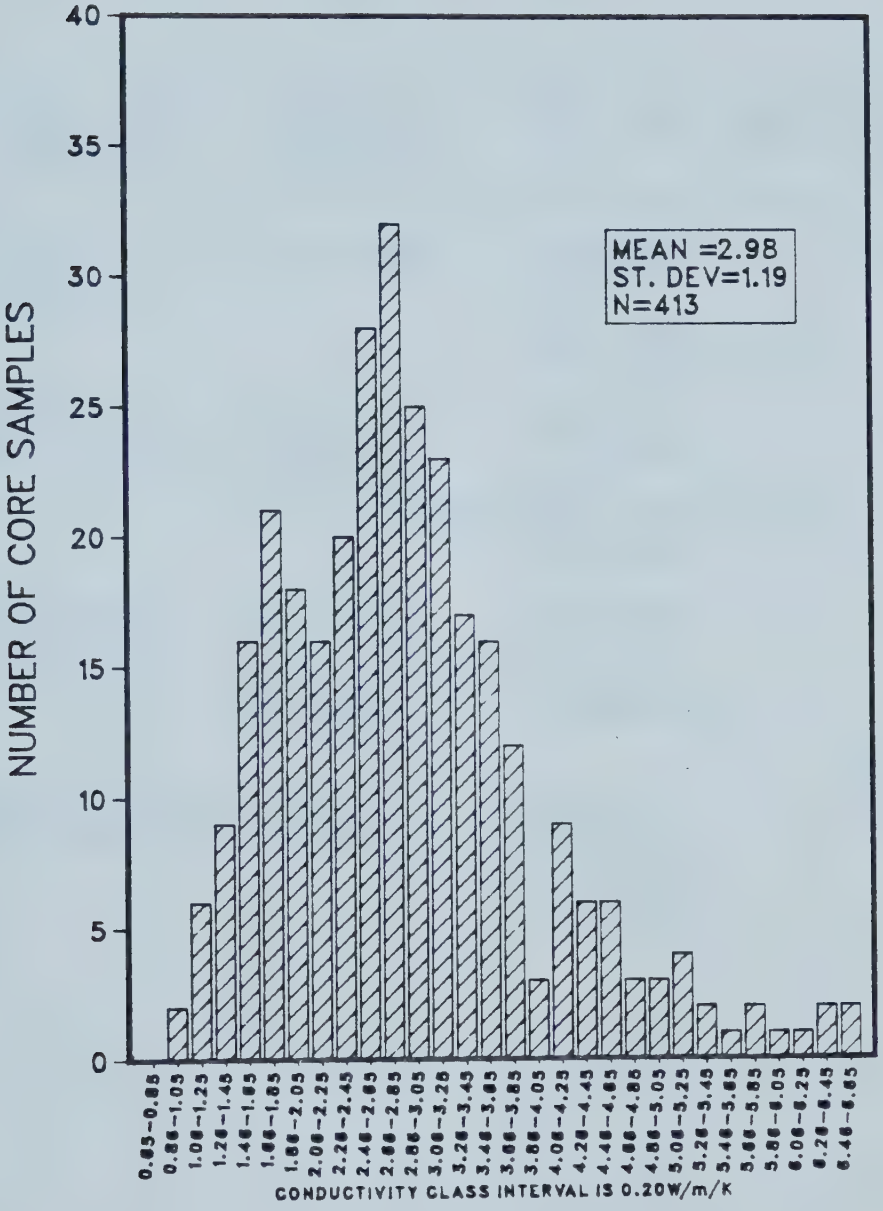


Figure 2.51 Histogram of thermal conductivity for all rock types with class interval of 0.20W/m/K for lithological interval (4), the upper Devonian to the Precambrian.

Table 2.2

Representative thermal conductivity for four lithological intervals based on measured rock samples.

| LITHOLOGICAL INTERVAL | GEOLOGICAL FORMATIONS | MAIN ROCK TYPES | MEAN K (W/m/K) | STD DEV |
|---|---|---|---|---|
| Colorado to Unconformity Surface | Cretaceous | Sandstone<br>Shale<br>Siltstone<br>Shaly-Siltstone | 2.90 | 1.11 |
| Colorado to Upper Devonian | Cretaceous<br>Jurassic<br>Triassic<br>Mississippian | Sandstone<br>Siltstone<br>Shale<br>Shaly-Siltstone<br>Limestone | 2.70 | 1.10 |
| Unconformity Surface to Precambrian | Jurassic<br>Triassic<br>Mississippian<br>Devonian<br>Precambrian | Limestone<br>Dolomite<br>Dolomite-Limestone | 2.77 | 1.14 |
| Upper Devonian to Precambrian | Devonian<br>Precambrian | Dolomite<br>Limestone<br>Dolomite-Limestone | 2.98 | 1.19 |

Table 2.3

Conductivity values on which the estimates of effective conductivity $K_{ef}$ were based. (The estimates are based on both actual measurements and published values.)

| Rock Type | Average Conductivity W/m/K | Minimum Conductivity W/m/K | Maximum Conductivity W/m/K | Comment |
|---|---|---|---|---|
| Limestone | 2.4 | 1.8 | 3.0 | Based on measurements of rocks from Hinton Region. |
| Dolomite | 3.1 | 1.7 | 3.0 | |
| Anhydrate | 5.5 | 4.3 | 5.8 | Majorowicz and Jessop (1981). Kapplemeyer and Haenel (1974). |
| Shale | 2.0 | 1.1 | 2.8 | Garland and Lennox (1962). Kapplemeyer and Haenel (1974). |
| Sandstone | 3.1 | 1.8 | 4.5 | Based on measurements of rocks from Hinton region. |
| Marlstone | 2.1 | 0.9 | 2.7 | Kapplemeyer and Haenel (1974). Hurtig et. al. (1976). |
| Chert | 4.2 | - | - | Majorowicz and Jessop (1981). |
| Coal | 0.3 | 0.2 | 0.5 | |
| Conglomerate | 2.4 | 0.9 | 4.6 | |
| Salt | 5.5 | 4.4 | 5.8 | |
| Siltstone | 2.8 | 1.7 | 3.8 | |
| Miscellaneous | 2.4 | 0.9 | 5.8 | |

Table 2.4

Calculated effective thermal conductivities (according to Jones et al. 1983 paper in preparation) based on net rock data and average conductivities as listed in Table 2.2.

| Stratigraphic Intervals | Well Locations | | | Average Conductivity W/m/K |
|---|---|---|---|---|
| | 9-29-53-10W5 | 11-33-51-16W5 | 6-13-58-18W5 | |
| Ground Surface to Top of Colorado | 2.42 | 2.50 | 2.46 | 2.46 |
| Top of Colorado to Top of Paleozoic | 2.30 | 2.48 | 2.21 | 2.33 |
| Paleozoic to Top of Devonian | - | 2.51 | 2.28 | 2.39 |
| Top of Paleozoic to Precambrian | - | 2.49 | 2.52 | 2.51 |
| Top of Devonian to Precambrian | - | 2.45 | 2.51 | 2.49 |

### 2.1.5 Calculation of Conductive Heat Flow

Conductive heat flow can be calculated from the steady-state heat flow equation

$$Q=KdT/dz \qquad 2.2$$

where Q=vertical heat flow, K=thermal conductivity, and dT/dz=temperature gradient.

To obtain heat flow estimates, average geothermal gradients were calculated for each of the lithological intervals considered and these were combined with the estimated thermal conductivities. The average geothermal gradients were calculated for each interval from the 3x3 township/range values.

Table 2.5 summarizes the thermal conductivities and average gradients for the intervals considered and gives the calculated heat flows for these intervals. Also, an error estimate is included for the conductive heat flow calculation. This error estimate is given by

$$\sigma_m=\sigma/\sqrt{n} \qquad 2.3$$

where

$\sigma_m$=standard error of estimate,

$\sigma$=standard deviation,

n=sample size.

Table 2.5

Heat flow estimates for the four lithological intervals based on the statistical averages of measured conductivities and gradT.

| LITHOLOGICAL INTERVAL | MEAN K (W/m/K) | MEAN GRADIENT (°C/km) | HEAT FLOW $mW/m^2$ | ERROR % |
|---|---|---|---|---|
| Colorado to Unconformity Surface | 2.90±1.11 | 23.86±4.89 | 69.19 | 19 |
| Colorado to Upper Devonian | 2.70±1.10 | 25.70±3.70 | 69.37 | 16 |
| Unconformity Surface to Precambrian | 2.77±1.14 | 30.53±6.64 | 84.57 | 18 |
| Upper Devonian to Precambrian | 2.95±1.19 | 31.89±8.99 | 95.03 | 22 |

Table 2.5 indicates a significant difference in heat flow above the unconformity surface compared with that below. Also, within the Paleozoic itself, there is a change in heat flow with depth as indicated by the results from the overlapping intervals from the unconformity surface to the Precambrian and the upper Devonian to the Precambrain.

For comparison, conductive heat flow was calculated from estimated effective conductivity values based on equation 2.1 and the heat conductivity values from Table 2.4.

The calculated heat flow values are given in Table 2.6. The results show that there is an increase in heat flow with depth, but for each lithological interval the values are considerably lower than those of Table 2.5 due to lower average conductivities calculated using equation 2.1.

Table 2.6

Heat flow estimates for the four lithological intervals based on calculated effective thermal conductivities and average gradT.

| Stratigraphic Interval | Average Conductivity W/m/K | Average grad T. °C/Km | Heat Flow $mWm^{-2}$ |
|---|---|---|---|
| Ground Surface to top of Colorado | 2.46 | - | - |
| Top of Colorado to top of Paleozoic | 2.3 | 23.9 | 55.6 |
| Paleozoic to top of Devonian | 2.39 | 25.7 | 61.4 |
| Top of Paleozoic to Precambrian | 2.51 | 30.5 | 76.6 |
| Top of Devonian to Precambrian | 2.49 | 31.9 | 79.4 |

# 3. DISCUSSION AND CONCLUSIONS

## 3.1 General Discussion of Results

The Paleozoic and the Precambrian surface maps of Figs. 2.4 and 2.5 indicate that the sediments dip in an approximately southwest direction toward the eastern limit of the disturbed belt. This is further confirmed by the profiles of Figs. 2.28, 2.30 and 2.32 and means that the overlying upper and lower Cretaceous Mesozoic formations become thicker toward the southwest. These southwestward dipping sedimentary formations extend relatively smoothly eastward well beyond the study area. Beyond the disturbed belt boundary to the west, toward the Rocky Mountains, the sediments are faulted and folded.

The geothermal gradient map of Fig 2.9 indicates that a high geothermal gradient occurs along the edge of the disturbed belt, with a regional trend that strikes in the northwest to southeast direction. Approximately perpendicular to this are three northeasterly trending high gradient zones which are indicated by arrows in Fig. 2.9.

It is apparent that the high gradient geothermal anomaly delineated by Lam et al. (1982) and striking in the southwest-northeast direction is part of a larger high gradient zone which borders the disturbed belt.

The geothermal gradient maps for the lithological intervals from the unconformity to the Precambrian surface Figs 2.18 and 2.19 do not show regional trends. However,

there are a number of isolated high and low gradient areas. Similarly, Figs. 2.16 and 2.17 do not indicate a regional geothermal gradient distribution that is consistent for the two intervals.

To better understand the thermal regime, the subsurface temperature distributions at 500m intervals, as illustrated in Figs. 2.20 to 2.26, were considered. These figures show that there is a gradual increase in subsurface temperature toward the northeast at a given depth. In addition, if profile (FF) of Fig. 2.31 is considered, there is an increase of temperature at any given level in the direction from the southwest toward the northeast. This implies that a horizontal geothermal gradient exists, and the magnitude of this gradient is greater near the limit of the disturbed belt.

Profile (AA) of Fig. 2.27 shows a similar result, but the effect is less pronounced at depths below the top of the upper Devonian surface. Similarly, profile (BB) of Fig. 2.29 shows such a result, but the effect seems to disappear at depths below the upper Devonian formations.

If profile (PP) of Fig. 2.33, which runs in the northwest-southeast direction, is considered, there is little change in temperature along the profile for any given depth.

By mapping geological surface information onto the maps illustrating temperatures for profile (FF), the temperatures along the various surfaces can be determined. From these,

horizontal gradients were estimated on the basis of a 200m grid. The horizontal gradients along the upper Devonian, the unconformity, and Colorado surfaces on profile (FF) are shown in Fig. 3.1.

From Fig. 3.1 it is seen that the horizontal temperature gradient is greater near the edge of the disturbed belt, and there is a general decrease in the horizontal gradient away from the disturbed belt. Furthermore, the figure shows that the horizontal gradient near the disturbed belt is greater along the surface of the upper Devonian than along the unconformity surface and much larger than along the Colorado.

The existence of a horizontal temperature gradient indicates that there is lateral heat flow and this may be associated with fluid motion. This effect can be due to the different hydrodynamic situation between the area close to the disturbed belt where most of the downward gravity imposed water flow occurs and the shallower part of the basin where fluid tends to flow laterally. This implication of heat transport by fluid flow is strengthened by results from model calculations by Dr. Rahman and included in a paper in preparation on results from this area (Jones et al, 1983). The model considers the influence of gravity induced water flow on the temperature as a function of depth. Such a situation was first described for one dimension by Bredelhoeft and Papadopulus (1965) and is represented by the equation:

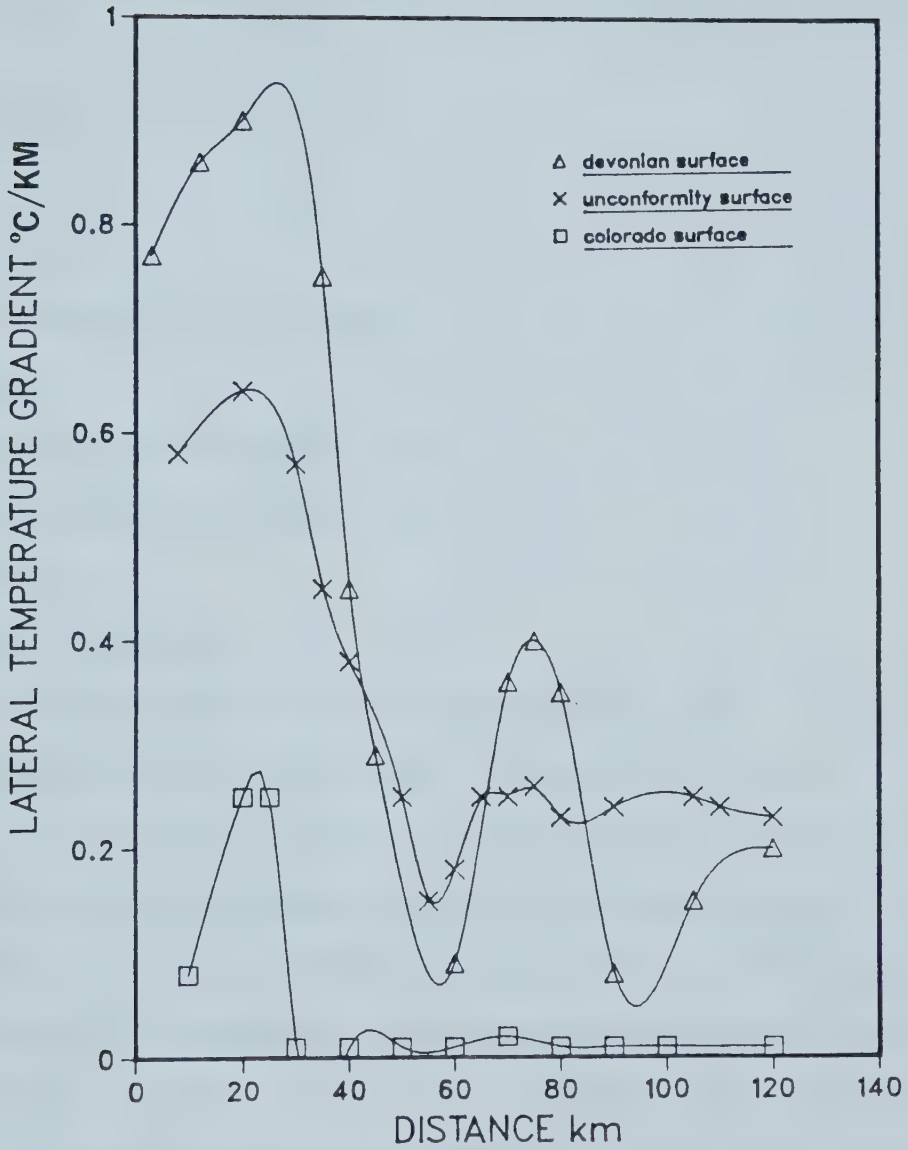


Figure 3.1 The horizontal gradients along the three geological surfaces shown in Fig. 2.32 for profile (FF) of Fig. 2.31.

$$T(z)=(T_H-T_o)(1-EXP(-P_1z/H)/(1-EXP(-P_1))+T_o \qquad 3.1$$

where $P_1$ is the Peclet number for vertical flow
(ie, the ratio of convective flow to conductive flow)

$$P_1=\rho C_f q_w H/\lambda_c$$

where

$T(z)$= temperature at depth z,

z=depth,

$T_H$=temperature at depth z=H,

$T_o$=temperature at depth z=0,

$\rho$ =density,

$C_f$=heat capacity,

$\lambda_c$= heat capacity of solid-fluid system and

$q_w$=groundwater flow per unit crossectional area.

The value $\lambda_c/\rho x C_f$ generally equals about $10^{-6}m^2sec^{-1}$. Temperature versus depth changes evaluated on the basis of equation (3.1) for $T_o$=5°C and $T_H$ =150°C and different values of downward groundwater flow velocity are given in Fig. 3.2. The result shows that even a downward water velocity of $10^{-10}$m/sec will produce an increase of thermal gradient with depth and downward velocities of $0.5x10^{-9}$m/sec and $10^{-9}$m/sec give even greater gradient increases with depth. Such velocities can explain the temperature gradient increase with depth in the area and the discrepancy between the average heat flow for the shallower and the deeper

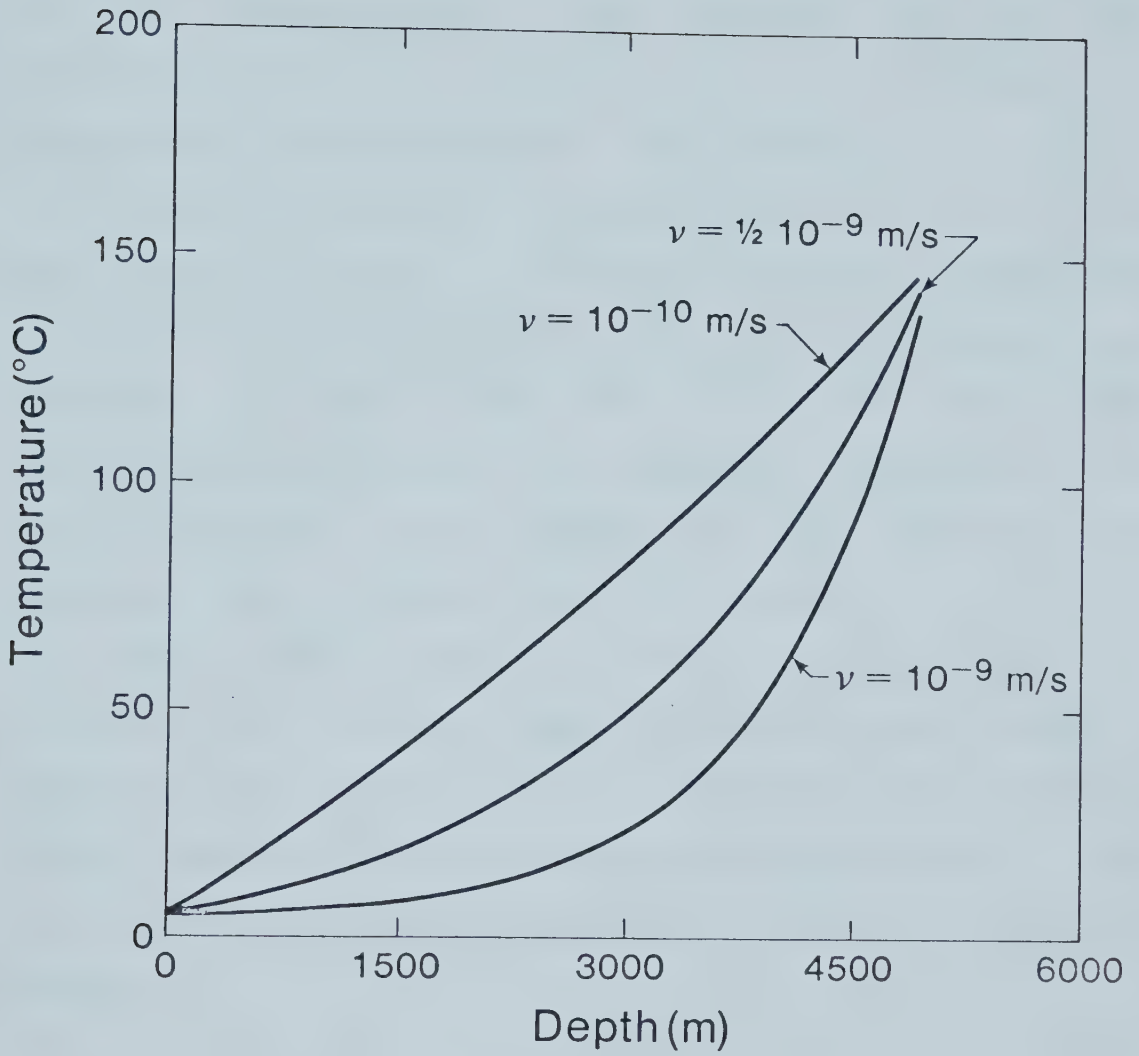


Figure 3.2 Temperature dependence with depth in the interval between ground level (5 degrees centigrade) and 5km (150 degrees centigrade) due to downward water movement with different velocities.

stratigraphic intervals.

Tables 2.5 and 2.6 show that there are discontinuities in the heat flow at various surfaces. These results indicate that lateral fluid movement within the permeable formations of the Mississippian, upper Devonian and the lower Cretaceous plays an important role in modifying the hydrodynamic situation and heat flow pattern.

A schematic model of the hydrodynamic situation in the study area is given in Fig.3.3. The model suggests that surface water percolates downward in the Rocky Mountains and foothills recharge area. The water then moves under hydraulic pressure along the permeable sediments of the lower Cretaceous, Mississippian and upper Devonian to the discharge area to the east and the northeast.

Such a model appears to satisfy the observations from the data, and it does not appear that some other source of heat, such as a magma intrusion or upwelling of partial melt occurs. Deep drilling and seismic reflection results (Price and Mountjoy, 1970) indicate that the Cambrian basement is unbroken.

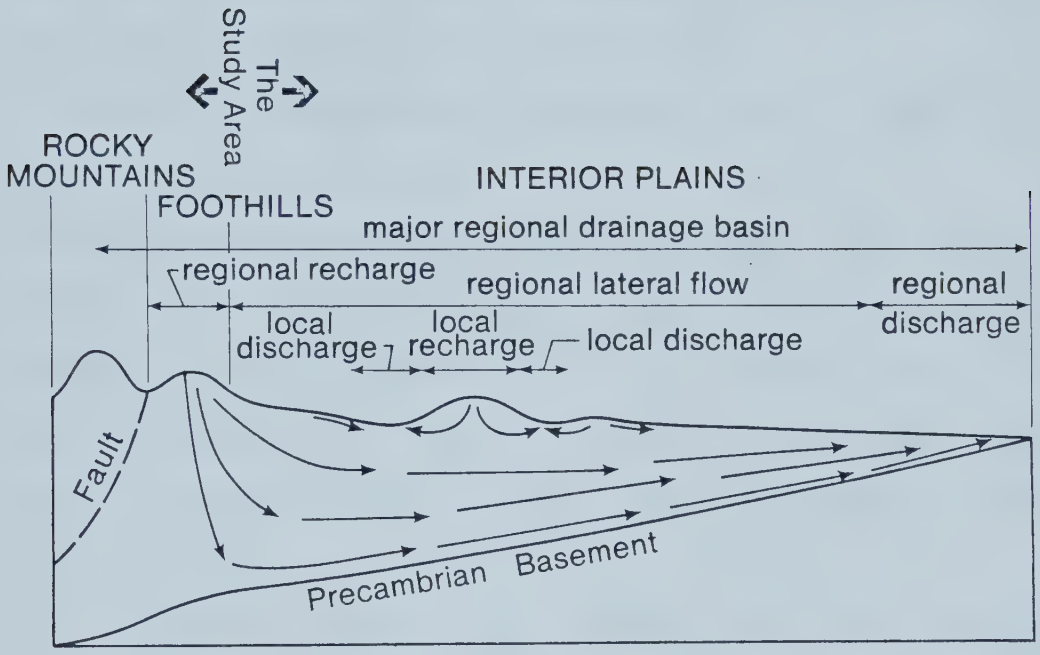


Figure 3.3 Hydrodynamic representation of the study area (after Hitchon, 1982).

## 3.2 Conclusions

The following conclusions can be reached from the work:

(1) Temperature gradients and heat flow increase with depth in the study area. This is especially evident in the high relief and the high hydraulic head region of the disturbed belt and the deeper part of the basin.

(2) Lateral temperature gradients occur along the main stratigraphic surfaces.

(3) The increase in heat flow with depth and the lateral temperature gradients can be explained by the hydrodynamic situation which is characterized by downward gravity imposed water movement to great depths and probably upward and lateral water movement in the deep permeable strata and through faults.

(4) Petroleum bottom-hole temperature data analyses in sedimentary basins are useful for detecting major heat flow features related to the basin hydrodynamics and are a necessary first step to determine the significance of detailed individual heat flow measurements.

(5) It is not sufficient to draw conclusions about terrestrial heat flow from a small number of even extremely accurate temperature measurements which come from depth intervals which include only part of the sedimentary section. The heat flow pattern within the strata can be significantly disturbed by the hydrodynamic situation.

(6) Steady-state "background" heat flow in the region can only be determined from careful measurements below the

sedimentary strata, ie, in the deeply buried Precambrian basement formations which may be less influenced by the water flow system.

## BIBLIOGRAPHY


American Association of Petroleum Geologists, 1976. *Bottom-hole temperature data file. University of Oklahoma.*

Anglin, F. M., and Beck, A. E. 1965. *Regional Heat Flow Pattern In Western Canada. Can. J. Earth Sci.*, **2:** *176-182.*

Balling, N., Kristiansen, J. I., Poulsen, D. K., and Saxon, S. 1980. *Proceedings of the II International Seminar on the Results of EC Geothermal Energy Research. Strasburg, March, 1980, Reidel Publishing Company.*

Birch, F. R., Roy, R. F., and Decker, E. R. 1968. *Heat Flow and Thermal History in New England and New York,* **In Studies of Appalachian Geology, ed. E-en Zen,** pp. 437-451 Interscience, New York.

Bodvarson, G. 1969. *On the Temperature of Water Flowing Through Fractures, J. of Geophys. Res.,* **74 pp. 1987-1992.**

Bott, M. H. P., 1982. *The Interior of the Earth: Its Structure, Constitution and Evolution. Edward Arnold (Publishers) Limited, London. pp. 266-295.*

Bredehoeft, J. D., and Papadopulus, T. S. 1965. *Rates of Vertical Ground Water Movement and Estimates from Earth's Thermal Profile.* **Water Resources Research, 4: 32-38.**

BRGM-1976 Report. *Potential Geothermique du Bassin Parissien, Bureau de Recherches Geologique et Minieres, Paris.*

Bullard, C. E. 1939. *Heat Flow in South Africa, Proc. Roy. Soc. London, A173(995) pp. 474-502.*

Burwash, R. A., 1979. *Uranium and Thorium in the Precambrian Basement of Western Canada. II. Petrologic and Tectonic Controls. Can. J. Earth Sci., 16: 972-484.*

Burwash, R. A., and Cumming, G. L. 1976. *Uranium and Thorium in the Precambrian Basement of Western Canada. Can. J. Earth Sci., 13: 284-293.*

Carvalho, M. D., Purwoko, S., Thamrin, M., and Vacquier, V. 1980. *Terrestrial Heat Flow In The Tertiary Basins Of Central Sumatra, Tectonophysics,* **69:** *pp. 163-188.*

Elder, J.W. 1981. *Thermal Systems. Academic Press, U.S.A.*

*pp. 21-38.*

Evans, T. R., and Coleman, N. C. 1979. *North Sea Geothermal Gradients, Nature,* **247**: *pp. 28-30.*

Fertl, W.M., and Wichmann, P. A. 1977. *How to Determine Static Bottom-hole Temperatures from Well Log Data. World Oil,* **184**: *pp. 105-106.*

Gable. R. 1979. *Draft of a Geothermal Flux Map of France pp.179-186. In Terrestrial Heat Flow Of Europe (L. Rybach, V Cermak eds.) Springer, 1979.*

Garland, G. D.,and Lennox, D. H. 1962. *Heat Flow in Western Canada.* Geophys. J., **6**: *pp. 245-262.*

*Harper, M. L., 1971. Approximate Geothermal Gradients in North Sea Basins, Nature* **230**: *235-236.*

Hitchon, B. 1982. *Fluid flow in Western Canada Sedimentary Basin. 1.* Effect of Topography. Water Resources Research, 5: 186-195.

Ingham, M. R., Bingham, D. K., and Gough, D. I. 1983. *A Magnetovariational Study of a Geothermal Anomaly.* Geophys. J. Roy. Astron. Soc. 72. (in press)

Jessop, A. M., Hobart, M. A., and Sclater, J. G. 1976. *The World Heat Flow Data Collection.* Can. Earth Physics Branch, 5; 125 pp.

Jessop, A. 1976. Geothermal Energy from Sedimentary Basins. *Can. Earth Physics. Geothermal Series 8; 10pp; Ottawa.*

Jones, F. W., Rahman, M., Majorowicz, J. A., and Lam, H. L. 1983. **REPORT** *"A Study of Thermal Properties of Sedimentary Rocks of Western Canada"* (UP-A-269-PHASE II )

Jones, F. W., Kushigbor, C., Lam, H. L., Majorowicz, J. A., and Rahman, M. 1983. *Estimates of Terrestrial Thermal Gradients and Heat Flow Variations with Depth in the Hinton-Edson Area of the Alberta Basin Derived from Petroleum Botton-Hole Temperature Data.* Submitted to Geophys. Prosp.

Kappelmeyer, O. and Haenel, R. 1974. *Geothermics with Special References to Application. Gebruder Borntraegen,* Berlin, Stuttgart. pp. 218-219.

Lachenbruch, A. H. and Sass, H. 1977. *Heat flow in the United States and the Thermal Regime of the Crust. In: The Earth's Crust. J. G. Heacock Ed. Amer. Geophys. Monograph 20, No.8, pp. 626-675. A G U, Washinton D.C.*

Lam, H. L., Jones, F. W. and Lambert, C. A. 1982. *Geothermal Gradients in the Hinton area of West central Alberta.* Can. J. of Earth Sci. 19: 755-766.

Majorowicz, J. A., Jones, F. W., and Lam, H. L. 1983b. *Terrestrial Heat Flow in Relation to Hydrodynamic in Alberta Basin* **Presented at the Proc. of IUGG Hamburg Conference.**

Majorowicz, J. A., Jones, F. W., and Lam, H. L. 1983a. *Comment on a Magnetovariational Study of a Geothermal Anomaly* by M. R. Ingham, D. K. Bingham and D .I. Gough. *Accepted for publication in the Geophys. J. R. Astro. Soc., 72.*

Majorowicz, J. A., and Jessop, A. M. 1981a. *Regional Heat Flow patterns in the Western Canadian Sedimentary Basin. Tectonophysics* 74: *209-238.*

Majorowicz, J. A., and Jessop, A. M. 1981b. *Present Heat Flow and a Preliminary Paleogeothermal History of Central Prairies Basin of Canada, Geothermics, Vol.10, No.2, pp. 81-93. London.*

McCrossan, R. G., and Glaister, R. P. 1970. Eds. *Geological History of Western Canada.* Published by Alberta Society of Petroleum Geologists, Alberta, Canada.

O' Brien, P. J., 1970.*Aquifer Transmissivity Distribution as Reflected by Overlying Soil Temperature Patterns: Ph.D thesis, The Pennsylvania State University.*

Oxburgh, E.R., and Andrews-Speed, C. P. 1981. *Temperature, Thermal Gradients and Heat Flow in the Southwest North Sea.* Petroleum Geology of the Continental Shelf of North-West Europe. pp.141-151.

Price, R. A., and Mountjoy, E. W. 1970. *Geological Structure of the Canadian Rocky Mountains between Bow and Athabasca Rivers-A Progress Report.* In *Structure of the Southern Canadian Cordillera.* Ed. J. O. Wheeler. *The Geological Association of Canada, Special Paper 6, pp. 7-26.*

Reiter, M., Jorge, C. and Tovar, R. 1982. *Estimates of Terrestrial Heat Flow in Northern Chihuahua, Mexico, Based upon Petroleum Bottom-hole Temperatures. Geological Soc. of America Bull. 93: pp. 613-624.*

Reiter, M., and Jessop, A. M. 1983. *Estimates Of Terrestrial Heat Flow in Offshore Eastern Canada derived from Petroleum Bottom-hole Temperature Data. (not published).*

Roberts, W. H. 1979. *Some Uses of Temperature Data in Petroleum Exploration:* Paper Presented to Sympossium II, Unconventional Methods in Exploration for Petroleum and Gas, Dallas, September 13-14, 1979.

Roy, R. E., Decker, E. R., Blackwell, D. D., and Birch, F. 1968. *Heat Flow in the United States, J. of Geophys. Res. 73: 5207-5221.*

Rybach, L., and Muffer, L. J. 1981. *Ed. Geothermal Systems: Principles and Case Histories, Wiley, 359 pp.*

Sclater, J. G., Jaupart, C. and Galson, D. 1980. *The Heat Flow Through Oceanic and Continental Crust and the Heat Loss of the Earth.* **Rev. Geophys. Space Phys., 18: 269-311.**

Sclater, J. G., and Parsons, B. 1981. *Oceans and Continents: Similarities and Differences in the Mechanisms of Heat Loss.* J. of Geophys. Res. vol.86, No. B12 pp. 11535-11552.

Smith, L., and Chapman, D. S. 1982. *On Thermal Effects of Groundwater Flow on Regional Systems, submitted to J. Of Geophys. Res., May 1982.*

Van Ostrand, C. E., 1939. *Temperature Gradients In Problems of Petroleum Geology, pp 989-1021, Amer. Assoc. Petrol. Geol., Tulsa, Okla, 1939.*

Yorath, C. J., and Hyndman, R. D. 1983. *Subsidence and Thermal History of Queen Charlotte Basin,* Can. J. Earth Sci. 20: 135-158.

B30401